CROSSTALK OF PROTEIN PHOSPHORYLATION AND LYSINE ACETYLATION ON 14-3-3 PROTEINS AND THEIR APPLICATIONS IN BRASSINOSTEROID SIGNALING AND PHOTOSYNTHESIS

BY

XIA WU

DISSERTATION

Submitted in partial fulfillment of the requirements
for the degree of Doctor of Philosophy in Biology
with a concentration in Physiological and Molecular Plant Biology
in the Graduate College of the
University of Illinois at Urbana-Champaign, 2011

Urbana, Illinois

Doctoral Committee:

Professor Steven Huber, Chair
Professor Donald Ort
Professor Peter Yau
Professor Raymond Zielinski

ABSTRACT

Protein phosphorylation and lysine acetylation are two important post-translational modifications (PTMs) in eukaryotes. However, the crosstalk between these two modifications is largely unknown. We demonstrated that both phosphorylation and lysine acetylation occurred to an Arabidopsis protein, 14-3-3ω. 14-3-3ω is a member of the 14-3-3 family of proteins that have been widely found in plants. 14-3-3s function mainly as phosphoserine/phosphothreonine-binding proteins that can affect the enzymatic activity, subcellular localization or protein turnover of their binding partners.

Phosphorylation of 14-3-3 proteins is one of the mechanisms regulating the binding of 14-3-3s to their target proteins. In animals, it was shown that the phosphorylation of 14-3-3s forced the release of their binding partners and resulted in signaling cascades. In contrast, little is known about the roles of 14-3-3 phosphorylation in signal transduction in plants. Thus, in Chapter 2 we characterized the phosphorylation of 14-3-3ω by the brassinosteroid receptor kinase BRI1 and its co-receptor BAK1. We identified eight novel Ser/Thr residues that were phosphorylated by BRI1 and/or BAK1 in vitro. Four of these phosphorylation sites (Thr-41, Thr-83, Thr94 and Thr-140) were confirmed to be present in planta in Arabidopsis and phosphorylation was greater in the 14-3-3ω that was associated with microsomal membranes compared to the soluble phase. 14-3-3ω was co-immunoprecipitated with the BRI1-BAK1 complex in vivo, and BRI1-bound 14-3-3ω was phosphorylated at Thr-94 and Thr-140 sites. Moreover, the phosphorylation of both sites responded to brassinolide (BL) with increased phosphorylation, suggesting the phosphorylation of 14-3-3ω is related to brassinosteroid (BR) signaling in Arabidopsis.

14-3-3ω expressed in *E. coli* was acetylated on Lys-53, a conserved residue that is known to be important for binding of target proteins. We demonstrated that directed mutant of 14-3-3ω (K53E) was unable to interact with neither BRI1 nor BAK1 in vitro and the phosphorylation of 14-3-3ω (K53E) by either kinase was dramatically decreased. On the other hand, the binding of the wildtype 14-3-3ω was shown to enhance its phosphorylation by BRI1 and BAK1, and phosphorylation of wildtype 14-3-3ω by BRI1 appeared to also enhance its binding to BRI1. The distinct responses of the directed mutant K53E suggests that acetylation of Lys-53 could be a negative regulator for the phosphorylation of 14-3-3ω by BRI1 and BAK1 kinases.

The acetylation of lysine was further studied in other proteins of Arabidopsis (Charter 3). We discovered that lysine acetylation is a widespread protein modification of diverse proteins in Arabidopsis. In particular, a group of photosynthesis-related proteins was newly identified to be acetylated on lysine residues in Arabidopsis, including light harvest proteins (LHCb1), Rubisco large and small subunits (RbCL and RbCS), subunits of PSII and PSI photoreaction centers, the ATP synthase beta subunit, and glyceraldehyde 3-phosphate dehydrogenase. We demonstrated that lysine acetylation of LHCb1 was correlated with its localization in relation to PSII photoreaction center; acetylation of RbCL may affect enzyme stability and the activity of Rubisco holoenzyme. Our data indicated that lysine acetylation is functionally important in photosynthesis.

In summary, we identified new roles of 14-3-3 protein phosphorylation in BR signaling and provided the first systematic study of the lysine acetylome in Arabidopsis. Protein phosphorylation and lysine acetylation appeared to be two inter-related modifications for 14-3-3ω proteins.

ACKNOWLEDGEMENTS

First and foremost, I would like to thank my revered advisor Dr. Steve Huber, who allowed me to conduct the Ph.D research in his lab. Steve designed great projects with me and supervised me at the highest standard. I learned so much from him both professionally and personally — I am indebted. I also want to thank the rest of my doctoral committee: Dr. Don Ort, Dr. Peter Yau and Dr. Ray Zielinski. They helped me through and made my Ph.D possible. I thank the past and present Huber lab family members: Dr. Man-Ho Oh, Dr. Kateri Duncan, Dr. Quansheng Qiu, Dr. Shane Hardin, Dr. Joan Huber, Dr. Clayton Larue, Dr. Jisen Zhang, Dr. Cathy Bermudez-Kandianis, Dr. Vladimir Brukhin, Dr. Tamara Lee, Dr. Vanita Jain, Dr. Jindong Sun, Dr. Hyoung Seok Kim, Suren Bandara, Rebekah Deter and Jose Soares. Together, we make the Huber team strong! Among them, I especially thank Man-Ho, who taught me numerous bench skills and gave my early research a jump start. Thanks are also extended to the Ray Ming lab, where I had a fun and productive rotation period during my first year and I thank Dr. Jong-Kuk Na and Dr. Jianping Wang for teaching me valuable cloning techniques. I also want to thank Dr. Hans Bohnert for the intellectual guidance, and Dr. Neil Kelleher and Dr. Adai Vellaichamy for the FTMS analysis. I am grateful to the people of Protein Sciences Facility, Immunological Resource Center, Core DNA Sequencing Facility, Microscopy Imaging Facility and Mass Spectrometry Lab at University of Illinois. They provided the state-of-the-art instruments and excellent services. I could not have collected as much data without them.

I would like to thank my parents, Zhiniu Wu and Haiyan Yuan. They are proud of me and I am proud of them. They kept me grounded and sane during the entire Ph.D effort — I am glad that I can succeed. I thank my family relatives, as they kept me motivated and cheered me on. I also want to thank my friends in Urbana-Champaign. It is they that make my life colorful as my research progressed!

My Ph.D dissertation won't have been possible without the generous funding from USDA-NIFA. My funding supports are also from Plant Molecular and Physiology Program, Campus Research Board, and School of Molecular and Cellular Biology at University of Illinois.

TABLE OF CONTENTS

LIST OF ABBREVIATIONS..... vii
CHAPTER 1: GENERAL INTRODUCTION..... 1
FIGURES..... 5
REFERENCES..... 8
CHAPTER 2: PHOSPHORYLATION OF 14-3-3ω BY THE RECEPTOR KINASES BRI1 AND BAK1 THAT FUNCTION IN BRASSINOSTEROID SIGNALING..... 13
INTRODUCTION..... 13
MATERIALS AND METHODS..... 14
RESULTS..... 17
DISCUSSIONS..... 25
FIGURES..... 29
TABLES..... 36
SUPPLEMENTAL FIGURES..... 37
SUPPLEMENTAL TABLES..... 45
SUPPLEMENTAL TEXTS..... 49
REFERENCES..... 54
CHAPTER 3: LYSINE ACETYLATION IS A WIDESPREAD PROTEIN MODIFICATION FOR DIVERSE PROTEINS IN ARABIDOPSIS..... 59
INTRODUCTION..... 59
MATERIALS AND METHODS..... 60
RESULTS..... 62
DISCUSSIONS..... 67
FIGURES..... 70
TABLES..... 75
SUPPLEMENTAL FIGURES..... 77
SUPPLEMENTAL TABLES..... 85
REFERENCES..... 88
CHAPTER 4: CONCLUDING REMARKS..... 91
TABLES..... 93

APPENDIX: THE ORIGIN OF THE NON-RECOMBINING REGION OF SEX CHROMOSOMES IN *CARICA* AND *VASCONCELLEA*..... 94
INTRODUCTION..... 94
MATERIALS AND METHODS..... 96
RESULTS..... 99
DISCUSSIONS..... 103
FIGURES..... 107
TABLES..... 109
SUPPLEMENTAL FIGURES..... 112
SUPPLEMENTAL TABLES..... 113
REFERENCES..... 118
CURRICULUM VITAE..... 122

LIST OF ABBREVIATIONS

PTM	Post-translational modification
Ser or S	Serine
Thr or T	Threonine
Lys or K	Lysine
pSer or pS	Phosphoserine
pThr or pT	Phosphothreonine
LysAc or acK	Lysine acetylation
Lysine acetylome	Entire set of proteins that are modified by lysine acetylation
Co-IP	Co-immunoprecipitation
SDS	Sodium dodecyl sulfate
SDS-PAGE	Sodium dodecyl sulfate polyacrylamide gel electrophoresis
IEF-2DE	Isoelectric focusing – two dimensional gel electrophoresis
LC-MS/MS	Liquid chromatography – tandem mass spectrometry
IMAC	Immobilized metal affinity chromatography (Fe^{3+})
TiO_2	Titanium dioxide chromatography
KDa	10^3 Dalton
MW	Molecular weight
pI	Isoelectric point of the protein
BSA	Bovine serum albumin
Ac-BSA	Acetyl- bovine serum albumin
BAX	Bcl-2–associated X protein
Bcl-2	B-cell lymphoma 2
C-Abl	Abelson murine leukemia oncogene
CKIα	Casein Kinase Iα
GRF2	General regulatory factor 2 (also known as 14-3-3ω)
FOXO3	Forkhead family of transcription factors
JNK	c-Jun N-terminal kinases
NR	Nitrate reductase
PKA	Protein kinase A
PKC	Protein kinase C
Raf	Proto-oncogene serine/threonine-protein kinase
SnRK2.8	Sucrose nonfermenting-related kinase 2.8
BR	Brassinosteroid
BL	Brassinolide
BRI1	Brassinosteroid Insensitive 1
BAK1	BRI1 associated kinase 1
BKI1	BRI1 kinase inhibitor 1
BSK1	BR-signaling kinase 1
BSU1	BRI1 suppressor 1
BIN2	Brassinosteroid Insensitive 2 (also known as GSK-3)
BES1	bri1-EMS-suppressor 1

BZR1	Brassinazole-resistant 1
EIF3	Translation initiation factor 3
eEF1A	Translation elongation factor 1A
GSK-3	Glycogen synthase kinase-3 (also known as BIN-2)
KAPP	Kinase-associated protein phosphatase
PP2A	Protein phosphatase 2A
TTL	Transthyretin-Like protein
RLK	Receptor-like kinase
RLK5	Receptor-like kinase 5 (also known as HAESA)
SERK1	Somatic embryogenesis receptor-like kinase 1
TMLK1	Transmembrane like kinase 1
LHCB1	Light harvesting chlorophyll a-b binding protein 1
Rubisco	Ribulose-1,5-bisphosphate carboxylase oxygenase
RbCL	Ribulose bisphosphate carboxylase large chain
RbCS	Ribulose bisphosphate carboxylase small chain
PSI	Photosystem I
PSII	Photosystem II
CaM	Calmodulin

CHAPTER 1: GENERAL INTRODUCTION

14-3-3 proteins and the phosphorylation of 14-3-3 proteins

14-3-3 proteins are a family of phospho-Ser/Thr binding proteins that are ubiquitous in eukaryotes. The name of "14-3-3" is ascribed to its first discovery from brain extracts, where these proteins were found in the 14th fraction of an ion-exchange column and at the subsequent 3.3 fraction of the starch gel electrophoresis (Moore and Perez, 1967). Since then, 14-3-3s have been identified in various tissues and species. In Arabidopsis, there are fifteen 14-3-3 genes and twelve expressed isoforms (Rosenquist et al., 2001; Sehnke et al., 2002), which are categorized into two groups based on the sequence homology to human isoforms: the epsilon 14-3-3s (more similar to human) and the non-epsilon 14-3-3s (less similar to human and distinct in plants) (Figure 1.1) (DeLille et al., 2001).

14-3-3 proteins function mainly as dimers through protein-protein interactions (Yaffe et al. 1997) and the binding of 14-3-3s generally requires a phospho-Ser/Thr on their client proteins in a so-called "14-3-3 binding motif". Several motifs have been identified, including mode 1 [(R/K)XX(pS/pT)XP], mode 2 [(R/K)XXX(pS/pT)XP] (represented both by nitrate reductase 530'-KKSVpSTPF-537') (Bachmann et al., 1996b) and mode 3 [(pS/pT)X_{1-2}-COOH] (such as H^+-ATPase 946'-YpTV-COOH 948') (Fuglsang et al., 1999). Recently, some other 14-3-3 binding motifs were also described (Ottmann et al., 2007; Chan et al., 2010). The binding of 14-3-3s can affect the enzymatic activity, subcellular localization or protein turnover of their binding partners (Bachmann, 1996a; Grozinger and Schreiber, 2000; Weiner and Kaiser, 1999). The regulation of 14-3-3 binding occurs at different levels. On one hand, reversible phosphorylation of the client proteins at the14-3-3 binding sites is required for the association of 14-3-3s. On the other hand, 14-3-3s themselves can be modified (such as by phosphorylation or lysine acetylation) and the binding ability of 14-3-3s is affected.

Most of the current understanding of 14-3-3 phosphorylation is from animal systems. For instance, phosphorylation of Ser58 on 14-3-3ζ (human isoform) by protein kinase A (PKA) affects the dimerization of 14-3-3ζ and inhibits binding to most client proteins (Woodcock et al., 2003; Ma et al, 2005). Phosphorylation of Ser184 on 14-3-3ζ by c-Jun NH_2-terminal kinase (JNK) results in the disassociation of apoptosis regulatory proteins Bax and c-Abl from 14-3-3ζ and the translocation of Bax to the mitochondria and c-Abl to the nucleus, which is a part of

apoptosis signaling cascades (Tsuruta et al., 2004 and Yoshida et al., 2005). Thr233 of 14-3-3ζ can be phosphorylated by casein kinase Iα, which affects the activation and association of Raf kinase (Dubois et al., 1997). In contrast, much less is known about 14-3-3 protein phosphorylation in plants. A recent study showed that Arabidopsis isoforms 14-3-3κ and 14-3-3χ could be phosphorylated on Ser 93 and Ser95 respectively, by sucrose nonfermenting-related kinase SnRK2.8, which provides a connection between 14-3-3 protein phosphorylation and plant metabolism (Shin et al., 2007). Arabidopsis 14-3-3ω has also been studied in relation to phosphorylation. Lu et al. (1994) reported that Arabidopsis14-3-3ω could be phosphorylated on Ser residues by organelle-membrane associated kinases. However, the identities of the kinases and the functions of the phosphorylation were not established in that study.

We are particularly interested in the non-epsilon family member 14-3-3ω (GRF2), because earlier studies on the interactions of 14-3-3s with nitrate reductase (NR) identified that 14-3-3ω possessed the highest binding and maximum inhibition of NR among the 14-3-3 isoforms tested (Bachmann et al., 1996b; Lambeck et al., 2010). In the dissertation, I studied the interactions of 14-3-3ω with the two new binding partners — the brassinosteroid insensitive 1 (BRI1) receptor kinase and its co-receptor brassinosteroid associated kinase 1 (BAK1) and I investigated the phosphorylation of 14-3-3ω by the receptor kinases and the impact on its interactions with BRI1 and BAK1.

Brassinosteroid (BR) signaling and the roles of 14-3-3 proteins

The brassinosteroids (BR) are a class of poly hydroxyl-steroids and are recognized as the sixth class of plant hormones (Fujioka and Yokota, 2003). BR signaling modulates plant growth and development as well as stress responses (Bishop and Koncz, 2002; Sakamoto et al., 2006; Nakashita et al., 2003). In general, BR signaling requires brassinosteroid receptor kinase, BRI1, which senses the BR molecules and activates the signal transduction cascade with its co-receptor, BAK1 (Kinoshita et al., 2005; Li et al., 2002; Nam et al., 2002). The details of BR intracellular signaling are described in Figure 1.2. It is noted that many checkpoints of BR signaling are regulated through protein phosphorylation and dephosphorylation. For example, the activation of both receptor kinases requires their sequential transphosphorylation within the BRI1-BAK1 complex (Wang et al., 2008). The localization of transcription factors BES1/ BZR1 is also attributed to the phosphorylation status of the proteins (Gampala et al., 2007; Tang et al., 2011).

The finding that 14-3-3 protein phosphorylation may occur during BR signal transduction will be an addition to the paradigm of BR signaling.

14-3-3 proteins have been reported in BR-related studies before. At the upstream end of BR signaling, 14-3-3 interacted with BRI1 and BAK1 (Oh et al., in submission), as well as with somatic embryogenesis receptor-like kinase 1 (SERK1), a receptor that has some overlap functions with BAK1 (Karlova et al. 2006). Downstream end of BR signaling, 14-3-3s bound to BZR1 impedes the nuclear shuffling of BZR1, thereby alleviating BR responses (Gampala et al. 2007). In addition, the protein levels of 14-3-3λ and 14-3-3κ were shown to increase upon BL treatment in a 2 DE-proteomics analysis (Deng et al., 2007). In my thesis, I further examined the roles of 14-3-3s in the upstream end of BR signaling in relation to BRI1 and BAK1.

Lysine acetylation of 14-3-3 proteins

Lysine acetylation (LysAc) is another form of reversible protein post-translational modification (PTM) in addition to protein phosphorylation. Lysine acetylation occurs to lysine residues where an acetyl moiety is attached to the ε-amino-group of lysine, and leads to the removal of the positive charge of lysine side chain and affects the electrostatic status of the modified protein. It is distinctly different from N-acetylation, which occurs frequently on the N-termini of the proteins (Glozak et al., 2005). Lysine acetylation is a well-known PTM of histone proteins and it is considered one of the mechanisms that regulates histone activities, impacting chromatin structure and gene expression (Jenuwein and Allis, 2000; Eberharter and Becker, 2002). Recent proteomic analyses in animal (Choudhary et al., 2009) and bacterial (Zhang et al., 2009) systems further expanded the scope of LysAc and identified thousands of LysAc proteins that are beyond histones. Thus, LysAc is quickly gaining people's attention and considered as another major in vivo PTM, comparable to protein phosphorylation (Norris et al., 2009).

In a 2-dimentional electrophoresis (2DE) analysis of 14-3-3ω proteins, we observed "charge trains" of 14-3-3ω purified from both *E.coli* and Arabidopsis (Figure 1.3). As lysine acetylation is an ancient protein modification, which can occur both in *E.coli* and Arabidopsis and can modify the isoelectric point (pI) of proteins (Zhang et al., 2009), we speculated that lysine acetylation may contribute to the patterns observed. We determined that 14-3-3ω expressed in *E. coli* was acetylated on Lys-53. Later, this observation was confirmed in the analysis of the human lysine acetylome, where additional lysine residues of 14-3-3 proteins were identified to

be acetylated and the LysAc was shown to affect the binding of 14-3-3s to their client proteins (Choudhary et al., 2009). Following the observation of LysAc on 14-3-3ω, we continued to look for LysAc on other proteins in Arabidopsis, and found that many Arabidopsis proteins were also modified by LysAc. As a result, the project of 14-3-3 lysine acetylation was extended to the overall lysine acetylome in Arabidopsis.

In plants, histone LysAc is essential for plant growth and development. The knockouts of the histone acetyltransferases or deacetylases were reported with altered levels of histone LysAc and displayed pleiotropic growth defects (Tian and Chen, 2001; Vlachonasios et al., 2003). However, little is known about LysAc of non-histone proteins in plants. Therefore, a proteomic analysis of lysine acetylome was designed to investigate the presence of LysAc of non-histone proteins in Arabidopsis.

Research Objectives and significance

The objectives of the dissertation were to 1) characterize the phosphorylation of 14-3-3ω in relation to BR signaling (Chapter 2), and 2) characterize the lysine acetylome in Arabidopsis (Chapter 3). Collectively, the results increase our understanding of two major PTMs in Arabidopsis – protein phosphorylation and LysAc and provide new perspectives in BR signaling and photosynthesis in Arabidopsis. These new findings can likely be extended to other plant species and have potential agricultural applications.

FIGURES

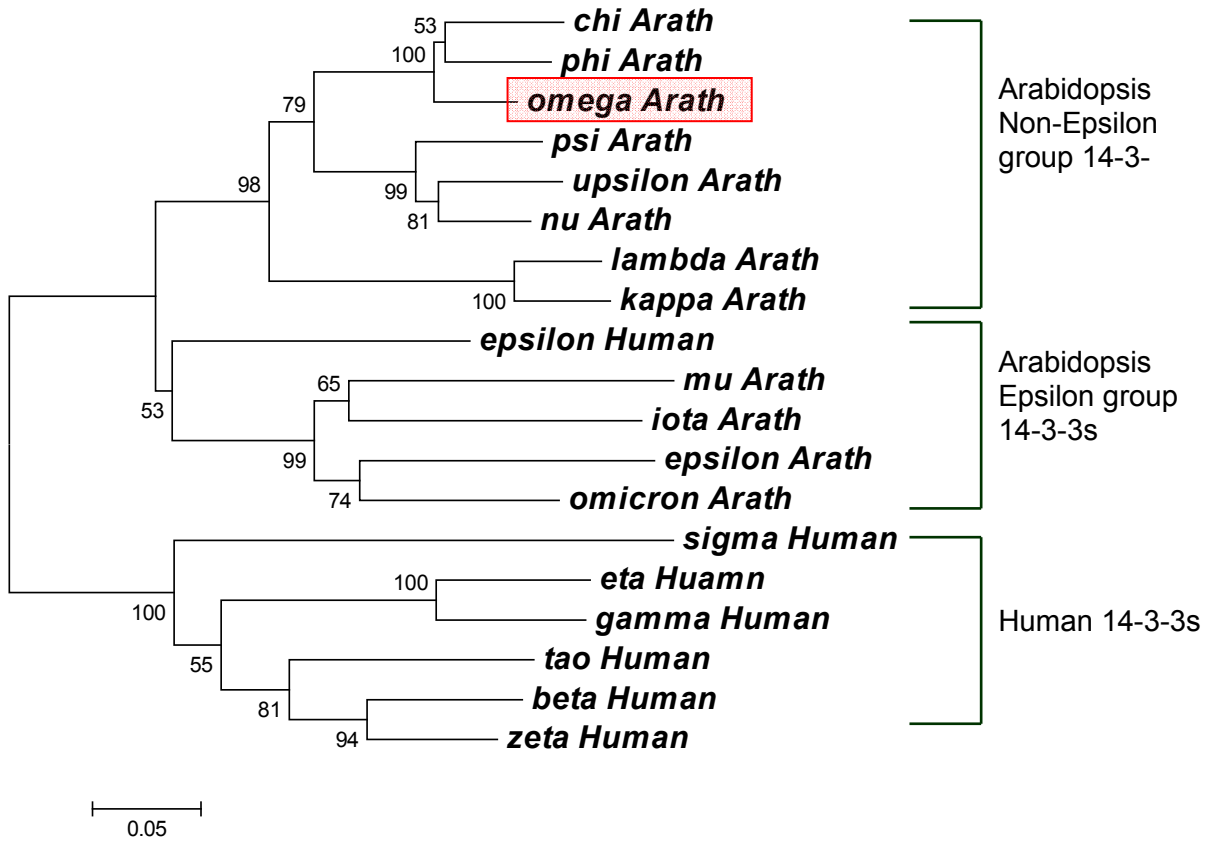


Figure 1.1 The phylogenetic tree of 14-3-3 isoforms in Arabidopsis and Human.
Protein sequences of 14-3-3s were aligned in Mega 4.0 (Tamura et al., 2007). The tree was drawn with the neighbor-joining method, and bootstrap values above 50 are shown. Based on the sequence identity to human isoforms, 14-3-3s in Arabidopsis were divided into the epsilon group 14-3-3s (more similar to human 14-3-3 epsilon) and the non-epsilon group 14-3-3s (less similar to human 14-3-3 epsilon). Arabidopsis 14-3-3ω belongs to the non-epsilon 14-3-3s and was highlighted in the graph.

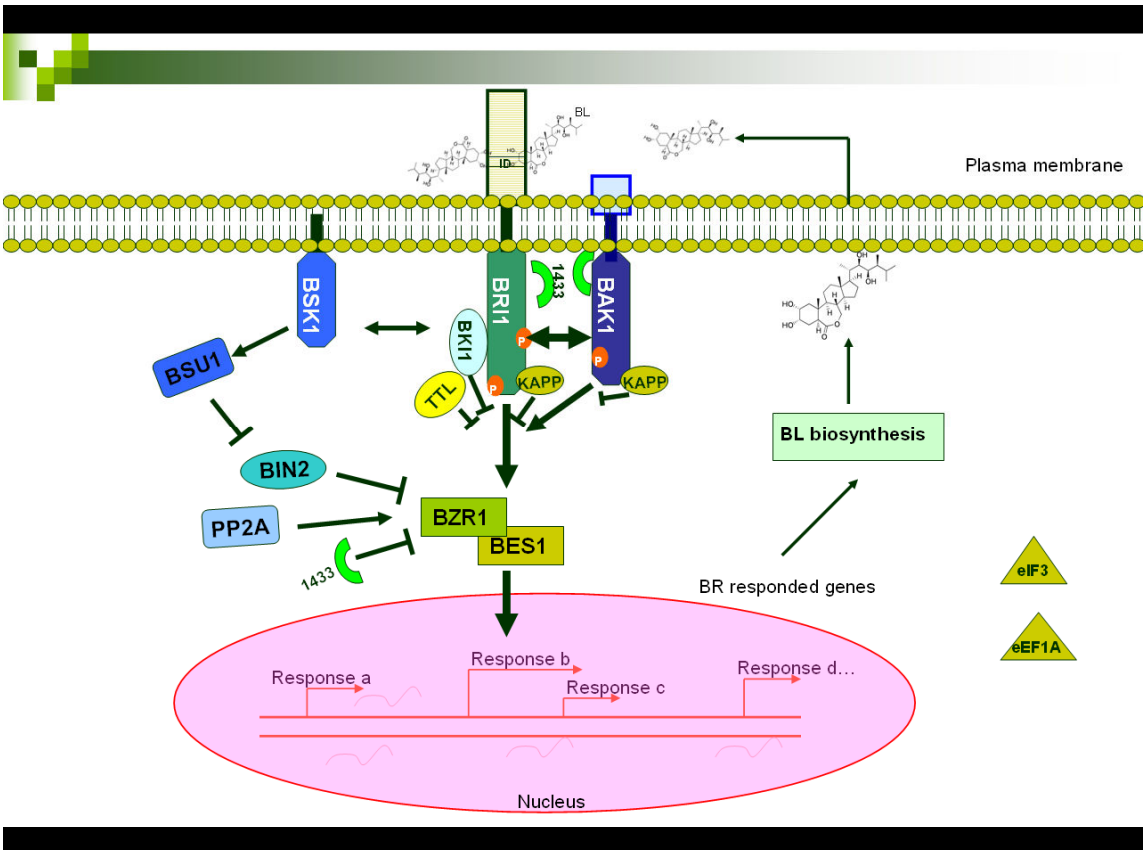


Figure 1.2 Simplified scheme of intracellular BR signaling (He et al., 2007; Kim and Wang, 2010).
The phytohormone brassinolide (BL) binds to BRI1 at its extracellular domain. BL binding triggers the autophosphorylation and conformational changes of BRI1, allowing the release of the BRI1 kinase inhibitor (BKI1). BAK1 dimerizes with BRI1 and further activates BRI1. The BR signaling cascade results in the dephosphorylation of the transcription factors, such as bri1-EMS-suppressor 1 (BES1) and brassinazole-resistant 1 (BZR1). Dephosphorylated BES1 and BZR1 shuttle from the cytoplasm to the nucleus and alter gene expression, including a set of BL-biosynthetic genes. The BL biosynthesis forms a negative feedback loop to balance BR signaling. Other BR signaling components include the family of glycogen synthase kinases, represented by GSK-3 (Brassinosteroid Insensitive 2, BIN2). BIN2 directly interacts with BES1/BZR1 and phosphorylates both transcription factors. The phosphorylation of BES1/BZR1 creates 14-3-3 binding sites, and the binding of 14-3-3s retains the cytoplasmic localization of BES1/BZR1, attenuating BR responses. The activity of BIN2 is inhibited by a protein phosphatase, BRI1 suppressor 1 (BSU1). Another phosphatase (PP2A) dephosphorylates BZR1, and assists the nuclear localization of BZR1. In addition, BRI1 interacts with and phosphorylates BR-signaling kinases (BSK1-BSK3), promoting the interaction of BSK1 with BSU1. BRI1 also interacts with Transthyretin-Like protein (TTL) and phosphorylates TTL in vitro. TTL was proposed as a negative regulator of BR signaling. Both BRI1 and BAK1 also interact with Kinase-associated protein phosphatase (KAPP), which is also negative regulator of BR signaling. Moreover, translation initiation factor 3 (eIF3) and translation elongation factor (eEF1A) were reported as BRI1 interacting proteins in vivo, but the actual roles have not been demonstrated to date. Interactions of 14-3-3ω with BRI1 and BAK1 are presented in this study. The phosphorylation of 14-3-3ω was correlated with the activation of BRI1-BAK1 complex in response to BL.

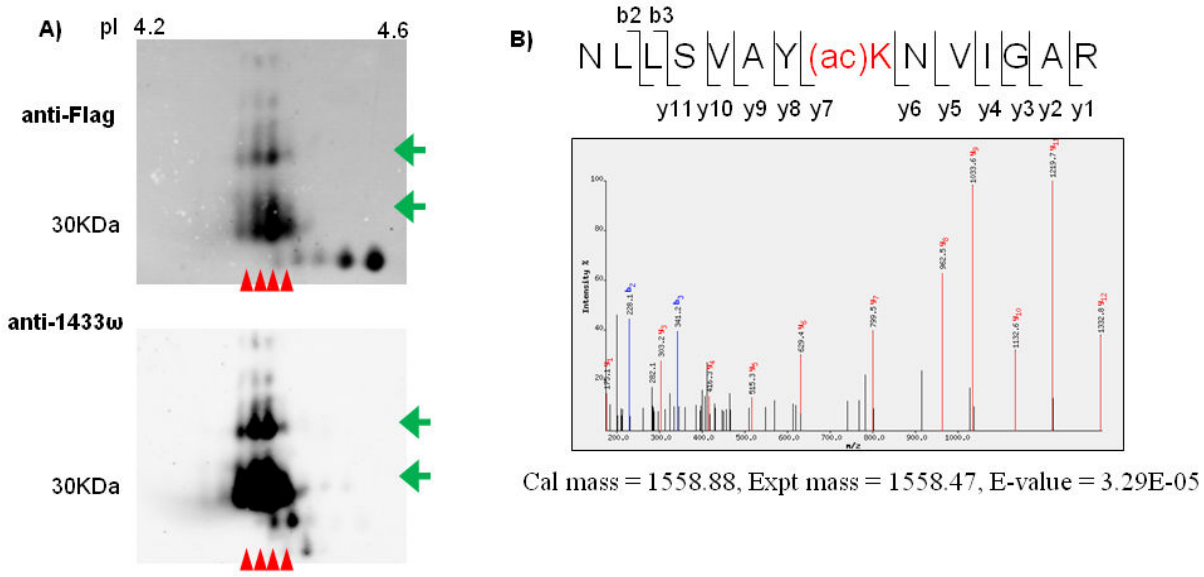


Figure 1.3 Lysine acetylation of 14-3-3ω in Arabidopsis and *E.coli*.

A) Flag-14-3-3ω purified from transgenic Arabidopsis and analyzed by probing 2DE immunoblots with anti-Flag and anti-1433ω antibodies. Both antibodies detected "charge trains" of 14-3-3ω – forms of 14-3-3ω with slightly different pI (red arrow head). Similar "charge trains" were also observed in the Flag-14-3-3ω that were expressed in *E. coli* (Figure 2.1C). It is possible that the alteration of pI is due to the modification of lysine acetylation. Forms of 14-3-3ω with different molecular weight (MW) were also observed from Arabidopsis (green arrow), which suggest some other unknown protein modifications may also occur to 14-3-3ω in Arabidopsis. B) Lysine acetylation of K53 was identified in the 14-3-3ω purified from *E. coli*. The equivalent modification was also identified in human 14-3-3s and it was shown the modification affect the binding of 14-3-3s to their client proteins (Choudhary et al., 2009).

REFERENCES

Bachmann, M., Huber, J.L., Liao, P.-C., Gage, D.A., Huber, S.C. (1996a) The inhibitor protein of phosphorylated nitrate reductase from spinach (Spinacia oleracea) leaves is a 14-3-3 protein. FEBS Lett. 387: 127-131.

Bachmann, M., Huber, J.L., Athwal, G.S., Wu, K., Ferl, R.J., Huber, S.C. (1996b) 14-3-3 proteins associate with the regulatory phosphorylation site of spinach leaf nitrate reductase in an isoform-specific manner and reduce dephosphorylation of Ser-543 by endogenous protein phosphatases. FEBS Lett. 398: 26-30.

Bishop G.J, Koncz C. (2002) Brassinosteroids and plant steroid hormone signaling. Plant Cell Suppl: S97-110.

Chan P.M., Ng Y.W., Manser E. (2010) A robust protocol to map binding sites of the 14-3-3 interactome: Cdc25C requires phosphorylation of both S216 and S263 to bind 14-3-3. Mol Cell Proteomics 10: M110.005157. Epub 2010 Dec 28.

Choudhary C., Kumar C., Gnad F., Nielsen M.L., Rehman M., Walther T.C., Olsen J.V., Mann M. (2009) Lysine acetylation targets protein complexes and co-regulates major cellular functions. Science 325: 834-840.

DeLille, J.M., Sehnke, P.C., Ferl, R.J. (2001) The Arabidopsis 14-3-3 family of signaling regulators. Plant Physiol. 126: 35-38.

Ding Z., Wang H., Liang X., Morris E.R., Gallazzi F., Pandit S., Skolnick J., Walker J.C., Van Doren S.R. (2007) Phosphoprotein and phosphopeptide interactions with the FHA domain from Arabidopsis kinase-associated protein phosphatase. Biochemistry 46: 2684-2696.

Dubois, T., Rommel, C., Howell, S., Steinhussen, U., Soneji, Y., Morrice, N., Moelling, K. and Aitken A. (1997) 14-3-3 is phosphorylated by casein kinase I on residue 233. Phosphorylation at this site in vivo regulates Raf/14-3-3 interaction. J Biol Chem. 272: 28882-28888.

Ehsan, H., Ray, W.K., Phinney, B., Wang, X., Huber, S.C., Clouse, S.D. (2005). Interaction of Arabidopsis BRASSINOSTEROID-INSENSITIVE 1 receptor kinase with a homolog of mammalian TGF-β receptor interacting protein. Plant J. 43: 251-261.

Fuglsang A.T., Visconti S., Drumm K., Jahn T., Stensballe A., Mattei B., Jensen O.N., Aducci P., Palmgren MG. (1999) Binding of 14-3-3 protein to the plasma membrane H(+)-ATPase AHA2 involves the three C-terminal residues Tyr(946)-Thr-Val and requires phosphorylation of Thr(947). J Biol Chem. 274: 36774-366780.

Gampala S.S., Kim, T.W., He, J.X., Tang, W., Deng, Z., Bai, M.Y., Guan, S., Lalonde, S., Sun, Y., Gendron, J.M., Chen, H., Shibagaki, N., Ferl, R.J., Ehrhardt, D., Chong, K., Burlingame, A.L. and Wang, Z.Y. (2007) An essential role for 14-3-3 proteins in brassinosteroid signal transduction in Arabidopsis. Dev Cell. 13:177-189.

Glozak M.A., Sengupta N., Zhang X., Seto E. (2005) Acetylation and deacetylation of non-histone proteins. Gene 363: 15-23.

Grozinger, C.M., Schreiber, S.L. (2000) Regulation of histone deacetylase 4 and 5 and transcriptional activity by 14-3-3-dependent cellular localization. Proc Natl Acad Sci U S A. 97: 7835-7840.

He, J.X., Gendron, J.M., Sun, Y., Gampala, S.S.L., Gendron, N., Sun, C.Q., Wang, Z.Y. (2005) BZR1 is a transcriptional repressor with dual roles in brassinosteroid homeostasis and growth responses. Science 307: 1634-1638.

He K., Gou X., Yuan T., Lin H., Asami T., Yoshida S., Russell S.D., Li J. (2007) BAK1 and BKK1 regulate brassinosteroid-dependent growth and brassinosteroid-independent cell-death pathways. Curr Biol. 17:1109-1115.

Jaillais, Y., Hothorn, M., Belkhadir, Y., Dabi, T., Nimchuk, Z.L., Meyerowitz, E.M., Chory, J. (2011) Tyrosine phosphorylation controls brassinosteroid receptor activation by triggering membrane release of its kinase inhibitor. Genes and Development 25: 232-237.

Jenuwein T., Allis C.D. (2000) Translating the Histone Code. Science 293: 1074-1080.

Karlova, R., Boeren, S., Russinova, E., Aker, J., Vervoort, J. and De Vries, S. (2006) The Arabidopsis somatic embryogenesis receptor-like kinase1 protein complex includes brassinosteroid-insensitive1. Plant Cell 18: 626-638.

Kim T.W., Guan S., Sun Y., Deng Z., Tang W., Shang J.X., Sun Y., Burlingame A.L., Wang Z.Y. (2009) Brassinosteroid signal transduction from cell-surface receptor kinases to nuclear transcription factors. Nat Cell Biol. 11: 1254-60.

Kim T.W, Wang Z.Y. (2010) Brassinosteroid signal transduction from receptor kinases to transcription factors. Annu Rev Plant Biol. 61: 681-704.

Lambeck, I., Chi, J.-C., Krizowski, S., Mueller, S., Mehlmer, N., Teige, M., Fischer, K., Schwarz, G. (2010) Kinetic analysis of 14-3-3-inhibited arabidopsis thaliana nitrate reductase. Biochemistry 49: 8177-8186.

Li, J., Wen, J., Lease, K.A., Doke, J.T., Tax, F.E., Walker, J.C. (2002). BAK1, an Arabidopsis LRR receptor-like protein kinase, interacts with BRI1 and modulates brassinosteroid signaling. Cell 110: 213-222.

Li L., Ye H., Guo H., Yin Y. (2009) Arabidopsis IWS1 interacts with transcription factor BES1 and is involved in plant steroid hormone brassinosteroid regulated gene expression. Proc Natl Acad Sci U S A. 107: 3918-3923.

Lu, G., Sehnke, P.C., Ferl RJ. (1994) Phosphorylation and calcium binding properties of an Arabidopsis GF14 brain protein homolog. Plant Cell 6: 501-510.

Ma, Y., Pitson, S., Hercus, T., Murphy, J., Lopez, A., and Woodcock, J. (2005) Sphingosine activates protein kinase A type II by a novel cAMP-independent mechanism. J Biol Chem. 280: 26011-26017.

Moore B.W., Perez V.J. (1967) F.D. Carlson. ed. Physiological and Biochemical Aspects of Nervous Integration. Prentice-Hall, Inc, The Marine Biological Laboratory, Woods Hole, MA. pp. 343–359.

Nakashita H., Yasuda M., Nitta T., Asami T., Fujioka S., Arai Y., Sekimata K., Takatsuto S., Yamaguchi I., Yoshida S. (2003) Brassinosteroid functions in a broad range of disease resistance in tobacco and rice. Plant J. 33: 887-898.

Nam, K.H., Li, J. (2002). BRI1/BAK1, a receptor kinase pair mediating brassinosteroid signaling. Cell 110: 203-212.

Norris K.L., Lee J.Y., Yao T.P. (2009) Acetylation goes global: the emergence of acetylation biology. Sci Signal. 2: pe76.

Ottmann C., Yasmin L., Weyand M., Veesenmeyer J.L., Diaz M.H., Palmer R.H., Francis M.S., Hauser A.R., Wittinghofer A., Hallberg B. (2007) Phosphorylation-independent interaction between 14-3-3 and exoenzyme S: from structure to pathogenesis. EMBO J. 26: 902-913.

Rosenquist, M., Alsterfjord, M., Larsson, C. and Sommarin, M. (2001) Data mining the Arabidopsis genome reveals fifteen 14-3-3 genes. Expression is demonstrated for two out of five novel genes. Plant Physiol. 127: 142-149.

Rozhon W., Mayerhofer J., Petutschnig E., Fujioka S., Jonak C. (2010) ASKθ, a group-III Arabidopsis GSK3, functions in the brassinosteroid signalling pathway. Plant J. 62: 215-223.

Sakamoto T., Morinaka Y., Ohnishi T., Sunohara H., Fujioka S., Ueguchi-Tanaka M., Mizutani M., Sakata K., Takatsuto S., Yoshida S., Tanaka H., Kitano H., Matsuoka M. (2006) Erect leaves caused by brassinosteroid deficiency increase biomass production and grain yield in rice. Nat Biotechnol. 24: 105-109.

Sehnke, P.C., DeLille, J.M. and Ferl, R.J. (2002) Consummating signal transduction: the role of 14-3-3 proteins in the completion of signal-induced transitions in protein activity. Plant Cell 14: S339-354.

Shin, R., Alvarez, S., Burch, A.Y., Jez, J.M. and Schachtman, D.P. (2007) Phosphoproteomic identification of targets of the Arabidopsis sucrose nonfermenting-like kinase SnRK2.8 reveals a connection to metabolic processes. Proc Natl Acad Sci U S A. 104: 6460-6465.

Sun Y., Fan X.Y., Cao D.M., Tang W., He K., Zhu J.Y., He J.X., Bai M.Y., Zhu S., Oh E., Patil S., Kim T.W., Ji H., Wong W.H., Rhee S.Y., Wang Z.Y. (2010) Integration of brassinosteroid

signal transduction with the transcription network for plant growth regulation in Arabidopsis. Dev Cell. 19: 765-777.

Tang W., Kim T.W., Oses-Prieto J.A., Sun Y., Deng Z., Zhu S., Wang R., Burlingame A.L., Wang Z.Y. (2008) BSKs mediate signal transduction from the receptor kinase BRI1 in Arabidopsis. Science 321: 557-560.

Tang W., Yuan M., Wang R., Yang Y., Wang C,. Oses-Prieto J.A., Kim T.W., Zhou H.W., Deng Z., Gampala S.S., Gendron J.M., Jonassen E.M., Lillo C., DeLong A., Burlingame A.L., Sun Y., Wang Z.Y. (2011) PP2A activates brassinosteroid-responsive gene expression and plant growth by dephosphorylating BZR1. Nat Cell Biol. 13: 124-131.

Tian L., Chen Z.J. (2001) Blocking histone deacetylation in Arabidopsis induces pleiotropic effects on plant gene regulation and development. Proc Natl Acad Sci U S A. 98: 200-205.

Tsuruta, F., Sunayama, J., Mori, Y., Hattori, S., Shimizu, S., Tsujimoto, Y., Yoshioka, K., Masuyama, N. and Gotoh, Y. (2004) JNK promotes Bax translocation to mitochondria through phosphorylation of 14-3-3 proteins. EMBO J. 23: 1889-1899.

Tamura K., Dudley J., Nei M., Kumar S. (2007) MEGA4: Molecular Evolutionary Genetics Analysis (MEGA) software version 4.0. Mol. Biol. Evol. 24: 1596-1599.

Vlachonasios K.E., Thomashow M.F., Triezenberg S.J. (2003) Disruption mutations of ADA2b and GCN5 transcriptional adaptor genes dramatically affect Arabidopsis growth, development, and gene expression. Plant Cell 15: 626-638.

Wang, X., Kota, U., He, K., Blackburn, K., Li, J., Goshe, M.B., Huber, S.C. and Clouse, S.D. (2008) Sequential transphosphorylation of the BRI1/BAK1 receptor kinase complex impacts early events in brassinosteroid signaling. Dev. Cell 15: 220-235.

Wang Z.Y, Nakano T, Gendron J, He J, Chen M, Vafeados D, Yang Y, Fujioka S, Yoshida S, Asami T, Chory J. (2002) Nuclear-localized BZR1 mediates brassinosteroid-induced growth and feedback suppression of brassinosteroid biosynthesis. Dev Cell. 2: 505-513.

Weiner, H., Kaiser, W.M. (1999) 14-3-3 proteins control proteolysis of nitrate reductase in spinach leaves. FEBS Lett. 455: 75-78.

Woodcock, J.M., Murphy, J., Stomski, F.C., Berndt, M.C. and Lopez, A.F. (2003) The dimeric versus monomeric status of 14-3-3ζ is controlled by phosphorylation of ser58 at the dimer interface. J Biol Chem. 278: 36323-36327.

Yaffe M.B., Rittinger K., Volinia S., Caron P.R., Aitken A., Leffers H., Gamblin S.J., Smerdon S.J., Cantley L.C. (1997) The structural basis for 14-3-3:phosphopeptide binding specificity. Cell 91: 961-971.

Yin, Y., Wang, Z.Y., Mora-Garcia, S., Li, J., Yoshida, S., Asami, T., Chory, J. (2002) BES1 accumulates in the nucleus in response to brassinosteroids to regulate gene expression and promote stem elongation. Cell 109: 181-191.

Yoshida, K., Yamaguchi, T., Natsume, T., Kufe, D., Miki, Y. (2005) JNK phosphorylation of 14-3-3 proteins regulates nuclear targeting of c-Abl in the apoptotic response to DNA damage. Nat Cell Biol. 7: 278-285.

Yuan T., Fujioka S., Takatsuto S., Matsumoto S., Gou X., He K., Russell S.D., Li J. (2007) BEN1, a gene encoding a dihydroflavonol 4-reductase (DFR)-like protein, regulates the levels of brassinosteroids in Arabidopsis thaliana. Plant J. 51: 220-233.

Zhang J., Sprung R., Pei J., Tan X., Kim S., Zhu H., Liu C.F., Grishin N.V., Zhao Y. (2009) Lysine acetylation is a highly abundant and evolutionarily conserved modification in *Escherichia coli*. Mol Cell Proteomics. 8: 215-225.

Zhao, J., Peng, P., Schmitz, R.J., Decker, A.D., Tax, F.E., Li, J. (2002) Two putative BIN2 substrates are nuclear components of brassinosteroid signaling. Plant Physiol. 130: 1221-1229.

CHAPTER 2: PHOSPHORYLATION OF 14-3-3ω BY THE RECEPTOR KINASES BRI1 AND BAK1 THAT FUNCTION IN BRASSINOSTEROID SIGNALING[1]

INTRODUCTION

14-3-3 proteins are a family of phospho-Ser/Thr binding proteins that are conserved in eukaryotes. In Arabidopsis, there are fifteen 14-3-3 genes and twelve expressed isoforms, and 14-3-3ω is one of the expressed isoforms (Rosenquist et al, 2001; Sehnke et al, 2002). 14-3-3 proteins function as dimers through protein-protein interactions (Yaffe et al. 1997), and the binding of 14-3-3s generally requires a phospho-Ser/Thr residue on their client proteins in a so-called "14-3-3 binding motif". Several motifs have been identified, including mode 1 [(R/K)XXpS/pTXP], mode 2 [(R/K)XXXpS/pTXP] and mode 3 [(pS/pT)X_{1-2}-COOH] (Aitken, 2006). Recently, some other 14-3-3 binding motifs were also described (Ottmann et al., 2007a; Chan et al., 2010). The binding of 14-3-3s can affect the enzymatic activity, subcellular localization and protein turnover of their binding partners (Bachmann, 1996; Grozinger and Schreiber, 2000; Weiner and Kaiser, 1999). The regulation of 14-3-3 binding occurs at different levels. On one hand, reversible phosphorylation of the client proteins at the 14-3-3 binding sites is required for the association of 14-3-3s. On the other hand, 14-3-3s themselves can be modified (such as by phosphorylation or lysine acetylation) and the binding ability of 14-3-3s is affected (Fu et al., 2000; Choudhary et al., 2009).

Most of our current understanding of 14-3-3 phosphorylation is from animal systems. For instance, phosphorylation of 14-3-3ζ on Ser58 by sphingosine activated protein kinase A (PKA) converted the normally dimeric 14-3-3s into monomers and interrupted the binding of 14-3-3s to most client proteins (Woodcock et al., 2003; Ma et al, 2005). Ser184 of 14-3-3ζ and Ser185 of 14-3-3σ were phosphorylated by c-Jun NH_2-terminal kinase (JNK) in responses to stress-induced apoptosis. The phosphorylation resulted in the disassociation of Bax and FOXO3a from 14-3-3s and the translocation of Bax to the mitochondria and FOXO3a to the nucleus (Tsuruta et al., 2004; Sunayama et al., 2005). Thr232 at the C-terminal of 14-3-3ζ can be phosphorylated by casein kinase Iα, which may affect the activation and association of Raf kinase (Dubois et al., 1997). Thus, phosphorylation of 14-3-3s plays important roles in signal transduction in animals.

[1] The content of this chapter is a part of the manuscript Wu et al. (2011) in preparation.

In contrast, our understandings of 14-3-3 protein phosphorylation in plants are very limited. In 1994, Ferl and colleagues reported that Arabidopsis14-3-3ω could be phosphorylated on Ser residues by organelle-membrane associated kinases. But the identity of the kinase and the functions of the phosphorylation were not established in that study. Using animal tyrosine kinase insulin growth factor receptor 1, Giacometti et al. (2004) observed that maize GF14-6 was phosphorylated on Tyr137, which inhibited the interaction of GF14-6 with H^+-ATPase. More recently, Arabidopsis isoforms 14-3-3κ and 14-3-3χ were found to be phosphorylated on Ser93 and Ser95 respectively, by sucrose nonfermenting-related kinase SnRK2.8 and revealed a connection between 14-3-3 protein phosphorylation and plant metabolic processes (Shin et al., 2007). Yet, the roles of 14-3-3 phosphorylation in signal transduction in plants have not been established to date.

Brassinosteroids (BRs) are recognized as the sixth class of plant hormones and modulate plant development and stress responses (Bishop and Koncz, 2002; Nakashita et al., 2003). In Arabidopsis, BR signaling requires brassinosteroid receptor kinase, BRI1, senses the BR molecules and activates the signaling cascades with its co-receptor, BAK1 (Kinoshita et al., 2005; Li et al., 2002; Nam et al., 2002). 14-3-3s were reported to interact with both BRI1 and BAK1. Prevention of the binding between BRI1 and14-3-3s resulted in BR deficient phenotypes, meaning that interactions of BRI1 and 14-3-3s are important to ensure the BR signaling input (Oh et al., in submission). Downstream end of BR signaling, 14-3-3s were also reported to interact with transcription factor BZR1, but the interaction retained the cytoplasmic localization of BZR1, attenuating the BR signaling output (Gampala et al. 2007). In addition, the protein levels of 14-3-3λ and 14-3-3κ were up-regulated in response to BL treatment (Deng et al., 2007). The objective of this study was to determine whether the 14-3-3ω might be the substrates of receptor-like kinases BRI1 and BAK1 in vitro and if so, whether the phosphorylation occurs in vivo and is responsive to BR signaling.

MATERIALS AND METHODS

Recombinant proteins

Recombinant proteins of His-14-3-3ω (vector pET15b), Flag-BRI1(vector pFlag-MAC) and Flag-BAK1(vector pFlag-MAC) were expressed in *E. coli* BL21(DE3) (Novagen) and purified

with affinity beads of His-Tag (QIAGEN) or Flag-Tag (Sigma), as described in the manufacturer's manuals. The His-tag of His-14-3-3ω was removed by cleavage with thrombin (Novagen) used at a 50:1 (w/w) ratio.

Antibodies

The custom antibodies anti-1433ω (antigen: DEIKEAAAPKPT) and anti-1433 loop8 (antigen: ELDTLGEESYKDST) were produced by Bethyl Laboratories; anti-pT41 (antigen: GDELpTVEERN), anti-pT83 (antigen: DDHVpTAIREY), anti-pT94 (antigen: RSKIEpTELSG), and anti-pT140 (antigen: AEFKpTGQERK) were produced by GenScript. Specificity of the antibodies was verified as shown in Figure 2.S3. Other antibodies that were used in this study included anti-BAK1 (Schulze et al., 2010), anti-1433-pS58 (PhosphoSolutions), anti-pS /pT-P (abcam), anti-pThr (Invitrogen) and anti-Flag (Sigma).

Arabidopsis tissues and BL treatment

Wild type WS-2 and transgenic Arabidopsis expressing BRI1-Flag or BAK1-Flag were grown under long days (16 h photoperiod from 8:00-24:00) in soil or in liquid culture (1/2 MS, 1% sucrose, pH 5.7). The 12 d-old BRI1-Flag transgenic seedlings in liquid culture were treated with 100 nM epi-BL (Sigma) for 1.5 h (12:00-13:30), 6 h (12:00-18:00), or 24 h (12:00-next day 12:00).

BIAcore analysis

BIAcore 3000 (GE, USA) was used to monitor the real-time interactions of 1433ω with BRI1 or BAK1. The running buffer was 20 mM MOPS (pH 7.5), 50 mM NaCl, 5 mM $MgCl_2$ (or 5 mM $MnCl_2$) and 0.05% (v/v) SP-20. Briefly, 130 (RU) ligand of His-1433ω was immobilized onto BIAcore NTA-Chip and different concentrations of analyte (BRI1 or BAK1) were injected at a flow rate of 20 µl/min for 2 min to examine the association. The disassociation (20 µl/min flow rate) was monitored for 10 min immediately after the analyte injections. After each run, the sensor chip was regenerated with the buffer of 20 mM MOPS (pH 7.5), 50 mM NaCl, 0.05% (v/v) SP-20 and 300 mM EDTA. The equilibrium constant (KD) was calculated with 1:1 Langmuir binding model. The injection of the analyte generally led to a bulk shift in the signals and only the curves without baseline drifts were used for kinetic analyses (Athwal et al., 2000).

In vitro phosphorylation assays

The phosphorylation reaction mixture (30 ul) containing 1 µg BRI1 (or 1 µg BAK1), 1 µg 14-3-3ω, 0.5 mM ATP, 5 mM $MnCl_2$ (or 5 mM $MgCl_2$) and 20 mM MOPS (pH 7.5) was incubated at room temperature for 50 min before addition of SDS sample buffer for SDS-PAGE analysis, or IEF buffer for 2-DE analysis (Wu et al., 2011).

In vitro co-immunoprecipitation assays

One microgram of BRI (or 1 µg BAK1) was immobilized onto Flag-beads by incubating in the binding buffer [5 mM $MnCl_2$ (or 5 mM $MgCl_2$), 50 mM MOPS (pH 7.5), 50 mM NaCl, 0.25% TX-100] for 4 h at 4ºC. Next, 1 µg 14-3-3ω was added to the mixture and incubated at room temperature for 30 min. The mixture was washed three times for 5 min each at room temperature with the washing buffer [5 mM $MnCl_2$ (or 5 mM $MgCl_2$), 50 mM MOPS (pH 7.5) and 75 mM NaCl] before dissolving in SDS sample buffer for SDS-PAGE analysis.

In vitro phosphorylation co-immunoprecipitation assays

First, the in vitro phosphorylation assay was performed as described above, but stopped by adding 10 volumes of $MgCl_2$-binding buffer on ice. Second, 20 µl of Flag-beads (preblocked with casein; Sigma) was added to the phosphorylation mixture to bind Flag-BRI1 and incubated for 4 h at 4ºC. Third, the beads were washed three times for 5 min each at 4ºC with $MgCl_2$-washing buffer. During the washing steps, the supernatants after bead pull downs were collected as the Super, and the subsequent first buffer wash was collected as the Wash. Fourth, proteins in the Super and Wash fractions were denatured and both fractions were dried down in the SpeedVac. Fifth, all three fractions: IP (bead immunoprecipitation), Super and Wash were dissolved in equal volumes of SDS sample buffer for analysis by SDS-PAGE and immunoblotting.

In vivo co-immunoprecipitation

Arabidopsis microsomal membranes were prepared in the extraction buffer [100 mM MOPS (pH 7.5), 20 mM NaF, 5 mM $NaMoO_4$, 1 mM Na_3VO_4, 1 µM MCLR, 1 mM AEBSF, 5 mM Caproic acid, 1 mM para-amino-benzamidine, 2 µM E64, 2 µM Leupeptine, 10 µM MG132 and 5 mM $MgCl_2$] as described in Duncan et al (2006). The microsomal pellet was briefly sonicated

to resuspend in the extraction buffer plus 0.25% TX-100 and 5% glycerol, and incubated with Flag-beads (preblocked with casein) overnight. The beads were washed three times for 5 min each with washing buffer [50 mM MOPS (pH 7.5), 75 mM NaCl, 5 mM $MgCl_2$], before boiling in SDS sample buffer for SDS-PAGE and immunoblot analysis.

Phosphopeptide enrichment and mass spectrometry analysis

Proteins in gel slices or on the Flag-beads were digested with 10 ng/µl trypsin (Promega) for 16 h. For phospho-select iron affinity enrichment (IMAC, Sigma), peptides were dissolved in IMAC buffer (pH 3.0, 30% acetonitrile and 250 mM acetic acid) and incubated with IMAC beads at room temperature for 35 min. Beads were washed three times for 5 min each with IMAC buffer and one time with water before elution with 400 mM ammonium hydroxide (pH 10.0) for 5 min. The eluted peptides were immediately mixed with sufficient 5% TFA to reduce pH to below 5.0. Peptides were dried down and cleaned with C18 ziptip (Millipore). MALDI analysis was performed on Applied Biosystems Voyager DE-STR (Mass Spectrometry Lab, University of Illinois). A matrix of DHB in 2% o-phosphoric acid was used to assist the detection of phosphopeptides (Kjellström and Jensen, 2004). Q-TOF analysis was performed as described in Wu et al. (2011).

RESULTS

14-3-3ω is phosphorylated by recombinant BRI1 and BAK1 cytoplasmic domains in vitro

As noted in the introduction, 14-3-3s co-immunoprecipitate with receptor kinases (RLKs) in vivo and bind directly to recombinant cytoplasmic domains (CDs) of BRI1 and BAK1 in vitro (Oh et al., in submission). A logical question is whether the 14-3-3s might be substrates of RLKs as well. To test this, we first performed in vitro phosphorylation assays of 14-3-3ω with BRI1 alone, BAK1 alone or (BRI1+BAK1) together (Figure 2.1A). As indicated by Pro-Q diamond staining (which detects phosphorylation on Ser, Thr and Tyr residues) and anti-pThr immunoblot (which detects phosphorylation on Thr residues), both BRI1 and BAK1 independently phosphorylated 14-3-3ω in vitro. Stronger phosphorylation signals were observed in the sample of 14-3-3ω incubated with (BRI1+BAK1) together. The divalent cation Mn^{2+} promoted higher

phosphorylation of 14-3-3ω over Mg^{2+}. The reaction also caused a mobility shift of 14-3-3ω in SDS-PAGE, resulting in an upper band that had greater phosphorylation signals, compared to the unshifted band. To further test the Mn^{2+} preference of the kinase activity of BRI1 and BAK1, the kinase-inactive mBAK1 (Wang et al. 2008) was used as another substrate phosphorylated by BRI1 or BAK1, in the presence of Mn^{2+} or Mg^{2+} (Figure 2.S1). Again, Mn^{2+} significantly stimulated the transphosphorylation of mBAK1 by BRI1 (Figure 2.S1A) and also by BAK1 (Figure 2.S1B). Therefore, Mn^{2+} was routinely used as the cofactor for all in vitro protein phosphorylation assays.

To identify the sites on 14-3-3ω phosphorylated by BRI1 and/or BAK1, the phospho 14-3-3ω bands were digested with trypsin and phosphopeptides were enriched by IMAC or TiO_2 columns before analysis by MALDI-TOF or LC-MS/MS. These efforts identified nine phosphopeptides (five unambiguous phosphorylation sites) of 14-3-3ω by BRI1, seven phosphopeptides (three unambiguous phosphorylation sites) of 14-3-3ω by BAK1 and thirteen phosphopeptides (five unambiguous phosphorylation sites) of 14-3-3ω by (BRI1+BAK1) together (Table 2.1). Representative tandem mass spectra are provided in Figure 2.S2. Consistent with the earlier observation that (BRI1+BAK1) together quantitatively enhanced the overall phosphorylation of 14-3-3ω (Figure 2.1A), higher peak intensities of phosphopeptides in the mass spectra were observed for samples of 14-3-3ω that were phosphorylated by (BRI1+BAK1) together. As both BRI1 and BAK1 are dual specificity kinases (Oh et al, 2009a and 2010), we also looked for phosphorylation on Tyr residues, but did not obtain positive evidence of Tyr phosphorylation on 14-3-3ω by mass spectrometry or with generic anti-phosphotyrosine antibodies (data not shown).

To confirm the mass spectrometry identifications, four phospho- and sequence- specific antibodies were generated: anti-pT41, anti-pT83, anti-pT94 and anti-pT140. The sequences used to generate these phosphopeptide antibodies are shown in Text 2.S1. The specificity of these custom antibodies was tested by peptide competition (Figure 2.S3), and all four antibodies can be used to infer sequence- and modification- specific information. The custom antibodies were then applied to time-course experiments to study the details of phosphorylation of 14-3-3ω by BRI1, BAK1 or (BRI1+BAK1) together (Figure 2.1B). Pro-Q staining showed that phosphorylation of 14-3-3ω occurred as early as 5 min after the incubation and increased with time. Interestingly, phosphorylation of 14-3-3ω at the Thr-83 site was catalyzed by BRI1 and not BAK1. In contrast, phosphorylation of 14-3-3ω at the Thr-94 site was much higher in the presence of BAK1.

Meanwhile, phosphorylation of 14-3-3ω at the Thr-41 site occurred to a limited extent with either BRI1 or BAK1 alone, but it was the combination (BRI1+BAK1) together that significantly boosted the phosphorylation at the Thr-41 site. Lastly, phosphorylation of 14-3-3ω at the Thr-140 was robust in all assays. The discriminative signals for the four phosphorylation sites (pT41, pT83, pT94 and pT140) confirmed the specificity of the antibodies; moreover, the results revealed the distinct kinase properties of BRI1 alone, BAK1 alone and (BRI1+BAK1) together. The custom antibodies were also used to probe IEF-2DE immunoblots to determine whether the mobility shift of 14-3-3ω in SDS-PAGE was due to the phosphorylation. As shown in Figure 2.1C, the sample of 14-3-3ω phosphorylated by BRI1 was analyzed and multiple spots of phospho 14-3-3ω were detected by the anti-pT140 antibodies. The spots with higher molecular weight (MW) also possessed lower pI – consistent with the phosphorylation. The time-zero (T0) sample without phosphorylation did not cross react with the phospho specific antibodies. The resolution of multiple spots of 14-3-3ω with different MW and pI documents the existence of different phospho forms of 14-3-3ω that were modified by BRI1.

Combining the sites identified by mass spectrometry and custom antibodies, 8 unambiguous in vitro phosphorylation sites of 14-3-3ω were identified. Residues T-41, Ser-120, Thr-140, Thr-151 and Ser-157 of 14-3-3ω are common sites phosphorylated by BRI1 and BAK1 (Table 2.S1). Thr-41, Ser-120, Thr-140 and Thr-151 are also widely shared among other 14-3-3 isoforms in Arabidopsis, whereas residues Thr-83, Thr-94, Ser-157 and Thr-255 are quite distinct for 14-3-3ω (Test 2.S1). At least one basic residue (Arg/Lys) was found adjacent to each phosphorylation sites ranging from -6 to +6 positions, but no specific favorable position was found (Table 2.1). When studied in terms of the 3-dimensional structure of the 14-3-3 protein, the phosphorylation sites are not limited to the flexible loop structure, and some are located on the region of α-helices (Figure 2.2A). Interestingly, a majority of the identified phospho-Ser/Thr sites were located on the outside surface of 14-3-3 protein structure and grouped in three regions, with the –OH groups facing outside of the protein. This directional control of the residues appeared to be specific, because there are other Ser/Thr residues, which were not highlighted, buried inside of the protein structure and these internal Ser/Thr residues were not identified to be phosphorylated. Thus, the directional clustering further demonstrated the specificity of the phosphorylation of 14-3-3ω by BRI1 and BAK1. It is noted that perhaps not all the phosphorylation sites occur simultaneously on one 14-3-3ω protein. As noted in 2DE analysis of in vitro phospho 14-3-3ω, various phospho

forms of 14-3-3ω with different pI and MW were observed (Figure 2.1C), and it is likely that one phospho 14-3-3ω protein may only consist of a few of these phosphorylation sites.

To understand the composition of individual phosphorylation sites to the overall phosphorylation of the 14-3-3ω protein, site directed mutagenesis of 14-3-3ω was performed, where Ser/Thr residues were substituted with Ala. As summarized in Table 2.S2, no single site-directed mutants (SDMs) or C-terminal truncated mutants of 14-3-3ω (T255*, S236* and T215*) were found to significantly reduce the overall phosphorylation. However, when multiple Ser/Thr residues were mutated to Ala, an impact on overall phosphorylation was apparent (Figure 2.2B). In particular, the quadruple mutant (T41A, T83A, T94A, T140A) had almost no phosphorylation on Thr residues catalyzed by BRI1, which suggested that these four sites may include the major Thr phosphorylation sites targeted by BRI1. In contrast, with BAK1 as kinase, the cross reacting with anti-pThr antibodies was still strong for the quadruple mutant (T41A, T83A, T94A, T140A), suggesting that additional major Thr phosphorylation sites of 14-3-3ω targeted by BAK1 may exist. The four Thr residues were also grouped with proximal Ser/Thr residues and mutated to Ala to identify the region that was more important for the initiation of the phosphorylation (Figure 2.2B). We found that the regional SDM of T140 (S109A, S117A, T140A, S157A) contained the least anti-pThr signals, which implied this T140 region (the loop between helix 5 and helix 6) may be important for the onset of BRI1 phosphorylation. It is noted that the major phospho-Ser sites were not identified in our SDM effort, as Pro-Q signals was not completely eliminated in any of the site directed mutants. We did not combine more SDMs on a single protein, as the identification may be confounded with the improper folding of 14-3-3ω.

Binding of 14-3-3ω to BRI1 and BAK1 in relation to the phosphorylation

Because 14-3-3ω binds directly to BRI1 and BAK1 (Oh et al., in submission), we wanted to determine the relationship between 14-3-3ω binding and the phosphorylation. To investigate this, we mutated the 14-3-3ω residues that are known to be important for 14-3-3 interactions with the client proteins (Fu et al., 2000, Aitken, 2006 and Telles, 2009): K53E, R60E, R133E, Y134F and F138V. We first tested the binding of these mutants to BRI1 and BAK1 in BIAcore binding assays. As shown in (Figure 2.S4A and S4B), the K53E, R60E, R133E and Y134F directed mutants did not interact with BRI1 or BAK1. The F138V mutant had a small decrease in binding to BAK1, and no effect on binding to BRI1. Next, we performed kinase assays on these mutants

to determine whether they could be phosphorylated by BRI1 and BAK1. Interestingly, phosphorylation of the R60E and R133E mutants was almost eliminated, and decreased phosphorylation was observed for the K53E and Y134F mutants, and there was no reduction in phosphorylation for the F138V mutant (Figure 2.3A). The mutants with decreased binding to BRI1 and BAK1 generally had reduced phosphorylation as well, although the correlation was not linear (Figure 2.3B). Residue of 14-3-3ζ Ser-58 (equivalent to 14-3-3ω Ser-62) is known to be important for 14-3-3 dimerization (Woodcock et al., 2003). The S62A mutant of 14-3-3ω had significant reduction in its binding to BRI1 and BAK1 and less phosphorylation was also observed (Figure 2.S5). However, the residue Ser-62 was identified not to be the phosphorylation site targeted by BRI1 or BAK1, using animal anti-pS58 antibodies (data not shown). Thus, the loss of phosphorylation of mutant S62A was likely due to the reduction in its binding. It is noted that the quadruple mutant (T41A, T83A, T94A, T140A) had normal binding to BRI1 and BAK1 (Figure 2.S4A and 2.S4B), and the reduction in phosphorylation of quadruple mutants was not due to less binding, but the elimination of Thr phosphorylation sites.

To further test the notion that binding of 14-3-3ω enhances its phosphorylation, the effects of Mn^{2+} concentration was examined in the binding and phosphorylation assays. First, we observed that the presence of minimolar level of divalent cation (such as Mn^{2+}) is essential for the occurrence of binding and phosphorylation. Second, the interactions of 14-3-3ω with BRI1 or BAK1 increased substantially at the presence of 5mM Mn^{2+}, which was also the concentration when phosphorylation of 14-3-3ω by BRI1 and/or BAK1 was evident (Figure 2.S6). The results support the hypothesis that binding promotes the phosphorylation. As noted earlier, both BRI1 and BAK1 preferred Mn^{2+} over Mg^{2+} to phosphorylate 14-3-3ω. Hence, we further compared the interactions of 14-3-3ω with BRI1 and BAK1 in the presence of Mn^{2+} or Mg^{2+} in BIAcore binding assays (Figure 2.3C). With both BRI1 and BAK1, higher association rate (Ka) and greater maximum binding (Rmax) to immobilized 14-3-3ω was observed in the presence of Mn^{2+} over Mg^{2+}. Thus, Mn^{2+} increased the binding of 14-3-3ω to both receptor kinases. To confirm these results, the ligand and analyte were switched and bead co-immunoprecipitation assays were performed. Equal amounts of BRI1 (or BAK1) were immobilized to the beads as the ligand and equal amounts of 14-3-3ω were added in solution as the analyte (Figure 2.3D). Again, more 14-3-3ω was co-immunoprecipitated with BRI1 (or BAK1) in the presence of Mn^{2+} compared to Mg^{2+}. Therefore, both binding assays confirmed that 14-3-3ω had greater binding to BRI1 and

BAK1 with Mn^{2+}, which may partially contribute to the higher degree of 14-3-3ω phosphorylation by BRI1 and BAK1 in the presence of Mn^{2+} over Mg^{2+}.

Our next question was whether the phosphorylation of 14-3-3ω protein would affect its binding to the receptor kinase. To test this, 14-3-3ω protein was first phosphorylated by the BRI1 in vitro, and the phosphorylation status of the 14-3-3ω co-immunoprecipitated with BRI1 was compared with that in the supernatant (unbound) fraction. Each fraction was adjusted to equal volumes so that immunoblot signals could be directly compared. The R60E mutant was used as the control for less binding and less phosphorylation. As shown in Figure 2.4, the phospho- and sequence- specific antibodies anti-pT83 and anti-pT140 only cross reacted with 14-3-3ω proteins in the immunoprecipitation fraction, suggesting the majority of the phospho 14-3-3ω was bound to BRI1. In similar experiments, the 14-3-3ω protein in each fraction was digested with trypsin and the peptides were analyzed by LC-MS/MS following phosphopeptide enrichment. Consistent with the results from immunoblotting, the phosphopeptides were only identified in the BRI1-immunoprecipitation fraction, and not from the supernatant fraction (data not shown). Specifically, we identified phosphopeptides containing the Thr-83, Ser-120, Thr-151 and Ser-157 phosphorylation sites, which represent a subset of the phosphorylation sites shown in Table 2.1. Thus, phospho 14-3-3ω appeared to have enhanced binding to BRI1. About 20% of the total 14-3-3ω interacted with BRI1 independent of in vitro phosphorylation (minus ATP treatment), whereas after the phosphorylation, about 40% of the total 14-3-3ω was found to be co-immunoprecipitated with BRI1 (Figure 2.4). Therefore, our data indicated that phosphorylation of 14-3-3ω enhanced its binding to BRI1. However, it is noted that phosphorylation of 14-3-3ω by BRI1 and BAK1 does not absolutely require binding, as indicated by the behaviors of the K53E and Y134F mutants.

Phosphorylation of 14-3-3ω in vivo in response to BL treatment

To test whether the phosphorylation of 14-3-3ω also occurs in vivo in Arabidopsis, we compared the phosphorylation of soluble 14-3-3ω and microsomal membrane associated 14-3-3ω, using the phospho- and sequence- specific antibodies (anti-pT41, anti-pT83, anti-pT94 and anti-pT140). The microsomal 14-3-3ω had much higher apparent phosphorylation on all four sites compared to the soluble fraction (Figure 2.5A). The corresponding 29KDa band in the microsomal fraction was also digested with trypsin and confirmed the presence of 14-3-3ω

protein (data not shown). The microsomal membrane associated 14-3-3ω was further analyzed by 2-DE followed by immunoblotting (Figure 2.5B). We identified the 14-3-3ω spots that also cross reacted with anti-pT94 antibodies and confirmed the phosphorylation of 14-3-3ω in vivo. The anti-1433ω antibodies also cross reacted with another 14-3-3 isoform 14-3-3φ, and the protein spot of 14-3-3φ was distinguished from 14-3-3ω by MW. In addition, the anti-14-3-3ω antibodies also weakly picked up another protein spot right next to 14-3-3ω with slightly lower MW and higher pI. The protein spot was confirmed to be a 14-3-3 protein by anti-loop8 antibodies, which react to a conserved sequence in the 14-3-3 cation binding loop (Athwal and Huber, 2002). After evaluation of the MW and pI of this 14-3-3 spot, we postulated it was a truncated form of 14-3-3ω and part of the C-terminal of this form may have been cleaved off, so it only weakly cross reacted to anti-1433ω antibodies. Meantime, this truncated form was also detected by anti-pT94 antibodies, but much less phosphorylation was observed. To test whether the C-terminal truncated 14-3-3ω was functional, we tested the binding of BRI1 (or BAK1) to the C-terminal truncation mutants (T255* and S236*), which likely covered the truncated region of the Arabidopsis 14-3-3ω truncated form. Interestingly, we observed both truncation mutants had improved binding to BRI1 and BAK1. In particular, S236* had about twice increase of maximum binding, compared to the wildtype 14-3-3ω (Figure 2.S7). Therefore, the occurrence of 14-3-3ω C-terminal truncated form in Arabidopsis was plausible.

To test whether the microsomal phospho 14-3-3ω contained the one that bound to BRI1 in vivo, 14-3-3ω was co-immunoprecipitated with BRI1 from the transgenic Arabidopsis that expressed BRI1-Flag (Wang et al., 2005b). We confirmed that 14-3-3ω interacted with BRI1 in vivo, as indicated by cross reaction with anti-1433ω antibodies. The interaction was specific, in reference to the wild-type WS-2 control. We further examined the phosphorylation of 14-3-3ω band using the phospho- and sequence- specific antibodies. We only observed signals from anti-pT94 and anti-pT140 antibodies (Figure 2.5C) and not from anti-pT41 or anti-pT83 antibodies (data not shown). Hence, the 14-3-3ω that was associated with BRI1-Flag complex was phosphorylated on Thr-94 and Thr-140 in vivo.

We applied the similar approach to examine the phosphorylation of 14-3-3ω bound to BAK1. We were able to confirm the interaction of 14-3-3ω with BAK1 in vivo. Moreover, the co-immunoprecipitated 14-3-3ω also cross reacted with anti-pT83 and anti-pT94 antibodies (Figure

2.5D), while not anti-pT41 or anti-pT140 antibodies. The results indicated that the14-3-3ω that interacted with BAK1-Flag complex was phosphorylated on Thr-83 and Thr-94 in vivo.

As the 14-3-3ω that co-immunoprecipitated with BRI1 (or BAK1) was phosphorylated in vivo, we hypothesized that phosphorylation of these sites may change in relation to the kinase activity of BRI1 (or BAK1). To test this, transgenic Arabidopsis seedlings expressing BRI1-Flag were treated with epi-brassinolide (epi-BL) for 1.5 h, 6 h and 24 h, and solvent ethanol for 1.5 h as the treatment control. 14-3-3ω was co-immunoprecipitated with BRI1-Flag and the phosphorylation of 14-3-3ω in different time points of BL treatment was examined. As shown in Figure 2.6, the anti-Flag antibodies confirmed that BRI1-Flag was immunoprecipitated from samples of different treatments. Both 14-3-3ω and BAK1 were successfully co-immunoprecipitated with the BRI1-Flag complex, as indicated by cross reaction with anti-BAK1 and anti-1433ω antibodies. Anti-pThr immunoblot indicated higher phosphorylation of BRI1 and BAK1 on Thr residues in samples purified after 1.5 h and 6 h exogenous BL treatment, indicating activation of BRI1 and BAK1 (Wang et al., 2008). The amount of 14-3-3ω that associated with BRI1 complex increased after BL treatment of 1.5 h, but decreased thereafter. The phosphorylation of 14-3-3ω at the Thr-94 site appeared to be transient following BL activation, as only the time point of 1.5 h had the strongest phosphorylation signals. In contrast, the phosphorylation of 14-3-3ω at the Thr-140 site was significantly enhanced by BL treatment of 1.5 h and 6 h and slightly decreased at the treatment of 24 h. However, the anti-pT140 antibodies cross reacted with a protein band at the size that matched the C-terminal of 14-3-3ω. Overall, the data suggest the binding and phosphorylation of 14-3-3ω were responded to BL activation.

DISCUSSIONS

We reported that the cytoplasmic domains (CDs) of integral membrane kinases BRI1 and BAK1 can directly interact and phosphorylate 14-3-3ω in vitro. Multiple residues of 14-3-3ω including Thr-41, Thr-83, Thr-94, Ser-120, Thr-140, Thr-151, Ser-157, Thr-255 were identified as in vitro phosphorylation sites by BRI1 and/or BAK1 (Table 2.1). None of these phosphorylation sites were identified in previous phosphoproteomics analyses of Arabidopsis (Sugiyama et al., 2008; Reiland et al., 2009). Using the sequence- and modification- specific antibodies, four of the phosphorylation sites of 14-3-3ω (Thr-41, Thr-83, Thr-94 and Thr-140) were established in planta. The phosphorylation of these four sites was more apparent in the microsomal membrane associated 14-3-3ω as opposed to the soluble fraction, suggesting that membrane-associated kinases may play a dominant role in the phosphorylation of 14-3-3s in Arabidopsis. Furthermore, the interactions of sphingosine, a primary component of membrane lipids, may also enhance the phosphorylation of 14-3-3s by membrane kinases in vivo, as reported in the animal systems (Woodcock et al., 2010). Hence, the combinational effects of membrane kinases and lipid binding in promotion of 14-3-3 phosphorylation may coincide to our observation that microsomal membrane associated 14-3-3ω had greater phosphorylation in Arabidopsis.

Our data showed that 14-3-3ω can be co-immunoprecipitated with BRI1-Flag complex and BAK1-Flag complex in vivo, as reported by Oh et al (in submission). 14-3-3s can also be co-immunoprecipitated with receptor kinase SERK1 complex (Rienties et al. 2005; Karlova et al., 2006). Thus, the binding of 14-3-3s to the receptor kinases may be widespread. Moreover, we demonstrated that the 14-3-3ω co-immunoprecipitated with BRI1-Flag complex was phosphorylated at Thr-94 and Thr-140 residues. The phosphorylation of both sites was responsive to exogenous BL treatment and correlated with the activation of BRI1-BAK1 signaling complex (Wang et al., 2008), indicating the phosphorylation of BRI1-bound 14-3-3ω may directly involve the activity of BRI1 and BAK1. Hence, the binding and phosphorylation of 14-3-3ω may be a part of the intracellular BR signaling in Arabidopsis.

The molecular actions between 14-3-3s and receptor kinases involve two types of events – binding and phosphorylation (Figure 2.7). Our results indicated that the binding of 14-3-3ω to BRI1 and phosphorylation by BRI1 may be two distinct processes, obligated by different protein

domains of BRI1. First, the binding of 14-3-3ω to BRI1 was not transient and the binding KD calculated from the BIAcore instrument was at the nM range, which was much tighter than the pure enzyme-substrate interaction. Second, Oh et al. (in submission) identified that the juxtamembrane domain (i.e., not kinase domain) of BRI1 was important for the interaction with the 14-3-3ω molecule. Third, the binding mutants (K53E and Y134F) lacked binding but still can be robustly phosphorylated by BRI1. Thus, the binding and phosphorylation can occur independently. On the other hand, we also documented the inter-relation between the binding of 14-3-3ω to BRI1 and phosphorylation by BRI1. Firstly, the 14-3-3ω mutants with higher binding to BRI1 was generally correlated with higher phosphorylation by BRI1 (Figure 2.3C), indicating 14-3-3ω binding to BRI1 enhanced its phosphorylation. Secondly, the majority of in vitro phospho 14-3-3ω modified by BRI1 were found in the BRI1 immunoprecipitation fraction not the supernatant (unbound) fraction, suggesting the phosphorylation of 14-3-3ω by BRI1 promote the binding of 14-3-3ω to BRI1 (Figure 2.4B). Therefore, a positively relation between the binding and phosphorylation was observed.

To our knowledge, this positive relationship between 14-3-3 phosphorylation and its binding is quite different from previous studies in animal system, most of which showed that phosphorylation events such as Ser-58, Ser-184 or Thr-232 on 14-3-3ζ inhibited the binding of 14-3-3s to their client proteins (Fu et al., 2000; Aitken, 2006). We used animal anti-pS58 antibodies and anti-pS/pT-P antibodies confirmed neither equivalent residues of 14-3-3ω Ser-62 nor Ser-190 were the targeted sites by BRI1 or BAK1. Besides, the Thr-232 residue was corresponding to an unphosphorylatable Met-238 residue in 14-3-3ω. Thus, the absence of these three phosphorylation sites on 14-3-3ω was consistent with the observation that phosphorylation of 14-3-3ω by BRI1 did not inhibit the binding of BRI1. Interestingly, most phosphorylation sites of 14-3-3ω by BRI1 and/or BAK1 were not conserved in human 14-3-3 isoforms. In particular, the phosphorylated residues Thr-83, Ser-157 and Thr-255 were unique for Arabidopsis 14-3-3s (Text 2.S2). Thus, although functionally conserved, 14-3-3s may have evolved certain distinct regulatory mechanism in plant and animal systems.

BRI1 forms homodimers in vivo (Wang et al., 2005a), and the phosphorylation of BRI1-bound 14-3-3ω can be the results of inter- or intra- molecule phosphorylation. We documented phosphorylation of 14-3-3ω by BRI1 or BAK1 strictly required the presence of divalent cation (such as Mn^{2+}) (Figure 2.S5). Moreover, cation Mn^{2+} promoted higher phosphorylation of 14-3-

3ω over Mg^{2+} (Figure 2.1). The preference of Mn^{2+} over Mg^{2+} for protein phosphorylation was also reported in some other RLKs in Arabidopsis, such as HEASA/RLK5 (Horn and Walker, 1994) and TMLK1 (Schaller and Bleecker, 1993). Considering the binding and phosphorylation of RLKs are positively related, and Mn^{2+} enhanced the binding of 14-3-3ω to BRI1 and BAK1 (Figure 2.3), we hypothesized the preference of Mn^{2+} over Mg^{2+} in substrate phosphorylation for BRI1 and BAK1 may be partially attributed to the enhanced interactions of substrates to RLKs under Mn^{2+}. Interestingly, Oh et al. (2000) observed the opposite preference of Mg^{2+}over Mn^{2+} for the phosphorylation of SP11 peptides by BRI1, which may hint the different characteristics of inter- and intra- molecule phosphorylation for BRI1. The phosphorylation motif for BRI1 kinase has not been reported before, so we summarized the current available information of BRI1 phosphorylation substrates (Table 2.S3) and performed a phosphorylation motif analysis (Crooks et al., 2004). As mentioned earlier, at least one basic residue (Arg/Lys) was located within the -6 to +6 position for each BRI1 phosphorylation site. Moreover, residue Ala was a more frequent residue at the -4 and +5 position (Figure 2.S8). Interestingly, BAK1 kinase also had similar preference for Ala residue at the -4 and +5 position (Table 2.S4). Furthermore, we propose the tertiary protein structure of the substrates may also play a role in the determination of the phosphorylation specificity of BRI1 and BAK1. As in the case of 14-3-3ω, most of the phosphorylated Ser/Thr by BRI1 and BAK1 are located on the outskirt of the protein structure, directly accessible by the receptor kinases. The roles of 3-DE structural information in prediction of the phosphorylation sites have been increasingly recognized (Jiménez et al. 2007; Durek et al., 2009). In addition, we also mentioned earlier that the phosphorylation specificity of BRI1 (or BAK1) was also partially achieved by substrate interactions to the juxtamembrane domain of the receptor kinase (Figure 2.7), and higher substrate binding would enhance the substrate phosphorylation.

Our 2-DE analysis of microsomal membrane associated 14-3-3s identified multiple forms of 14-3-3s besides 14-3-3ω. One of these members was likely a C-terminal truncated 14-3-3ω (Figure 2.5). In barley, a similar C-terminal truncated variant for 14-3-3A was reported and it was present specifically during the embryo germination of barley (Testerink et al., 2002). The C-terminal of 14-3-3 protein is considered as an autoinhibitor for the binding to their client proteins and the truncation of the C-terminal has been reported to enhance the binding of 14-3-3s to nitrate reductase and H^+-ATPase (Shen et al., 2003; Visconti et al., 2008). Our data also

indicated that truncated forms of 14-3-3ω had greater binding to both BRI1 and BAK1 proteins in vitro (Figure 2.S7). Therefore, it appeared that the interactions of 14-3-3s with BRI1 and BAK1 can also be regulated through the cleavage of the autoinhibitory C-terminal of 14-3-3 proteins. The exact mechanism of the 14-3-3 C-terminal truncation remained to be studied in future.

To summarize, 14-3-3ω in Arabidopsis is phosphorylated at least at four sites (Thr-41, Thr-83, Thr-94 and Thr-140) and the phosphorylation of 14-3-3ω likely plays a role in BR signal transduction in plants. Binding and phosphorylation of 14-3-3s emerge as two inter-related molecular mechanism in regulation of receptor kinases.

FIGURES

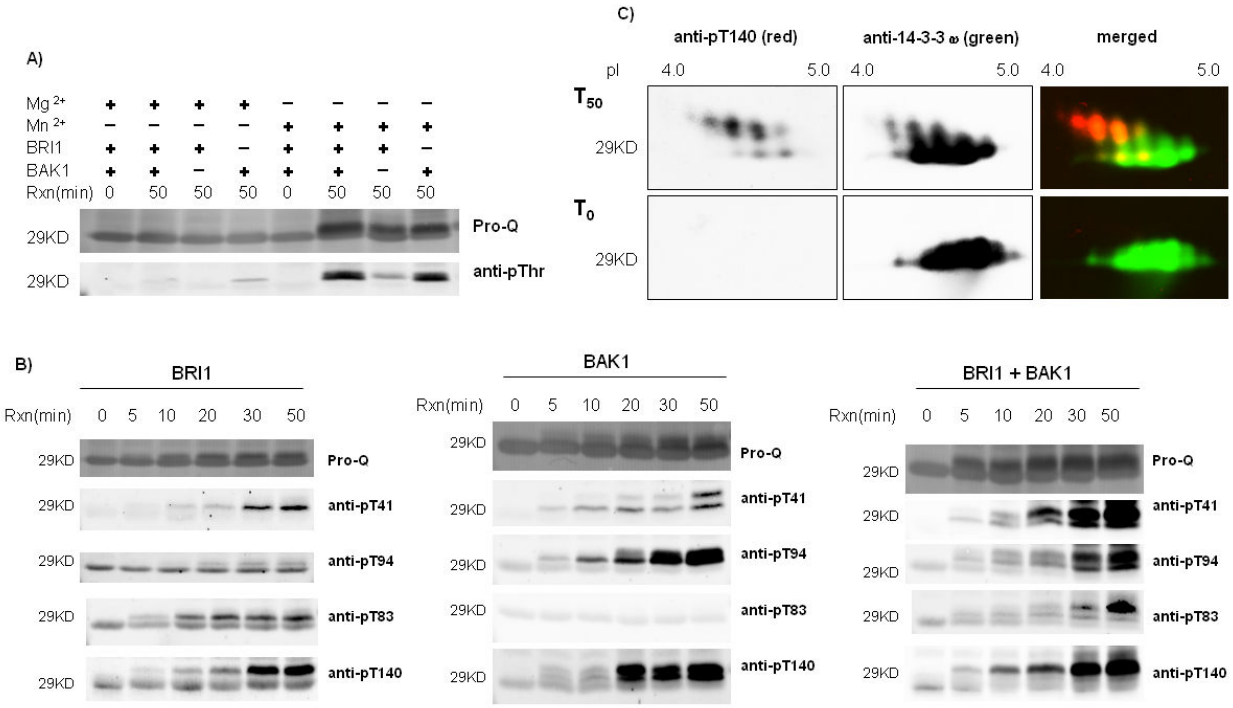


Figure 2.1 14-3-3ω was phosphorylated by both BRI1 and BAK1 in vitro.
A) The phosphorylation reaction required Mn^{2+} and caused a mobility shift of 14-3-3ω. Mn^{2+} created significantly higher level of transphosphorylation to 14-3-3ω than Mg^{2+}, as indicated by Pro-Q and anti-pThr antibody. "+" addition, "-" without addition, "Rxn" reaction time. B) Characterization of in vitro phosphorylation of 14-3-3ω by BRI1 alone, BAK1 alone, (BRI1+BAK1) together with phospho- and sequence- specific antibodies. Time course experiments showed the phosphorylation occurred as early as 5 min. Phosphorylation of 14-3-3ω at the Thr-83 was only catalyzed by BRI1. Phosphorylation of 14-3-3ω at the Thr-94 was much higher in the presence of BAK1. Phosphorylation of 14-3-3ω at the Thr-41 was dramatically bolstered with (BRI1+BAK1) together. Phosphorylation of 14-3-3ω at the Thr-140 was robust in all assays. The distinct phosphorylation patterns demonstrated the specificity of the antibodies and the unique kinases properties of BRI1 alone, BAK1 alone, and BRI1 and BAK1 together. C) The phospho 14-3-3ω by BRI1 is further analyzed by IEF-2D immunoblotting and shown to have migration shifts in pI and molecular weight (MW). The spots of greater mass were moved to acidic pI, which are consistent with increased phosphorylation.

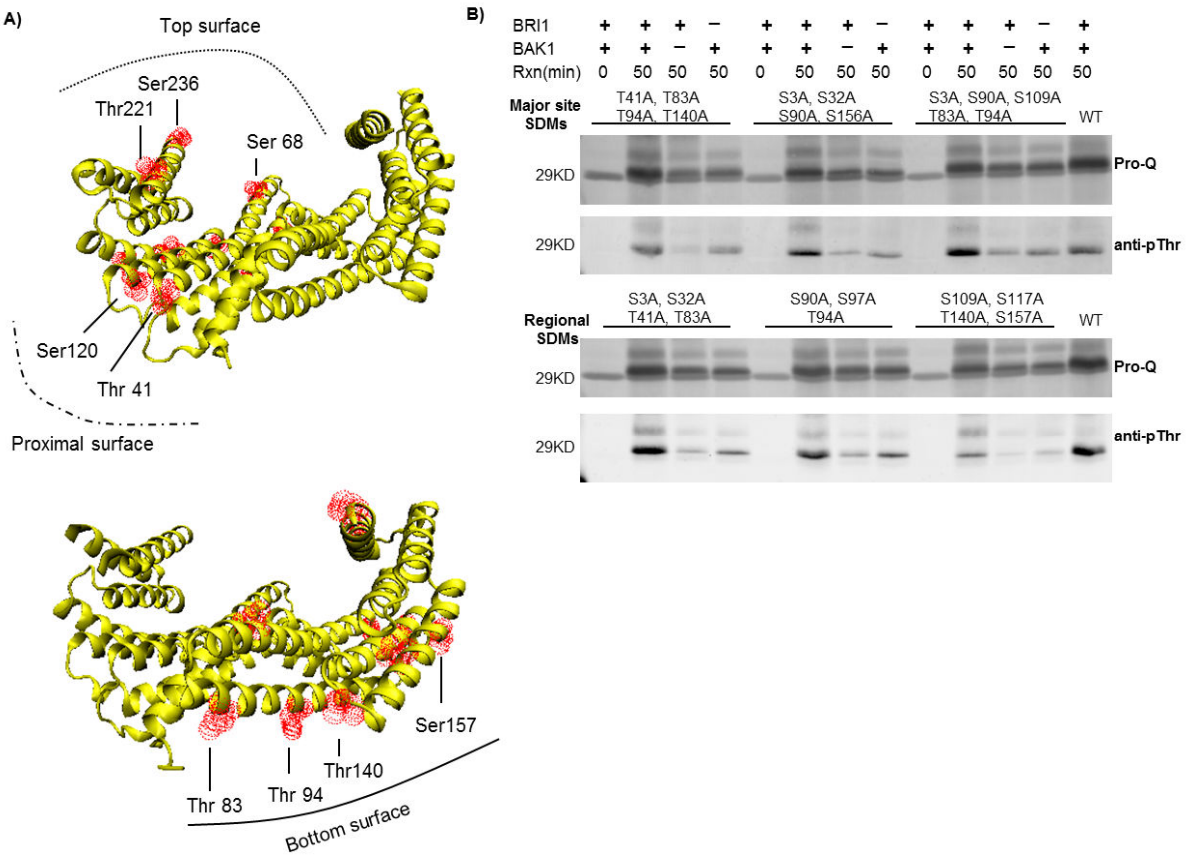


Figure 2.2 The localization of identified phosphorylation sites on 14-3-3ω and the effects of the mutagenesis on these sites.

A) Majority of the identified phosphorylation sites were located on the outside of the 14-3-3 structural surface, meaning that they are accessible to direct kinase interaction. Lacking the structure information of 14-3-3 isoforms in Arabidopsis, the structure thread of tobacco 14-3-3 homolog was adapted and analyzed in VMD (PDB:2O98, Ottmann et al. 2007b; Humphrey et al., 1996). B) Site directed mutagenesis (SDM) of multiple Ser/Thr to Ala residues on 14-3-3ω had decreased level of phosphorylation, compared to the wildtype (WT). However, the decrease was not complete, and the major phosphorylation site(s) may not be identified.

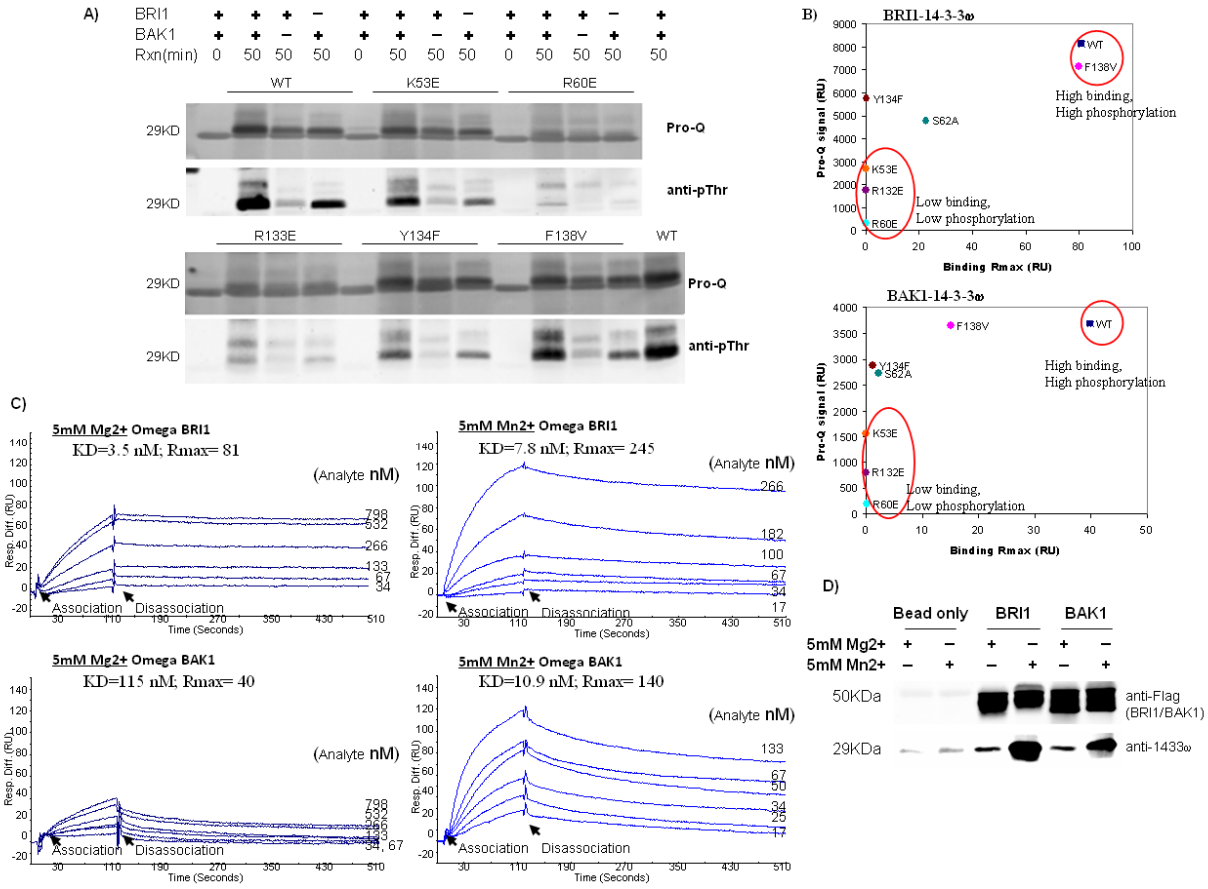


Figure 2.3 Binding mutants of 14-3-3ω had decreased level of phosphorylation and the preference of Mn^{2+} in phosphorylation may be due to Mn^{2+} increased the binding of 14-3-3ω to BRI1 and BAK1. A) Mutation of 14-3-3ω residues that are essential in binding resulted in less phosphorylation by BRI1 and BAK1. R60E and R133E showed dramatic decrease in phosphorylation, while K53E and Y134F showed small decrease in phosphorylation. The results indicated the binding of 14-3-3ω to BRI1 and BAK1 may be important for the phosphorylation on 14-3-3ω. B) Plot of maximum binding (Rmax) and Pro-Q phosphorylation signal of BRI1-1433ω and BAK1-1433ω. It revealed the correlation of binding and phosphorylation, but the relationship was not linear. C) The real-time interactions of 1433ω-BRI1 and 1433ω-BAK1 were studied in BIAcore 3000. His-1433ω was immobilized as the ligand, and series concentration of BRI1 or BAK1 were injected as the analyte. Mn^{2+} enhanced the overall binding of 14-3-3ω to BRI1 and BAK1 with higher association rate (Ka) and greater maximum binding (Rmax). The increase of Mn^{2+} in binding may be related to earlier observation that Mn^{2+} enhanced the phosphorylation. D) In vitro bead pull down assay of 14-3-3ω by Flag-BRI1 or Flag-BAK1 confirmed the BIAcore data that Mn^{2+} elevated the 14-3-3ω binding to BRI1 and BAK1.

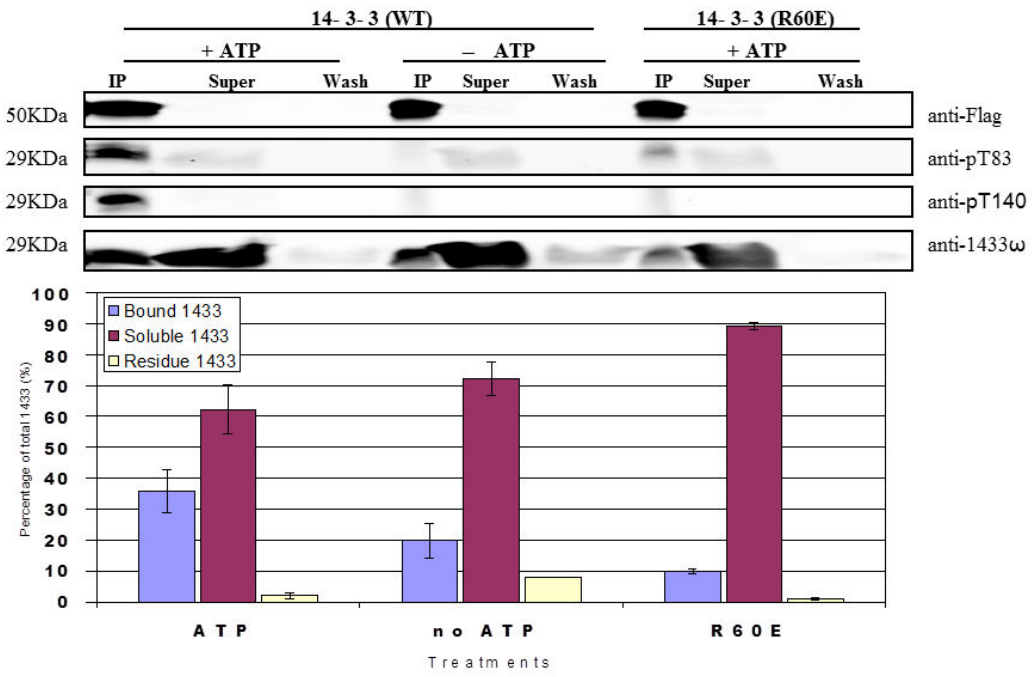


Figure 2.4 The phosphorylation of 14-3-3ω by BRI1 enhanced its binding to BRI1.

In vitro co-immunoprecipitating of phospho 14-3-3ω by BRI1. Reaction without ATP was used to compare the effect of phosphorylation. Reaction of R60E demonstrated less binding was accompanied with less phosphorylation. IP: the fraction of immunoprecipitation with BRI1; Super, the fraction of supernatant after the immunoprecipitation; Wash, the fraction of solution after the first washing. The whole supernant and wash fraction were dried down and resuspended in SDS sample buffer in equal amount as immunoprecipitation fraction, but the resultant concentrated salts and detergents expanded the band size of both fractions. Nevertheless, the phospho signals of anti-pT83 and anti-pT140 were mostly found in the IP fraction, despite that more 14-3-3ω proteins were found in the supernatant fraction. It is likely that most of the phospho14-3-3ω proteins were associated with BRI1. The quantitative comparison of the 14-3-3ω proteins in each fraction was shown in the diagram. Under the experimental conditions, about 20% of 14-3-3ω can be co-immunoprecipitated with BRI1, independent of the phosphorylation. The ratio of 14-3-3ω binding to BRI1 increased to about 40% after the phosphorylation. The results indicated that the phosphorylation of 14-3-3ω by BRI1 enhanced its binding to BRI1.

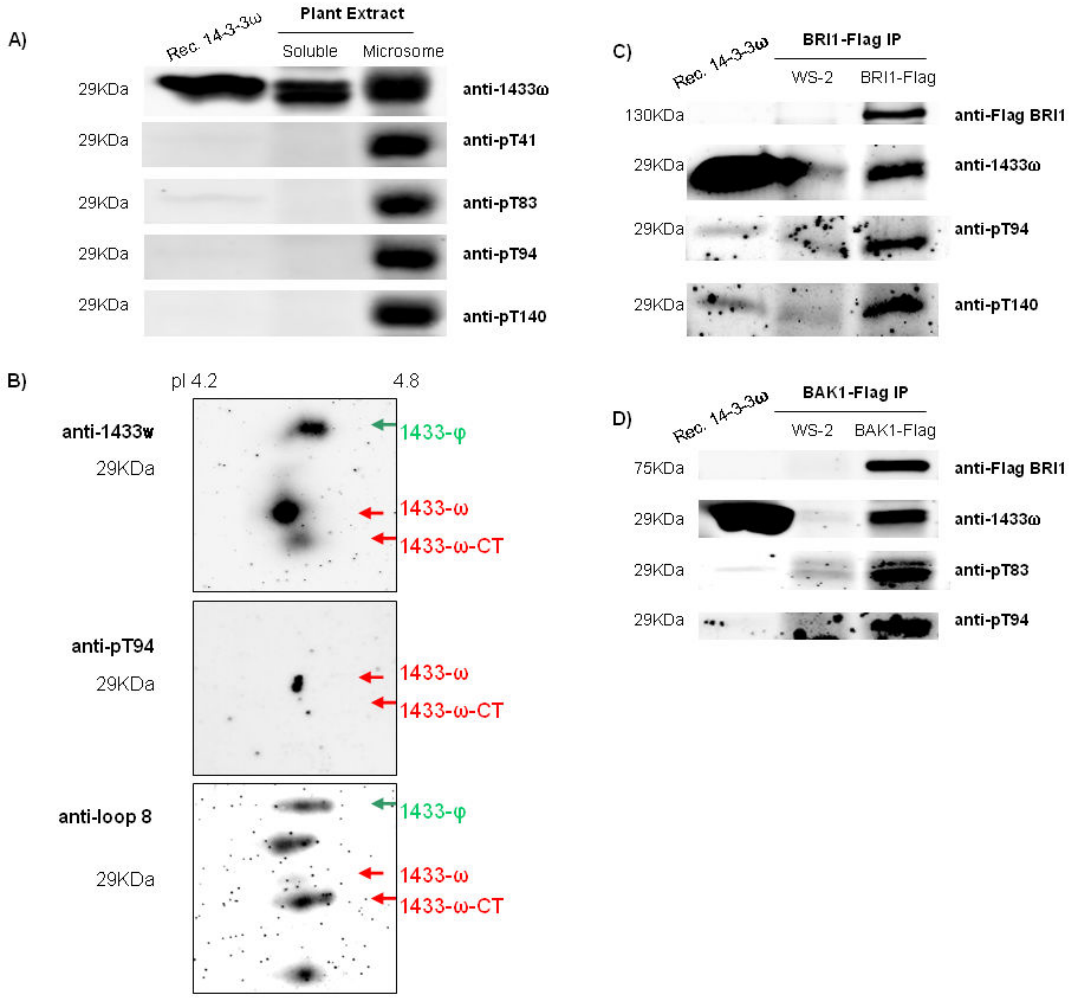


Figure 2.5 Phosphorylation of 14-3-3ω in Arabidopsis. A) Higher phosphorylation on Thr-41, Thr-83, Thr-94 and Thr-140 residues of 14-3-3ω was observed in the 14-3-3ω that associated with the microsomal membranes. Recombinant 14-3-3ω was loaded as a molecular weight (MW) reference, and it also indicated the phosphorylation specificity of the antibodies. B) IEF-2DE immunoblots of anti-1433ω and anti-pT94 confirmed 14-3-3ω was phosphorylated in vivo. Anti-1433ω antibodies also reacted to 14-3-3φ, which was distinguished from 14-3-3ω by MW. Anti-1433ω antibodies may also have reacted to a truncated form of 14-3-3ω (1433-ω-CT), and this form contained much less phosphorylation on the Thr-94 site. Anti-loop8 antibodies further confirmed that there were multiple forms of 14-3-3 proteins associated with the microsomal membranes in Arabidopsis. C) The phosphorylation on Thr-94 and Thr-140 residues was observed in the 14-3-3ω that co-immunoprecipitated with BRI1 from the transgenic plants that expressed BRI1-Flag. WS-2 was processed simultaneously and the unspecific interactions were not observed. The phosphorylation of Thr-41 and Thr-83 sites was not identified in the same experiment. D) The phosphorylation of Thr-83 and Thr-94 residues was observed in the 14-3-3ω that co-immunoprecipitated with BAK1-Flag from the transgenic plants that expressed BAK1-Flag. WS-2 showed the co-immunoprecipitation was specific. The phosphorylation of Thr-41 and Thr-140 sites was not identified in the same experiment.

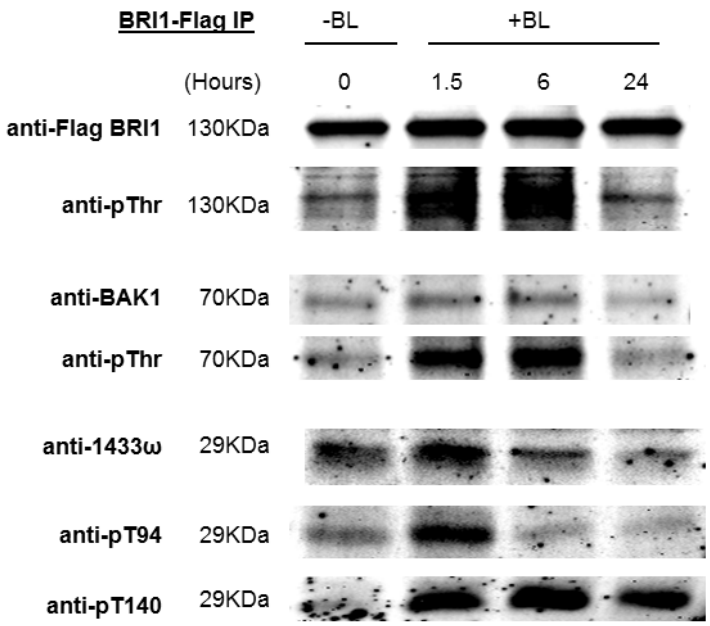


Figure 2.6 Phosphorylation of 14-3-3ω in response to BL treatment.

BRI1-Flag transgenic seedlings (12 d-old) were treated with epi-BL for 1.5 h, 6 h and 24 h or with solvent ethanol for 1.5 h as the control. BRI1-Flag was immunoprecipitated from the microsomal extract with anti-Flag beads. Both BAK1 and 14-3-3ω were co-immunoprecipitated in the BRI1-Flag complex. The protein level and the phosphorylation status of the 14-3-3ω were compared across the treatments.

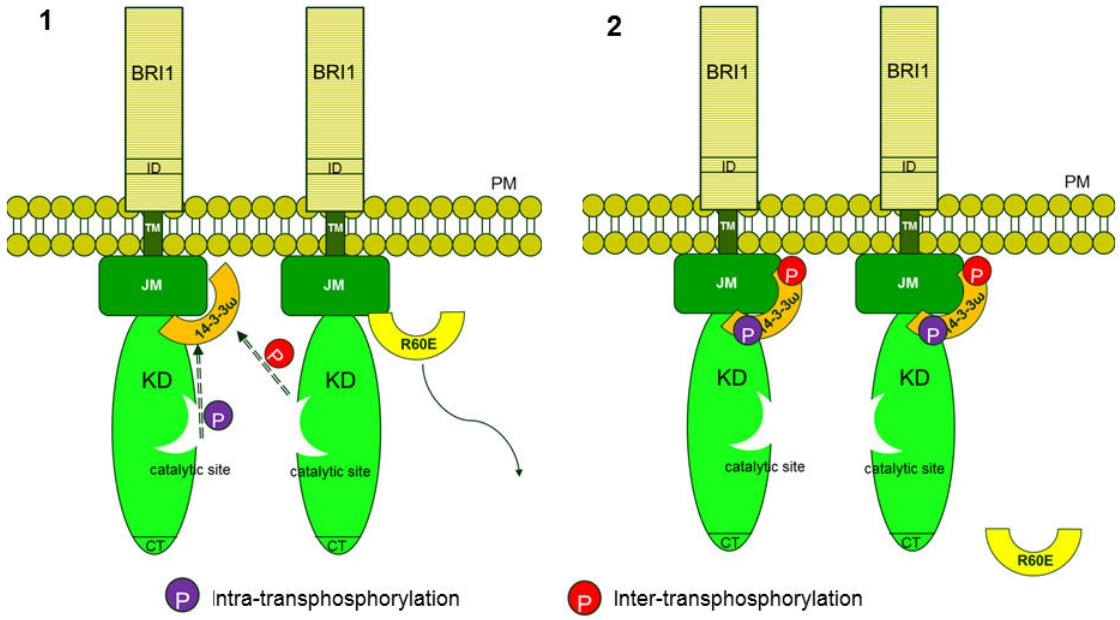


Figure 2.7 Simplified model of binding and phosphorylation of 14-3-3ω by BRI1.
PM, plasma membrane; ID, island domain TM, transmembrane domain; JM, jaxtamembrane domain; KD, kinase domain; CT, C-terminal domain. BRI1 forms homodimers in vivo (Wang et al., 2005a). 14-3-3ω binds to the jaxtamembrane domain of BRI1 (Oh et al., in submission). The kinase domain of BRI1 phosphorylates 14-3-3ω by intra/inter- phosphorylation. The phosphorylation of 14-3-3ω enhances the binding to BRI1. 14-3-3ω mutant R60E lacks binding to the juxtamembrane domain of BRI1 and was less phosphorylated by BRI1. The events of binding and phosphorylation of 14-3-3ω by BRI1 is inter-related.

TABLES

Table 2.1 In vitro phosphorylation sites of 14-3-3ω by BRI1 and BAK1

Identification	Peptides	Cal aveMass[a]	MALDI-TOF			Q-TOF		
			BRI1	BAK1	BRI1+ BAK1	BRI1	BAK1	BRI1+ BAK1
pS67 or pS68	(R)IISSIEQK(E)	998.0643	997.49	n/a	n/a	n/a	n/a	n/a
pT83	(R)GNDDHVpTAIR(E)	1178.1472	1178.15	n/a	n/a	1176.3972	n/a	1176.4606
pT151	(R)DAAEHpTLAAYK(S)	1270.2858	1270.55	1270.02	1270.19	n/a	1268.4722	1268.5058
pS220 or pT221	(K)DSTLI(ox)MQLLR(D)	1286.4354	1286.55	n/a	n/a	n/a	n/a	n/a
pT255	(K)EAAAPKPpTEEQQ(-)	1379.3680	1379.46	n/a	1379.55	n/a	n/a	n/a
pT151	(R)KDAAEHpTLAAYK(S)	1398.4609	1398.68	1398.19	1398.52	1396.5082	1396.5478	1396.5838
pT140	(R)YLAEFKpTGQER(K)	1422.4832	1422.76	n/a	1422.70	n/a	n/a	1420.6034
pT41	(K)VSAAVDGDELpTVEER(N)	1670.6741	n/a	n/a	1671.29	n/a	n/a	n/a
pT83	(K)EESRGNDDHVpTAIR(E)	1679.6469	n/a	n/a	1679.56	n/a	n/a	n/a
pS120	(R)LIPAAASGDpSKVFYLK(M)	1760.9769	1760.98	1760.92	1760.68	1758.7024	n/a	n/a
pS157	(K)pSAQDIANAELAPTHPIR(L)	1884.9926	1885.01	1884.77	1884.70	n/a	1882.8010	1882.8494
pT232 or pT235 or pS236	(R)DNLTLWTSDMQDDAADEIK(E)	2262.3184	n/a	2261.77	2262.06	n/a	n/a	n/a
pT232 or pT235 or pS236	(R)DNLTLWTSD(ox)MQDDAADEIK(E)	2278.3178	n/a	2277.93	2278.02	n/a	n/a	n/a
pT151 and pS157	(K)DAAEHpTLAAYKpSAQDIANAELAPTHPIR(L)	3136.2556	n/a	n/a	3135.23	n/a	n/a	3133.3306
pT151 and pS157	(R)KDAAEHpTLAAYKpSAQDIANAELAPTHPIR(L)	3264.4308	n/a	n/a	3262.89	n/a	n/a	3261.4077

[a] The calculated average theoretical mass, (ox)M oxidized methionine residue
[b] MALDI-TOF average mass. The peaks of phosphopeptides in MALDI-TOF were specific and were compared to the peptide peaks of non-phospho 14-3-3ω digests.
[c]Q-TOF monoisotopic mass. Detail spectra of Q-TOF were presented in Figure 2.S2.

SUPPLEMENTAL FIGURES

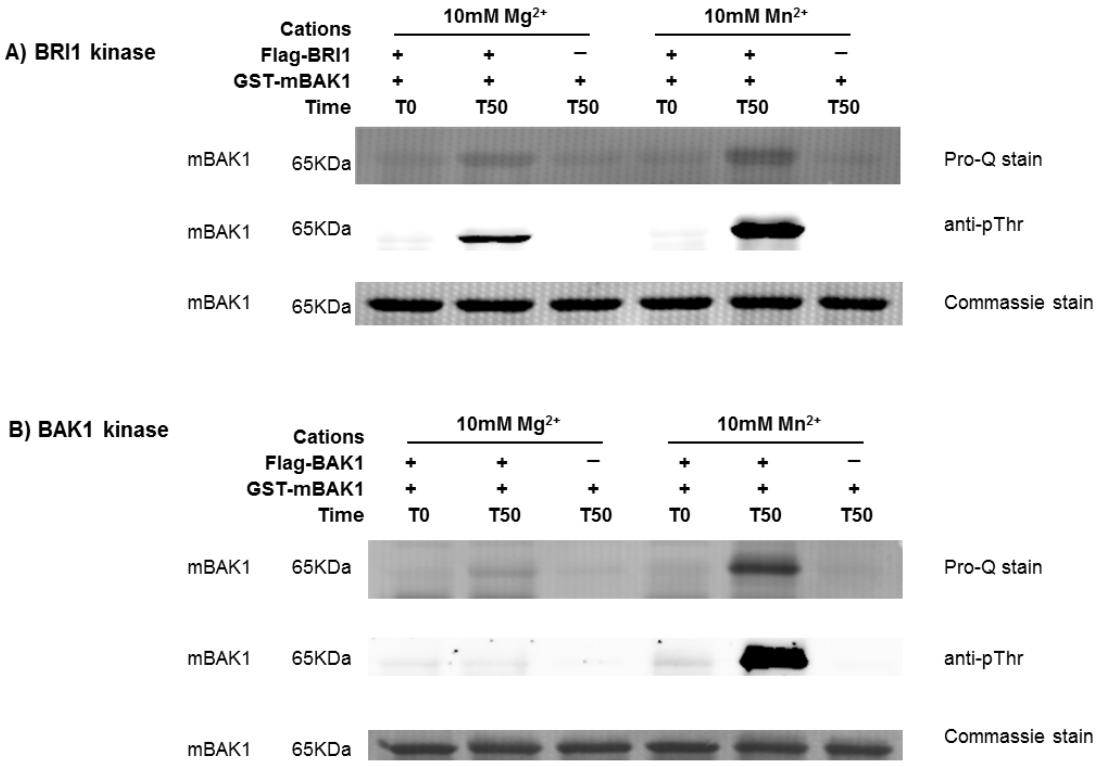
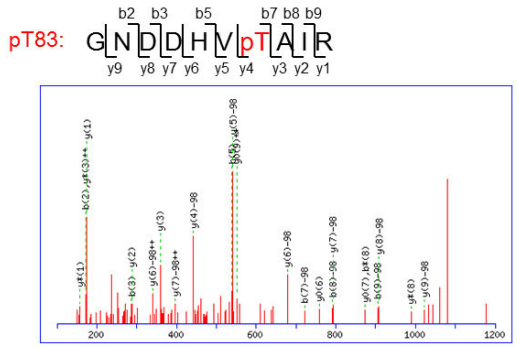
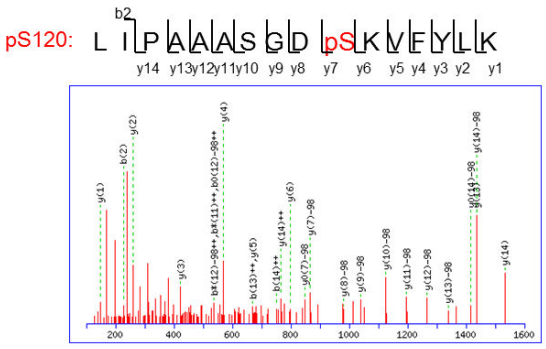


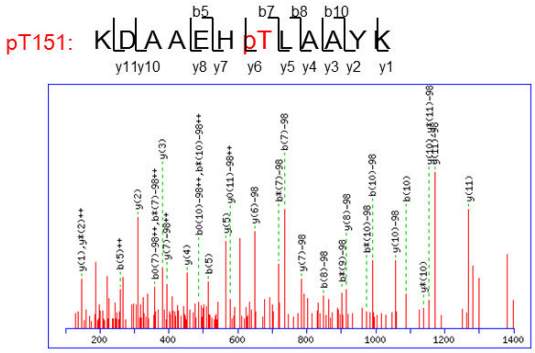
Figure 2.S1 mBAK1 was used as another substrate to demonstrate that Mn^{2+} is a better cofactor over Mg^{2+} for BRI1-mBAK1 transphosphorylation and BAK1-mBAK1 autophosphorylation.



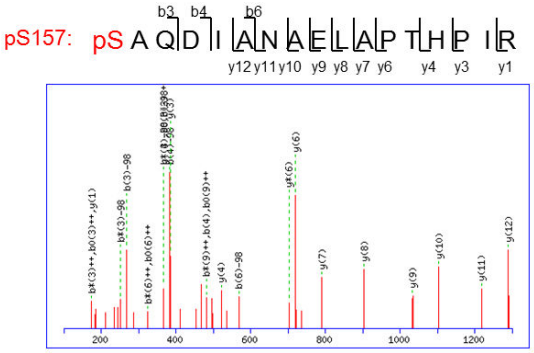
Mr (expt) 1176.3972, Mr(calc)1176.4925, Mascot Score 66, Expect 0.00011



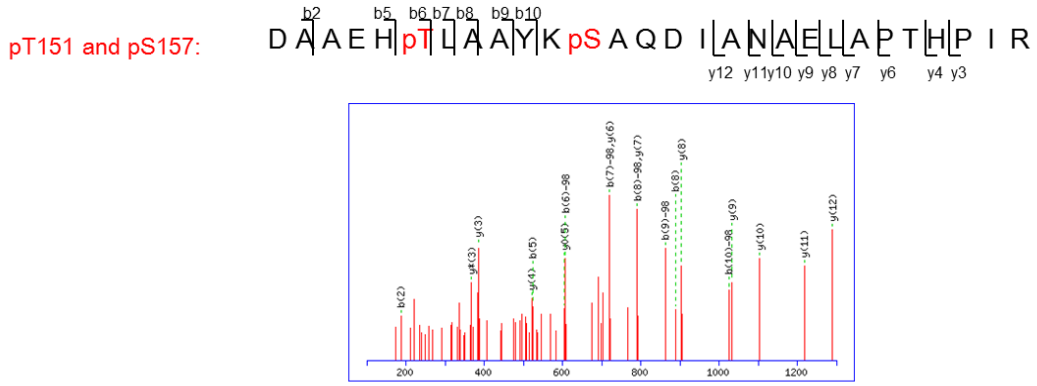
Mr (expt) 1758.7524, Mr(calc) 1758.8957, Mascot Score 87, Expect 3.5e-07



Mr (expt) 1396.5082, Mr(calc) 1396.6387, Mascot Score 80, Expect 4.8e-06



Mr (expt) 1882.8494, Mr(calc) 1882.8938, Mascot Score 82, Expect 3.8e-06



Mr (expt) 3133.3306, Mr(calc) 3133.4275, Mascot Score 80, Expect 1.1e-05

Figure 2.S2 Representative spectra phosphopeptides of 14-3-3ω phosphorylated by BRI1 and/or BAK1 identified in Q-TOF. The mass spectra were searched in Mascot server. The peptide scores and the confidence of the identification are indicated below the spectra. The matched b- or y- ions are indicated in the sequences.

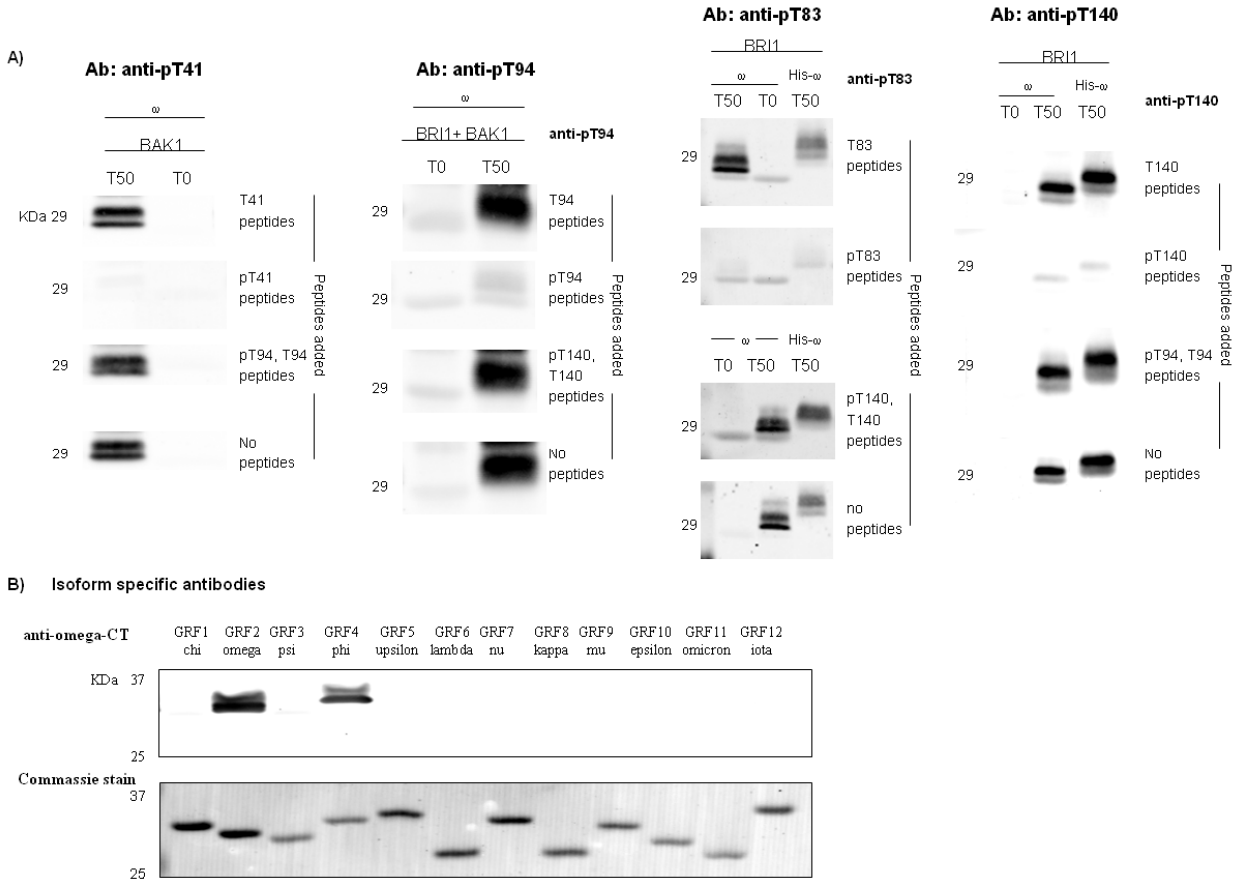


Figure 2.S3 A) Peptide competition showed the specificity of custom phospho- and site- specific antibodies: anti-pT41, anti-pT83, anti-pT94 and anti-pT140. All four antibodies are phosphorylation and site specific. B) Examination of isoform specific antibodies of anti-1433ω. The anti-1433ω cross reacted with the recombinant proteins of 14-3-3ω and 14-3-3φ out of twelve 14-3-3 isoforms tested. As proteins of 14-3-3ω and 14-3-3φ can be distinguished based on the molecular weight in SDS-PAGE, the antibody anti-1433ω can be applied in an isoform specific manner.

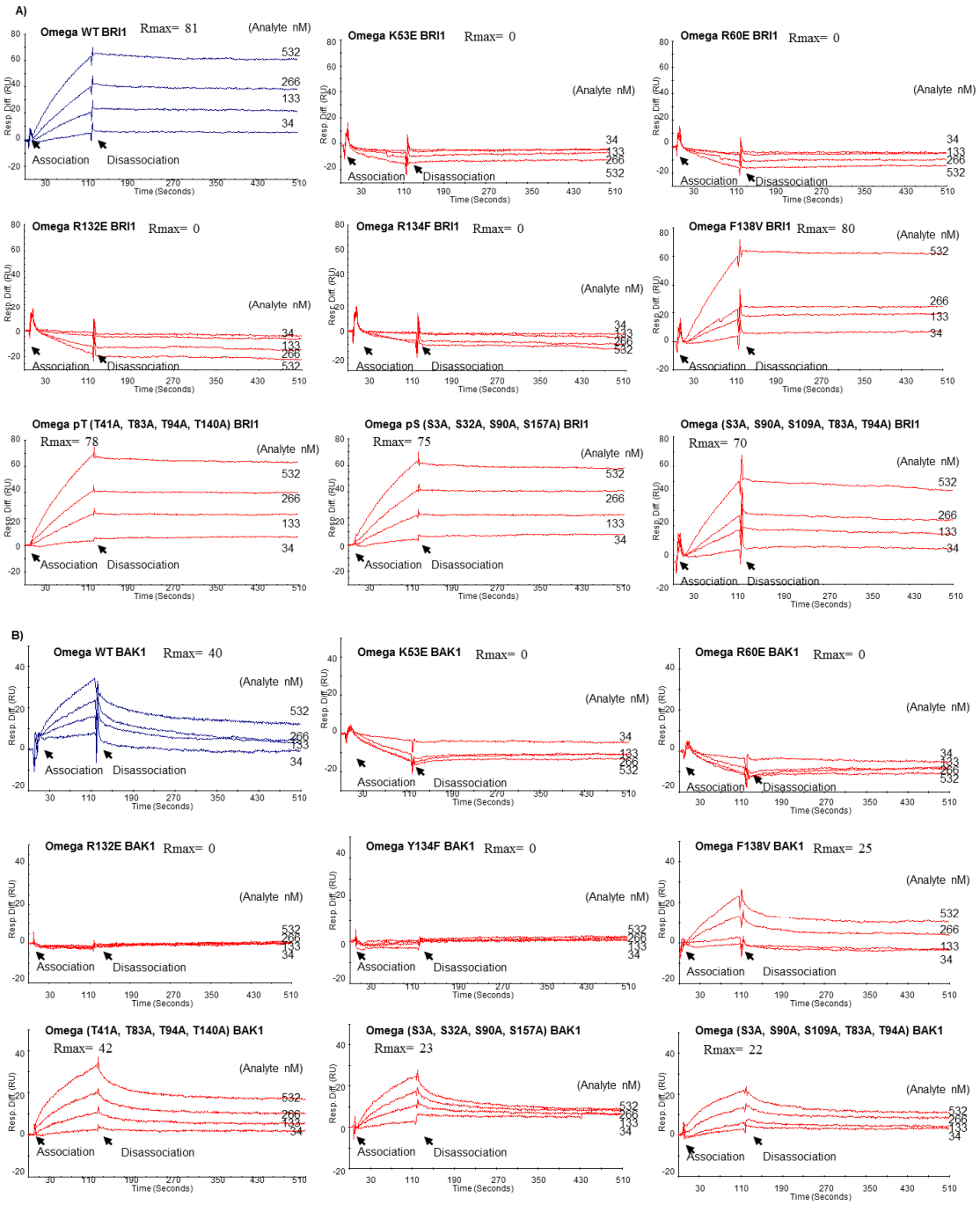


Figure 2.S4 A) Interactions of 14-3-3ω binding mutants with BRI1 in BIAcore analysis. Under 5mM Mg^{2+}, 14-3-3ω mutants K53E, R60E, R133E and Y134F were unable to bind to BRI1. Mutant F138V and phosphorylation quadruple mutants had no effects in binding to BRI1. B) Interactions of 14-3-3ω binding mutants with BAK1 in BIAcore analysis. The interactions were tested in the presence of 5mM Mg^{2+}. Similar to the results of BRI1 interactions, mutants K53E, R60E, R133E and Y134F were unable bind to BAK1; mutant F138V, (S3A, S32A, S90A, S157A), (S3A, S90A, S109A, T83A, T94A) had small decrease in binding to BAK1. Mutant (T41A, T83A, T94A, T140A) had normal binding to BAK1.

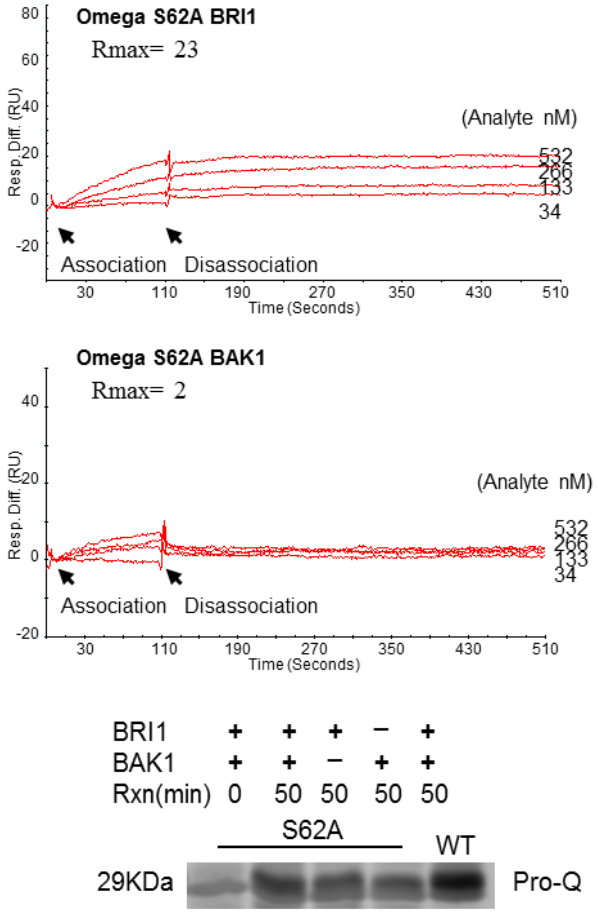


Figure 2.S5 Real-time interaction of 14-3-3ω S62A mutant to BRI1 and BAK1. Mutation of 14-3-3ω S62A significantly compromised the binding to BRI1 and BAK1. Considerable less phosphorylation of S62A was also observed. The results suggest the Ser-62, which is important in 14-3-3ω dimerization, may also modulate the interactions of 14-3-3ω to BRI1 and BAK1.

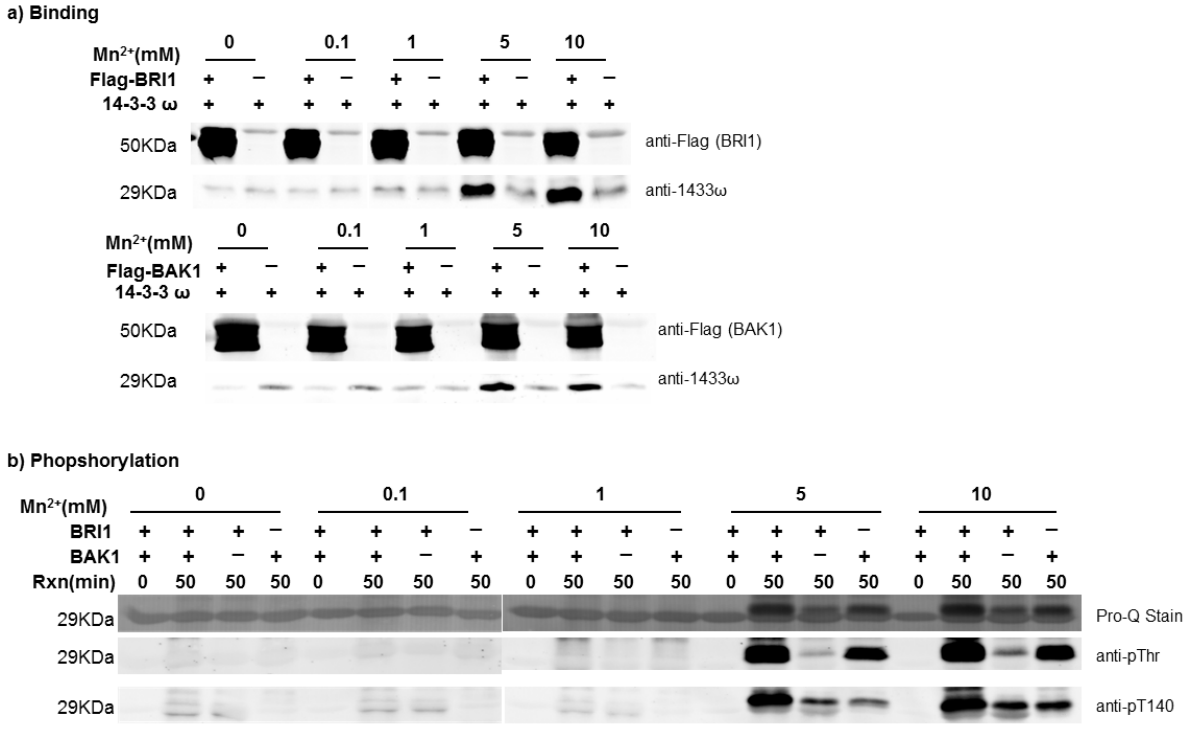


Figure 2.S6 A) The effects of different concentrations of Mn^{2+} on 14-3-3ω binding to BRI1 and BAK1 in vitro showed that mM level of Mn^{2+} was required for the interactions. B) The effects of different concentrations of Mn^{2+} on 14-3-3ω phosphorylation by BRI1 and BAK1 in vitro. mM level of Mn^{2+} was required for the phosphorylation. The results supported the notion that binding enhanced the phosphorylation.

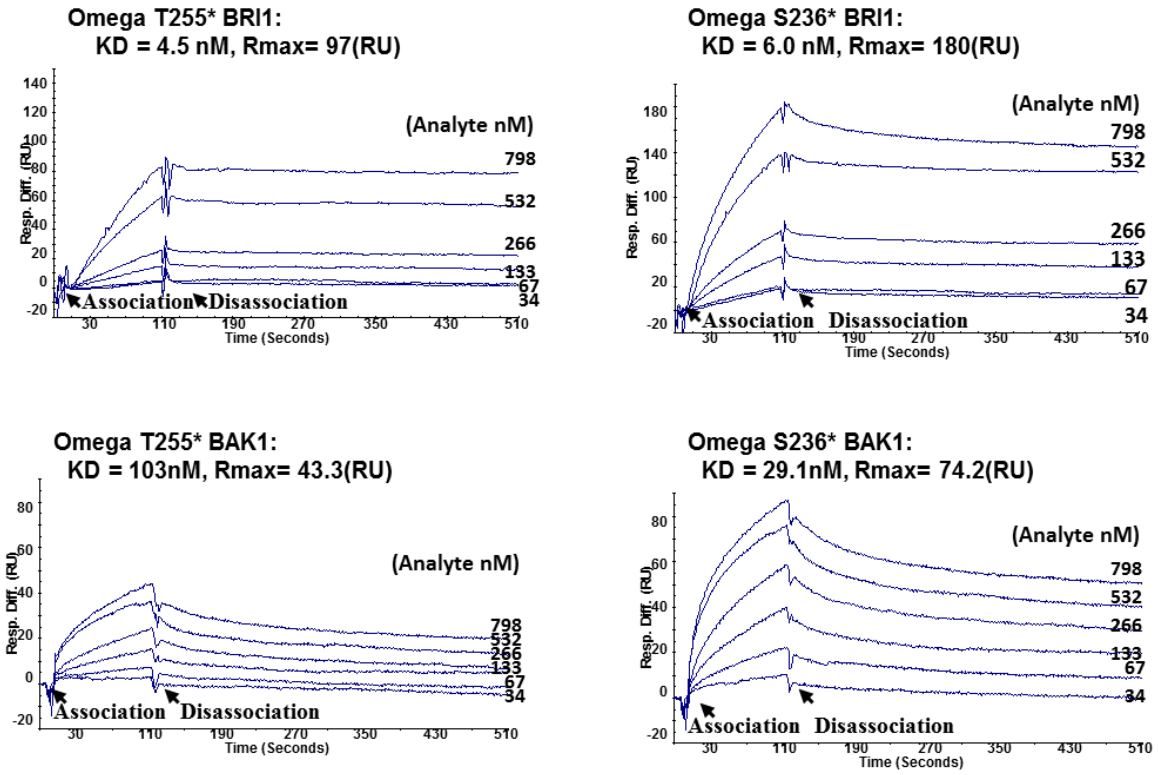


Figure 2.S7 BIAcore analysis of interactions of 14-3-3ω C-terminal truncation mutants (T255* and S236*) with BRI1 and BAK1. The binding was tested in the presence of 5mM Mg^{2+}. Mutant T255* had small enhance in binding to BRI1 and BAK1. Mutant S236* had dramatic increase in binding to BRI1 and BAK1.

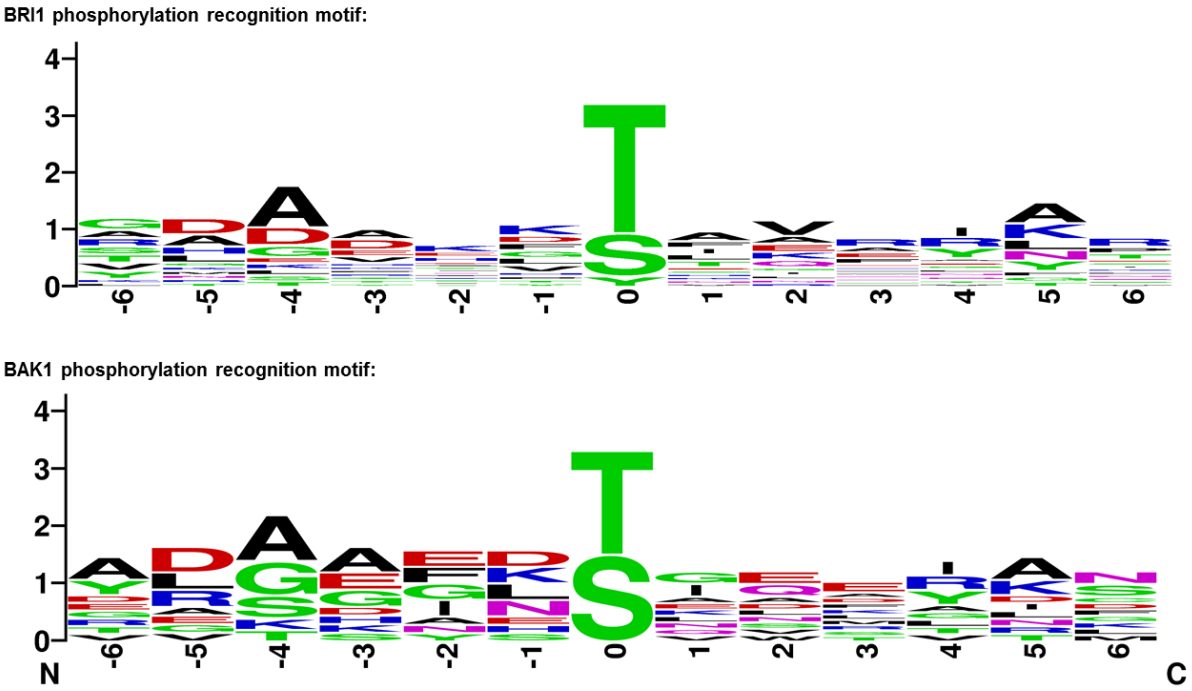


Figure 2.S8 Phosphorylation motif of BRI1 and BAK1.

Sequence information of BRI1 or BAK1 phosphorylation substrates (Table 2.S3 and Table 2.S4) was analyzed by the WebLogo software (Crooks et al., 2004). The size of each amino acid logo reflects the percentage that they are found at certain position. The amino acid Ala was more probable to be found in the BRI1 phosphorylation substrates at the -4 and +5 position. BAK1 phosphorylation substrates also tend to have Ala at the -4 and +5 position.

SUPPLEMENTAL TABLES

Table 2.S1 Residues of 14-3-3ω phosphorylated by BRI1 and BAK1 in vitro

Phosphorylation sites	BRI1	BAK1	BRI1+BAK1
pT41	A	A	A, C
pS67 or pS68	C		
pT83	A, B, C		A, B, C
pT94	A	A	A
pS120	B, C	C	C
pT140	A, C	A	A, C
pT151	B, C	B, C	B, C
pS157	C	B, C	B, C
pS220 or pT221		C	
pT255	C	C	
pT232 or pT235 or pS236		C	C

A: Identified by phospho- site- specific antibody
B: Identified by Q-TOF
C: Identified by MALDI

Table 2.S2 Summary of 14-3-3ω SDMs and their effects on the phosphorylation

Description	Site SDM	Effect on phosphorylation
Single site SDM	S3A	no
	S32A	no
	T41A	no
	S67A	no
	S75A	no
	T83A	no
	S90A	no
	T94A	no
	T140A	no
	S157A	no
	T169A	no
	S190A	no
	T216A	no
	Y217F	no
	T235A	no
Multiple site SDM	T94A, T140A	no
	T41A, T83A, T94A, T140A	small
	S3A, S32A, S90A, S157A	small
	S3A, S90A, S109A, T83A, T94A	small
	S3A, S32A, T41A, T83A	small
	S90A, S97A, T94A	small
	S109A, S117A, T140A, S157A	small
Truncation SDM	T215*	small
	S236*	no
	T255*	no
Binding SDM	K53E	small
	R60E	large
	R133E	large
	Y134F	small
	F138V	no
	S62A	small

No: less than 10% decrease
Small: 10%-50% decrease
Large: more than 50% decrease

Table 2.S3 The sequence information of BRI1 phosphorylation substrates included in the motif analysis

Protein	Position	Peptides	Identification Method	Reference
mBAK1	S290	VASDNF**pS**NKNILG	Mass Spec	Wang et al., 2008
	T312	GRLADG**pT**LVAVKR	Mass Spec	
	T446	LMDYKD**pT**HVTTAV	Mass Spec	
	T449	YKDTHV**pT**TAVRGT	Mass Spec	
	T450	KDTHVT**pT**AVRGTI	Mass Spec	
	T455	TTAVRG**pT**IGHIAP	Mass Spec	
eEFI3	T14	GHERPL**pT**FLRYNR	Mass Spec	Ehsan et al., 2005
	T89	SGKELF**pT**FKFNAP	Mass Spec	
14-3-3ω	T83	GNDDHV**pT**AIREYR	Mass Spec, phospho Abs	This study
	T151	RDAAEH**pT**LAAYKS	Mass Spec	
	T255	AAAPKP**pT**EEQQ(-)	Mass Spec	
	T140	YLAEFK**pT**GQERKD	Mass Spec, phospho Abs	
	T41	VDGDEL**pT**VEERNL	Mass Spec, phospho Abs	
	S120	AAASGD**pS**KVFYLK	Mass Spec	
	S157	TLAAYK**pS**AQDIAN	Mass Spec	
BSK1	S230	RDGKSY**pS**TNLAYT	Site directed mutagenesis	Tang et al., 2008
BKI1	Y211	SHAVKK**pY**IRMLFQ	Site directed mutagenesis	Jaillais et al., 2011

Table 2.S4 The sequence information of BAK1 phosphorylation substrates included in the motif analysis

Protein	Position	Peptides	Identification Method	Reference
mBRI1	S838	AEGHGN**pS**GDRTAN	Mass Spec	Wang et al., 2008
	T846	DRTANN**pT**NWKLTG	Mass Spec	
	S858	GVKEAL**pS**INLAAF	Mass Spec	
	S1166	AGSGID**pS**QSTIRS	Mass Spec	
	T1169	EDGGFS**pT**IEMVDM	Mass Spec	
1433 omega	S120	AAASGD**pS**KVFYLK	Mass Spec	This study
	S157	TLAAYK**pS**AQDIAN	Mass Spec	
	T151	RDAAEH**pT**LAAYKS	Mass Spec	
	T41	VDGDEL**pT**VEERNL	Phospho Abs	
	T94	YRSKIE**pT**ELSGIC	Phospho Abs	
	T140	YLAEFK**pT**GQERKD	Phospho Abs	

Text 2.S1 Protein sequence alignment of 14-3-3 isoforms in Arabidopsis

```
GRF3-psi          -------MSTREENVYMAKLAEQAERYEEMVEFMEKVAKTVD-VEELSVEERNLLSVAYK
GRF5-upsilon      ----MSSDSSREENVYLAKLAEQAERYEEMVEFMEKVAKTVE-TEELTVEERNLLSVAYK
GRF7-nu           ------MSSSREENVYLAKLAEQAERYEEMVEFMEKVAKTVD-TDELTVEERNLLSVAYK
GRF1-chi          -MATPGASSARDEFVYMAKLAEQAERYEEMVEFMEKVAKAVD-KDELTVEERNLLSVAYK
GRF4-phi          MAAPPASSSAREEFVYLAKLAEQAERYEEMVEFMEKVAEAVD-KDELTVEERNLLSVAYK
GRF2-omega        ------MASGREEFVYMAKLAEQAERYEEMVEFMEKVSAAVD-GDELTVEERNLLSVAYK
GRF6-lambda       ----MAATLGRDQYVYMAKLAEQAERYEEMVQFMEQLVTGATPAEELTVEERNLLSVAYK
GRF8-kappa        ----MATTLSRDQYVYMAKLAEQAERYEEMVQFMEQLVSGATPAGELTVEERNLLSVAYK
GRF10-epsilon     ------MENEREKQVYLAKLSEQTERYDEMVEAMKKVAQLDV---ELTVEERNLVSVGYK
GRF11-omicron     ------MENERAKQVYLAKLNEQAERYDEMVEAMKKVAALDV---ELTIEERNLLSVGYK
GRF12-iota        -MSSSGSDKERETFVYMAKLSEQAERYDEMVETMKKVARVNS---ELTVEERNLLSVGYK
GRF9-mu           ----MGSGKERDTFVYLAKLSEQAERYEEMVESMKSVAKLNV---DLTVEERNLLSVGYK
                            *   **:*** **:***:***: *:.:        :*::*****:**.**

GRF3-psi          NVIGARRASWRIISSIEQKEESKGNEDHVAIIKDYRGKIESELSKICDGILNVLEAHLIP
GRF5-upsilon      NVIGARRASWRIISSIEQKEDSRGNSDHVSIIKDYRGKIETELSKICDGILNLLEAHLIP
GRF7-nu           NVIGARRASWRIISSIEQKEESRGNDDHVSIIKDYRGKIETELSKICDGILNLLDSHLVP
GRF1-chi          NVIGARRASWRIISSIEQKEESRGNDDHVSLIRDYRSKIETELSDICDGILKLLDTILVP
GRF4-phi          NVIGARRASWRIISSIEQKEESRGNDDHVTTIRDYRSKIESELSKICDGILKLLDTRLVP
GRF2-omega        NVIGARRASWRIISSIEQKEESRGNDDHVTAIREYRSKIETELSGICDGILKLLDSRLIP
GRF6-lambda       NVIGSLRAAWRIVSSIEQKEESRKNDEHVSLVKDYRSKVESELSSVCSGILKLLDSHLIP
GRF8-kappa        NVIGSLRAAWRIVSSIEQKEESRKNEEHVSLVKDYRSKVETELSSICSGILRLLDSHLIP
GRF10-epsilon     NVIGARRASWRILSSIEQKEESKGNDENVKRLKNYRKRVEDELAKVCNDILSVIDKHLIP
GRF11-omicron     NVIGARRASWRILSSIEQKEESKGNEQNAKRIKDYRTKVEEELSKICYDILAVIDKHLVP
GRF12-iota        NVIGARRASWRIMSSIEQKEESKGNESNVKQIKGYRQKVEDELANICQDILTIIDQHLIP
GRF9-mu           NVIGSRRASWRIFSSIEQKEAVKGNDVNVKRIKEYMEKVELELSNICIDIMSVLDEHLIP
                  ****: **:***.*******  : *. :.  :: *  ::* **: :* .*: :::  *:*

GRF3-psi          SASPAESKVFYLKMKGDYHRYLAEFKAGAERKEAAESTLVAYKSASDIATAELAPTHPIR
GRF5-upsilon      AASLAESKVFYLKMKGDYHRYLAEFKTGAERKEAAESTLVAYKSAQDIALADLAPTHPIR
GRF7-nu           TASLAESKVFYLKMKGDYHRYLAEFKTGAERKEAAESTLVAYKSAQDIALADLAPTHPIR
GRF1-chi          AAASGDSKVFYLKMKGDYHRYLAEFKSGQERKDAAEHTLTAYKAAQDIANSELAPTHPIR
GRF4-phi          ASANGDSKVFYLKMKGDYHRYLAEFKTGQERKDAAEHTLTAYKAAQDIANAELAPTHPIR
GRF2-omega        AAASGDSKVFYLKMKGDYHRYLAEFKTGQERKDAAEHTLAAYKSAQDIANAELAPTHPIR
GRF6-lambda       SAGASESKVFYLKMKGDYHRYMAEFKSGDERKTAAEDTMLAYKAAQDIAAADMAPTHPIR
```

anti-pT41

anti-pT83

anti-pT94

anti-pT140

Text 2.S1 cont-

```
GRF8-kappa          SATASESKVFYLKMKGDYHRYLAEFKSGDERKTAAEDTMIAYKAAQDVAVADLAPTHPIR
GRF10-epsilon       SSNAVESTVFFYKMKGDYYRYLAEFSSGAERKEAADQSLEAYKAAVAAAENGLAPTHPVR
GRF11-omicron       FATSGESTVFYYKMKGDYFRYLAEFKSGADREEAADLSLKAYEAATSSASTELSTTHPIR
GRF12-iota          HATSGEATVFYYKMKGDYYRYLAEFKTEQERKEAAEQSLKGYEAATQAASTELPSTHPIR
GRF9-mu             SASEGESTVFFNKMKGDYYRYLAEFKSGNERKEAADQSLKAYEIATTAAEAKLPPTHPIR
                     :   ::.**: ******.**:***.:  :*: **: :: .*: *   *   :..***:*

GRF3-psi            LGLALNFSVFYYEILNSPDRACSLAKQAFDDAIAELDTLGEESYKDSTLIMQLLRDNLTL
GRF5-upsilon        LGLALNFSVFYYEILNSSDRACSLAKQAFDEAISELDTLGEESYKDSTLIMQLLRDNLTL
GRF7-nu             LGLALNFSVFYYEILNSPDRACSLAKQAFDEAISELDTLGEESYKDSTLIMQLLRDNLTL
GRF1-chi            LGLALNFSVFYYEILNSPDRACNLAKQAFDEAIAELDTLGEESYKDSTLIMQLLRDNLTL
GRF4-phi            LGLALNFSVFYYEILNSPDRACNLAKQAFDEAIAELDTLGEESYKDSTLIMQLLRDNLTL
GRF2-omega          LGLALNFSVFYYEILNSPDRACNLAKQAFDEAIAELDTLGEESYKDSTLIMQLLRDNLTL
GRF6-lambda         LGLALNFSVFYYEILNSSDKACNMAKQAFEEAIAELDTLGEESYKDSTLIMQLLRDNLTL
GRF8-kappa          LGLALNFSVFYYEILNSSEKACSMAKQAFEEAIAELDTLGEESYKDSTLIMQLLRDNLTL
GRF10-epsilon       LGLALNFSVFYYEILNSPESACQLAKQAFDDAIAELDSLNEESYKDSTLIMQLLRDNLTL
GRF11-omicron       LGLALNFSVFYYEILNSPERACHLAKRAFDEAIAELDSLNEDSYKDSTLIMQLLRDNLTL
GRF12-iota          LGLALNFSVFYYEIMNSPERACHLAKQAFDEAIAELDTLSEESYKDSTLIMQLLRDNLTL
GRF9-mu             LGLALNFSVFYYEIMNAPERACHLAKQAFDEAISELDTLNEESYKDSTLIMQLLRDNLTL
                    ***************:*:.: ** :**:**::**:***:*.*:******************

GRF3-psi            WTSDMTDEAG-DEIKEASKPDGAE----------
GRF5-upsilon        WTSDLNDEAG-DDIKEAPKEVQKVDEQAQPPPSQ
GRF7-nu             WNSDINDEAGGDEIKEASKHEPEEGKPAETGQ--
GRF1-chi            WTSDMQDDVA-DDIKEAAPAAAKPADEQQS----
GRF4-phi            WTSDMQDESP-EEIKEAAAPKPAEEQKEI-----
GRF2-omega          WTSDMQDDAA-DEIKEAAAPKPTEEQQ-------
GRF6-lambda         WTSDMQEQMDEA---------------------
GRF8-kappa          WTSDMQEQMDEA---------------------
GRF10-epsilon       WTSDLNEEGDERTKGADEPQDEN----------
GRF11-omicron       WTSDLEEGGK-----------------------
GRF12-iota          WTSDLPEDGGEDNIKTEESKQEQAKPADATEN--
GRF9-mu             WTSDISEEGGDDAHKTNGSAKPGAGGDDAE----
                    *.**: :
```

anti-loop8

anti-1433ω

Text 2.S1 cont-

S T Unequivocal phosphorylation sites of 14-3-3ω identified in this study.

Based on the epitodes for the antibodies,

anti-pT41 and anti-pT83 antibodies are specific for 1433-omega(ω);

anti-pT94 antibodies cross reacts to 1433-omega(ω), 1433-chi(χ) and 1433-nu(υ);

anti-pT140 antibodies cross reacts to 1433-omega(ω) and 1433-phi(φ);

anti-loop8 antibodies cross reacts to 14-3-3 isoforms of the non-epsilon group;

anti-1433ω antibodies cross reacts to 1433omega(ω) and 1433-phi(φ). However, 1433ω and 1433φ can be distinguished by MW (Figure 2.S3).

Text 2.S2 Protein sequence alignment of Arabidopsis 14-3-3ω and human 14-3-3 isoforms

```
Human-beta            MTMDKSELVQKAKLAEQAERYDDMAAAMKAVTEQGH--ELSNEERNLLSVAYKNVVGARR 58
Human-zeta            --MDKNELVQKAKLAEQAERYDDMAACMKSVTEQGA--ELSNEERNLLSVAYKNVVGARR 56
Human-theta           --MEKTELIQKAKLAEQAERYDDMATCMKAVTEQGA--ELSNEERNLLSVAYKNVVGGRR 56
Human-sigma           --MERASLIQKAKLAEQAERYEDMAAFMKGAVEKGE--ELSCEERNLLSVAYKNVVGGQR 56
Human-gamma           -MVDREQLVQKARLAEQAERYDDMAAAMKNVTELNE--PLSNEERNLLSVAYKNVVGARR 57
Human-eta             -MGDREQLLQRARLAEQAERYDDMASAMKAVTELNE--PLSNEDRNLLSVAYKNVVGARR 57
Human-epsilon         -MDDREDLVYQAKLAEQAERYDEMVESMKKV-AGMD-VELTVEERNLLSVAYKNVIGARR 57
Arath-GRF2-omega      MASGREEFVYMAKLAEQAERYEEMVEFMEKVSAAVDGDELTVEERNLLSVAYKNVIGARR 60
                          : .::  *:********::*.  *: .        *: *:************:*.:*

Human-beta            SSWRVISSIEQKT--ERNEKKQQMGKEYREKIEAELQDICNDVLELLDKYLIPNATQP-- 114
Human-zeta            SSWRVVSSIEQKT--EGAEKKQQMAREYREKIETELRDICNDVLSLLEKFLIPNASQA-- 112
Human-theta           SAWRVISSIEQKT--DTSDKKLQLIKDYREKVESELRSICTTVLELLDKYLIANATNP-- 112
Human-sigma           AAWRVLSSIEQKSNEEGSEEKGPEVREYREKVETELQGVCDTVLGLLDSHLIKEAGDA-- 114
Human-gamma           SSWRVISSIEQKTSADGNEKKIEMVRAYREKIEKELEAVCQDVLSLLDNYLIKNCSETQY 117
Human-eta             SSWRVISSIEQKTMADGNEKKLEKVKAYREKIEKELETVCNDVLSLLDKFLIKNCNDFQY 117
Human-epsilon         ASWRIISSIEQKEENKGGEDKLKMIREYRQMVETELKLICCDILDVLDKHLIPAANTG-- 115
Arath-GRF2-omega      ASWRIISSIEQKEESRGNDDHVTAIREYRSKIETELSGICDGILKLLDSRLIPAAASG-- 118
                       ::**::******      :.:    : **. :* **  :*  :* :*:. **  .

Human-beta            ESKVFYLKMKGDYFRYLSEVASGDNKQTTVSNSQQAYQEAFEISKKEMQPTHPIRLGLAL 174
Human-zeta            ESKVFYLKMKGDYYRYLAEVAAGDDKKGIVDQSQQAYQEAFEISKKEMQPTHPIRLGLAL 172
Human-theta           ESKVFYLKMKGDYFRYLAEVACGDDRKQTIDNSQGAYQEAFDISKKEMQPTHPIRLGLAL 172
Human-sigma           ESRVFYLKMKGDYYRYLAEVATGDDKKRIIDSARSAYQEAMDISKKEMPPTNPIRLGLAL 174
Human-gamma           ESKVFYLKMKGDYYRYLAEVATGEKRATVVESSEKAYSEAHEISKEHMQPTHPIRLGLAL 177
Human-eta             ESKVFYLKMKGDYYRYLAEVASGEKKNSVVEASEAAYKEAFEISKEQMQPTHPIRLGLAL 177
Human-epsilon         ESKVFYYKMKGDYHRYLAEFATGNDRKEAAENSLVAYKAASDIAMTELPPTHPIRLGLAL 175
Arath-GRF2-omega      DSKVFYLKMKGDYHRYLAEFKTGQERKDAAEHTLAAYKSAQDIANAELAPTHPIRLGLAL 178
                      :*:*** ******.***:*.  *:.:    . :  **. * :*:  .: **:********

Human-beta            NFSVFYYEILNSPEKACSLAKTAFDEAIAELDTLNEESYKDSTLIMQLLRDNLTLWTSEN 234
Human-zeta            NFSVFYYEILNSPEKACSLAKTAFDEAIAELDTLSEESYKDSTLIMQLLRDNLTLWTSDT 232
Human-theta           NFSVFYYEILNNPELACTLAKTAFDEAIAELDTLNEDSYKDSTLIMQLLRDNLTLWTSDS 232
Human-sigma           NFSVFHYEIANSPEEAISLAKTTFDEAMADLHTLSEDSYKDSTLIMQLLRDNLTLWTADN 234
Human-gamma           NYSVFYYEIQNAPEQACHLAKTAFDDAIAELDTLNEDSYKDSTLIMQLLRDNLTLWTSDQ 237
Human-eta             NFSVFYYEIQNAPEQACLLAKQAFDDAIAELDTLNEDSYKDSTLIMQLLRDNLTLWTSDQ 237
Human-epsilon         NFSVFYYEILNSPDRACRLAKAAFDDAIAELDTLSEESYKDSTLIMQLLRDNLTLWTSDM 235
Arath-GRF2-omega      NFSVFYYEILNSPDRACNLAKQAFDEAIAELDTLGEESYKDSTLIMQLLRDNLTLWTSDM 238
                      *:***:*** * *: *  *** :**:*:*:*.**.*:********************::
```

Text 2.S2 cont-

```
Human-beta              QGDEG-DAGEG-EN------- 246
Human-zeta              QGDEA-EAGEGGEN------- 245
Human-theta             AGEEC-DAAEGAEN------- 245
Human-sigma             AGEEGGEAPQEPQS------- 248
Human-gamma             QDDDG---GEGNN-------- 247
Human-eta               QDEEA---GEGN--------- 246
Human-epsilon           QGDGEEQNKEALQDVEDENQ- 255
Arath-GRF2-omega        QDDAADEIKEAAAPKPTEEQQ 259
                         .:      :
```

S **T** Unequivocal phosphorylation sites of 14-3-3ω identified in this study.

S **T** Phosphorylation sites of 14-3-3ζ in the literatures

REFERENCES

Aitken, A. (2006) 14-3-3 proteins: A historic overview. Seminars in Cancer Biology 16: 162-172.

Athwal, G.S., Lombardo, C.R., Huber, J.L., Masters, S.C., Fu, H. and Huber, S.C. (2000) Modulation of 14-3-3 protein interactions with target polypeptides by physical and metabolic effectors. Plant Cell Physiol. 41: 523-533.

Athwal G.S., Huber S.C. (2002) Divalent cations and polyamines bind to loop 8 of 14-3-3 proteins, modulating their interaction with phosphorylated nitrate reductase. Plant J. 29: 119-29.

Bachmann, M., Huber, J.L., Liao, P.-C., Gage, D.A., Huber, S.C. (1996) The inhibitor protein of phosphorylated nitrate reductase from spinach (Spinacia oleracea) leaves is a 14-3-3 protein. FEBS Lett. 387: 127-131.

Bishop G.J., Koncz C. (2002) Brassinosteroids and plant steroid hormone signaling. Plant Cell Suppl: S97-110.

Chan P.M., Ng Y.W., Manser E. (2010) A robust protocol to map binding sites of the 14-3-3 interactome: Cdc25C requires phosphorylation of both S216 and S263 to bind 14-3-3. Mol Cell Proteomics 10: M110.005157.

Choudhary C., Kumar C., Gnad F., Nielsen M.L., Rehman M., Walther T.C., Olsen J.V., Mann M. (2009) Lysine acetylation targets protein complexes and co-regulates major cellular functions. Science 325: 834-840.

Crooks G.E., Hon G., Chandonia J.M., Brenner S.E. (2004) WebLogo: a sequence logo generator. Genome Res 14: 1188–1190.

Deng, Z., Zhang, X., Tang, W., Oses-Prieto, J.A., Suzuki, N., Gendron, J.M., Chen, H., Guan, S., Chalkley, R.J., Peterman, T.K., Burlingame, A.L., Wang Z.Y. (2007) A proteomics study of brassinosteroid response in Arabidopsis. Mol Cell Proteomics 6: 2058-2071.

Dubois, T., Rommel, C., Howell, S., Steinhussen, U., Soneji, Y., Morrice, N., Moelling, K., Aitken A. (1997) 14-3-3 is phosphorylated by casein kinase I on residue 233. Phosphorylation at this site in vivo regulates Raf/14-3-3 interaction. J Biol Chem. 272: 28882-28888.

Duncan, K.A., Hardin, S.C., Huber, S.C. (2006) The three maize sucrose synthase isoforms differ in distribution, localization, and phosphorylation. Plant Cell Physiol. 47: 959-971.

Durek P., Schudoma C., Weckwerth W., Selbig J., Walther D. (2009) Detection and characterization of 3D-signature phosphorylation site motifs and their contribution towards improved phosphorylation site prediction in proteins. BMC Bioinformatics 10: 117.

Fu, H., Subramanian, R.R., Masters, S.C. (2000). 14-3-3 Proteins: Structure, function, and regulation. Annual Review of Pharmacology and Toxicology 40: 617-647.

Gampala S.S., Kim, T.W., He, J.X., Tang, W., Deng, Z., Bai, M.Y., Guan, S., Lalonde, S., Sun, Y., Gendron, J.M., Chen, H., Shibagaki, N., Ferl, R.J., Ehrhardt, D., Chong, K., Burlingame, A.L., Wang, Z.Y. (2007) An essential role for 14-3-3 proteins in brassinosteroid signal transduction in Arabidopsis. Dev Cell. 13:177-189.

Giacometti, S., Camoni, L., Albumi, C., Visconti, S., De Michelis, M.I., Aducci, P. (2004) Tyrosine phosphorylation inhibits the interaction of 14-3-3 proteins with the plant plasma membrane H^+-ATPase. Plant Biology 6: 422-431.

Grozinger, C.M., Schreiber, S.L. (2000) Regulation of histone deacetylase 4 and 5 and transcriptional activity by 14-3-3-dependent cellular localization. Proc Natl Acad Sci U S A. 97: 7835-7840.

Horn, M.A., Walker, J.C. (1994). Biochemical properties of the autophosphorylation of RLK5, a receptor-like protein kinase from *Arabidopsis thaliana*. Biochimica et Biophysica Acta. 1208: 65-74.

Humphrey, W., Dalke, A. and Schulten, K. (1996) "VMD - Visual Molecular Dynamics", J. Molec. Graphics. 14: 33-38.

Jiménez J.L., Hegemann B., Hutchins J.R.A., Peters J.-M., Durbin R. (2007) A systematic comparative and structural analysis of protein phosphorylation sites based on the mtcPTM database. Genome Biology 8: R90.

Karlova, R., Boeren, S., Russinova, E., Aker, J., Vervoort, J. and De Vries, S. (2006) The Arabidopsis somatic embryogenesis receptor-like kinase1 protein complex includes brassinosteroid-insensitive1. Plant Cell 18: 626-638.

Kinoshita, T., Caño-Delgado, A., Seto, H., Hiranuma, S., Fujioka, S., Yoshida, S., Chory, J. (2005) Binding of brassinosteroids to the extracellular domain of plant receptor kinase BRI1. Nature 433: 167-171.

Kjellström, S., Jensen, O.N. (2006) Phosphoric acid as a matrix additive for MALDI MS analysis of phosphopeptides and phosphoproteins. Anal Chem.76 : 5109-5117.

Li, J., Wen, J., Lease, K.A., Doke, J.T., Tax, F.E., Walker, J.C. (2002). BAK1, an Arabidopsis LRR receptor-like protein kinase, interacts with BRI1 and modulates brassinosteroid signaling. Cell 110: 213-222.

Lu, G., Sehnke, P.C., Ferl R.J. (1994) Phosphorylation and calcium binding properties of an Arabidopsis GF14 brain protein homolog. Plant Cell 6: 501-510.

Nakashita H., Yasuda M., Nitta T., Asami T., Fujioka S., Arai Y., Sekimata K., Takatsuto S., Yamaguchi I., Yoshida S. (2003) Brassinosteroid functions in a broad range of disease resistance in tobacco and rice. Plant J. 33: 887-898.

Nam, K.H., Li, J. (2002). BRI1 and BAK1, a receptor kinase pair mediating brassinosteroid signaling. Cell 110: 203-212.

Ma, Y., Pitson, S., Hercus, T., Murphy, J., Lopez, A.,Woodcock, J. (2005) Sphingosine activates protein kinase A type II by a novel cAMP-independent mechanism. J Biol Chem. 280: 26011-26017.

Oh, M.-H., Ray, W.K., Huber, S.C., Asara, J.M., Gage, D.A., Clouse, S.D. (2000) Recombinant brassinosteroid insensitive 1 receptor-like kinase autophosphorylates on serine and threonine residues and phosphorylates a conserved peptide motif in vitro. Plant Physiol. 124: 751-765.

Oh, M.-H., Wang, X., Kota, U., Goshe, M.B., Clouse, S.D., Huber, S.C. (2009). Tyrosine phosphorylation of the BRI1 receptor kinase emerges as a component of brassinosteroid signaling in Arabidopsis. Proc. Natl. Acad. Sci. USA 106: 658-663.

Oh, M.-H., Wang, X., Wu, X., Zhao, Y., Clouse, S.D., Huber, S.C. (2010). Autophosphorylation of Tyr-610 in the receptor kinase BAK1 plays a role in brassinosteroid signaling and basal defense gene expression. Proc. Natl. Acad. Sci. USA 107: 17827-17832.

Ottmann, C., Marco, S., Jaspert, N., Marcon, C., Schauer, N., Weyand, M., Vandermeeren, C., Duby, G., Boutry, M., Wittinghofer, A., Rigaud, J.-L., Oecking, C. (2007b). Structure of a 14-3-3 Coordinated Hexamer of the Plant Plasma Membrane H+-ATPase by Combining X-Ray Crystallography and Electron Cryomicroscopy. Mol Cell. 25: 427-440.

Ottmann C., Yasmin L., Weyand M., Veesenmeyer J.L., Diaz M.H., Palmer R.H., Francis M.S., Hauser A.R., Wittinghofer A., Hallberg B. (2007a) Phosphorylation-independent interaction between 14-3-3 and exoenzyme S: from structure to pathogenesis. EMBO J. 26: 902-913.

Reiland, S., Messerli, G., Baerenfaller, K., Gerrits, B., Endler, A., Grossmann, J., Gruissem, W., Baginsky, S. (2009) Large-scale arabidopsis phosphoproteome profiling reveals novel chloroplast kinase substrates and phosphorylation networks. Plant Physiol. 150: 889-903.

Rienties, I.M., Vink, J., Borst, J.W., Russinova, E., and de Vries, S.C. (2005). The Arabidopsis SERK1 protein interacts with the AAA-ATPase AtCDC48, the 14-3-3 protein GF14lambda and the PP2C phosphatase KAPP. Planta 221: 394–405.

Rosenquist, M., Alsterfjord, M., Larsson, C., Sommarin, M. (2001) Data mining the Arabidopsis genome reveals fifteen 14-3-3 genes. Expression is demonstrated for two out of five novel genes. Plant Physiol. 127: 142-149.

Schaller G.E., Bleecker A.B. (1993) Receptor-like kinase activity in membranes of Arabidopsis thaliana. FEBS Lett. 333: 306-310.

Schulze, B., Mentzel, T., Jehle, A.K., Mueller, K., Beeler, S., Boller, T., Felix, G., Chinchilla, D. (2010) Rapid heteromerization and phosphorylation of ligand-activated plant transmembrane receptors and their associated kinase BAK1. J Biol Chem. 285: 9444-9451.

Sehnke, P.C., DeLille, J.M., Ferl, R.J. (2002) Consummating signal transduction: the role of 14-3-3 proteins in the completion of signal-induced transitions in protein activity. Plant Cell 14: S339-354.

Shen W., Clark A.C., Huber S.C. (2003) The C-terminal tail of Arabidopsis 14-3-3omega functions as an autoinhibitor and may contain a tenth alpha-helix. Plant J. 34: 473-484.

Shin, R., Alvarez, S., Burch, A.Y., Jez, J.M., Schachtman, D.P. (2007) Phosphoproteomic identification of targets of the Arabidopsis sucrose nonfermenting-like kinase SnRK2.8 reveals a connection to metabolic processes. Proc Natl Acad Sci U S A. 104: 6460-6465.

Sugiyama, N., Nakagami, H., Mochida, K., Daudi, A., Tomita, M., Shirasu, K. and Ishihama, Y. (2008) Large-scale phosphorylation mapping reveals the extent of tyrosine phosphorylation in Arabidopsis. Molecular Systems Biology 4: 193.

Sunayama, J., Tsuruta, F., Masuyama, N., Gotoh, Y. (2005) JNK antagonizes Akt-mediated survival signals by phosphorylating 14-3-3. J Cell Biol. 170: 295-304.

Telles, E., Hosing, A.S., Kundu, S.T., Venkatraman, P., Dalal, S.N. (2009) A novel pocket in 14-3-3epsilon is required to mediate specific complex formation with cdc25C and to inhibit cell cycle progression upon activation of checkpoint pathways. Experimental Cell Research 315:1448-1457.

Testerink C., van Zeijl M.J., Drumm K., Palmgren M.G., Collinge D.B., Kijne J.W., Wang M. (2002) Post-translational modification of barley 14-3-3A is isoform-specific and involves removal of the hypervariable C-terminus. Plant Mol Biol. 50: 535-542.

Tsuruta, F., Sunayama, J., Mori, Y., Hattori, S., Shimizu, S., Tsujimoto, Y., Yoshioka, K., Masuyama, N., Gotoh, Y. (2004) JNK promotes Bax translocation to mitochondria through phosphorylation of 14-3-3 proteins. EMBO J. 23:1889-1899.

Visconti S., Camoni L., Marra M., Aducci P. (2008) Role of the 14-3-3 C-terminal region in the interaction with the plasma membrane H+-ATPase. Plant Cell Physiol. 49:1887-1897.

Wang, X., Li, X., Meisenhelder, J., Hunter, T., Yoshida, S., Asami, T., Chory, J. (2005a) Autoregulation and homodimerization are involved in the activation of the plant steroid receptor BRI1. Dev Cell. 8: 855-865.

Wang X., Goshe M.B., Soderblom E.J., Phinney B.S., Kuchar J.A., Li J., Asami T., Yoshida S.,

Huber S.C., Clouse S.D. (2005b) Identification and functional analysis of in vivo phosphorylation sites of the Arabidopsis BRASSINOSTEROID-INSENSITIVE1 receptor kinase. Plant Cell 17: 1685-1703.

Wang, X., Kota, U., He, K., Blackburn, K., Li, J., Goshe, M.B., Huber, S.C., Clouse, S.D. (2008). Sequential Transphosphorylation of the BRI1 and BAK1 Receptor Kinase Complex Impacts Early Events in Brassinosteroid Signaling. Dev Cell. 15: 220-235.

Weiner, H., Kaiser, W.M. (1999) 14-3-3 proteins control proteolysis of nitrate reductase in spinach leaves. FEBS Lett. 455: 75-78.

Woodcock, J.M., Murphy, J., Stomski, F.C., Berndt, M.C., Lopez, A.F. (2003) The Dimeric Versus Monomeric Status of 14-3-3ζ Is Controlled by Phosphorylation of Ser58 at the Dimer Interface. J Biol Chem. 278: 36323-36327.

Woodcock, J.M., Ma, Y., Coolen, C., Pham, D., Jones, C., Lopez, A.F., Pitson, S.M. (2010) Sphingosine and FTY720 directly bind pro-survival 14-3-3 proteins to regulate their function. Cell Signal. 22: 1291-1299.

Wu, X., Oh, M.-H., Schwarz, E., Larue, C.T., Sivaguru, M., Imai, B.S., Yau, P.M., Ort, D.R. and Huber, S.C. (2011) Lysine Acetylation is a Widespread Protein Modification for Diverse Proteins in Arabidopsis. Plant Physiol. 155: 1769-1778.

Yaffe M.B., Rittinger K., Volinia S., Caron P.R., Aitken A., Leffers H., Gamblin S.J., Smerdon S.J., Cantley L.C. (1997) The structural basis for 14-3-3:phosphopeptide binding specificity. Cell 91: 961-971.

CHAPTER 3: LYSINE ACETYLATION IS A WIDESPREAD PROTEIN MODIFICATION FOR DIVERSE PROTEINS IN ARABIDOPSIS[3]

INTRODUCTION

Protein lysine acetylation (LysAc) is a post-translational modification whereby an acetyl moiety is transferred to the ε–amino group of lysine residues and is distinct from the acetylation that occurs frequently on the N-terminus of a protein. Importantly, acetylation of the ε-N of lysine removes the positive charge of the side chain and therefore directly impacts the electrostatic status of the modified protein (Glozak et al., 2005). Lysine acetylation is best known for its regulation of histone proteins, affecting chromatin structure and gene expression (Eberharter and Becker, 2002). Recent proteomic analyses further extended the scope of LysAc. In Salmonella, LysAc is found to be widespread in the central metabolic enzymes and the occurrence of LysAc correlates with alterations of carbon fluxes (Wang et al., 2010). In humans, LysAc is particularly abundant in protein complexes where it regulates protein-protein interactions and enzyme activities (Choudhary et al., 2009; Zhao et al., 2010).

Although LysAc is considered to be an evolutionarily conserved modification from prokaryotes to eukaryotes (Choudhary et al., 2009; Zhang et al., 2009), little is known about LysAc beyond histone proteins in plants. In Arabidopsis, histone LysAc is essential for plant growth and development, as mutants of Arabidopsis lacking certain members of the histone acetyltransferases or deacetylases have altered levels of histone LysAc and display pleiotropic growth defects (Tian and Chen, 2001; Vlachonasios et al., 2003).

The first objective of this study was to determine if non-histone LysAc also occurs in Arabidopsis as in other reported organisms. We used immunoblotting with generic anti-LysAc antibodies to answer this question. We further identified the sites of LysAc modification, using peptide affinity enrichment (Choudhary et al., 2009; Zhang et al., 2009) prior to LC/MS analysis. The second objective of this study was to determine the functional signficance of LysAc on two selected, abundant LysAc proteins (LHCb and eEF-1A).

[3] The central content of the chapter was published in the article Wu et al. (2011) Plant Physiol. 2011 Feb 10. [Epub ahead of print].

MATERIALS AND METHODS

Plant Material

Arabidopsis ecotype Ws-2 was used in the study and grown in soil as described previously (Oh et al., 2009) and described further in the Supplemental Information.

Antibodies

Generic anti-lysine acetylation antibodies were obtained from Cell signaling (#9681S) and Immunechem (#ICP0380) and were used for LysAc peptide affinity 2 enrichment. Immunechem antibodies (#ICP0380) was also used for the immunoblotting. Sequence- and modification-specific antibodies were produced and affinity purified against the following peptides: anti-eEF-1A-acK306, KNVAVacKDLKRG; and antieEF- 1A-acK227, QINEPacKRPSDK, by GenScript and were used to confirm specific lysine acetylation sites on eEF-1A. Generic anti-lysine trimethylation antibodies were obtained from Immunechem (#ICP0601). Sequence-specific antibodies against LHCb were obtained from Agrisera (#AS01 004-10) and custom anti-EF1α antibodies were produced and affinity purified against the peptide IDRRSGKEIEKEPK and were produced by GenScript. Blots were blocked with 2% fish gelatin (Sigma-Aldrich) and Alexa Fluor 680 (Invitrogen) or IRDye 800 (Rockland) was used as the secondary antibodies. Images were viewed using a Li-Cor Odyssey and analyzed using Odyssey software.

Protein Extraction

Frozen tissue powder was mixed with extraction buffer containing 100 mM Tris (pH 8.0), 1.5 M 2-mercaptoethanol, 4% SDS, 15% glycerol, 5 mM NaF, 1 mM Na_3VO_4, 1 mM AEBSF, 2 mM EDTA and 0.005% bromophenol blue and vortexed for 30 s. The mixture was heated at 95° C for 5 min, and vortexed another 30 s. Supernatants were collected after centrifugation at 16,000g for 15 min at room temperature and extracts were analyzed by 1-DE and 2-DE followed by immunoblotting as described in the Supplemental Information.

Green Native Gels

Shoots were homogenized in 50 mM Tris (pH 7.4), 10 mM $MgCl_2$, and 5 mM KCl, and normalized for chlorophyll content before centrifugation at 6,000g for 10 min. The thylakoid

pellets were solubilized and loaded for first dimension native green gel analysis according to Allen and Staehelin (Allen and Staehelin, 1991). Individual bands were excised from green gels and resolved by SDS-PAGE before transfer to PVDF for immunoblotting.

LC-MS Analysis

Denatured and alkylated proteins were digested with Trypsin or Glu-C (Roche) as described by Shevchenko (2007) and reconstituted for immunoenrichment of acetylated peptides as described by Choudhary (2009). In addition, selected spots of 1- or 2-DE gels were plugged and digested. LC-MS/MS analysis was performed on a Waters Q-Tof API-US Quad-ToF mass spectrometer with a nanoAcquity UPLC system, with a linear gradient of 1% to 60% acetonitrile in 0.1% formic acid over 60 min. MS/MS data were collected using the Data Directed Analysis (DDA) method in MassLynx to fragment the top four ions in each survey scan. ProteinLynx (Waters) was used to process the mass spectral data into peak list files (PKL) for analysis by Mascot (Matrix Science) and/or Phenyx (Genebio).

The mass spectra were searched against the NCBI nr database using the Mascot search engine, version 2.3. The search was limited with a taxonomy filter of Arabidopsis thaliana and mass tolerance was set to 0.5 Da for peptide and MS/MS masses. The significance threshold was set to the default p value of 0.05. The reverse decoy database setting within Mascot was used to determine the False Discovery Rate (FDR) for the searches that was typically less than 5%. Relevant spectra were visually inspected to confirm the proper assignment of peaks for acetylated residues, and selected spectra annotated to identify the characteristic acetyl-ion peaks are shown in Supplemental Figure 3.S8. Database searches were performed against the NCBI non-redundant database limited to Arabidopsis thaliana.

Immunocytochemistry

Fully expanded leaves were fixed with 4% paraformaldehyde (Electron Microscopy Sciences), dehydrated in a graded ethanol series, and embedded in paraffin using an automatic tissue processor (ASP 300, Leica). Sections were blocked by Image-iT™ FX signal enhancer (Invitrogen), incubated in a cocktail of anti-LysAc mouse monoclonal antibodies (Cell Signaling) overnight, and probed with Alexa 488 Goat anti-Mouse secondary antibody (Invitrogen) and counter stained with either a membrane dye (10µg/mL) FM143 (Invitrogen) or a

nuclear dye (100μg/mL in water) Hoechst 33342 (Invitrogen). Samples were imaged using a Zeiss LSM 710 laser scanning confocal microscope (Carl Zeiss) as described in the Supplemental Information.

Protein Interaction Analysis

Real-time interactions between recombinant CaM and immobilized biotinylated eEF-1A peptides were monitored with an Octet QK (Forte-Bio, Menlo Park, CA) that is based on biolayer biointerferometry (Abdiche et al., 2008).

RESULTS

Abundant Lysine Acetylation of Non-Histone Proteins in Arabidopsis

The presence of lysine acetylation in different organs and tissues of Arabidopsis was demonstrated by immunoblotting with anti-LysAc antibodies (Figure 3.1A). The two most prominent acetylated protein bands from shoot and leaf tissues comigrated with the 50 and 25 kDa standard proteins. Silique and flower tissues also contained these two dominant bands, but they were less abundant. For the root, the proteins cross reacting with the anti-LysAc antibodies were numerous but in general less abundant. Seeds contained major lysine acetylated proteins at 25 and 18 kDa that corresponded to major storage proteins previously identified as cruciferin 2 α-subunit and cruciferin 3 β-subunit (Wan et al., 2007).

To better define the composition of the major LysAc proteins at 50 and 25 kDa in leaf extracts, we separated proteins by 2-dimensional electrophoresis (2-DE) followed by immunoblotting with anti-LysAc antibodies (Figure 3.1B). It was determined that the 50 kDa LysAc band consisted of two acetylated proteins: eEF-1A, pI 9.2, and RbcL, pI 5.9. From the Commassie staining intensities it was clear that there was less eEF-1A protein but greater cross reactivity with the anti-LysAc antibodies compared to RbcL suggesting a higher stoichiometry of LysAc. The 50-kDa acetylated protein spot with an apparent pI 3.0, was identified by LC/MS as a mixture of RbcL, ATP synthase β subunit, and other proteins that did not match the pI. We therefore reasoned that these proteins were incompletely focused during the initial IEF step. In contrast, the 25 kDa acetylated protein band consisted of three neighboring spots, identified as

LHCb1 and LHCb2 by LC/MS. The surrounding small spots were other LHCb minor isoforms, consistent with the report of Galetskiy et al. (Galetskiy et al., 2008).

The specificity of the anti-LysAc immunoblots was demonstrated by strong competition with acetyl-BSA but not unmodified BSA (Supplemental Figure 3.S1), as also reported by Zhang et al. (2009) in studies of lysine acetylation in *E. coli*. The specificity was also supported by the observation that although the major bands in the anti-LysAc immunoblots were also abundant proteins by commassie staining, not all of the abundant proteins were strongly recognized by the anti-LysAc antibodies (Figure 3.1A). However, one contrasting note is that the anti-LysAc antibodies appeared to recognize carbamylated-lysine residues as well. As shown in Supplemental Figure 3.S2, extended heating of samples with SDS sample buffer containing urea resulted in strong cross reaction with the generic antibodies. Thus, we avoided the use of urea for sample preparations in this study, except where mentioned.

Identification of lysine modified proteins by LC-MS

We identified 64 different lysine modification sites from 57 proteins and each site was verified manually (Table 3.1 and Supplemental Table 3.S2). Consistent with Figure 3.1, the major lysine acetylated proteins from immunoblotting all had at least one positive site, such as Lys-306 of eEF-1A, Lys-252 of RbcL and Lys-37 of LHCb1. However, an acetylated peptide has the monoisotopic mass gain of 42.0105 units, which is nearly the same as trimethylation (42.0468 mass units). Thus, the two modifications differ by only 0.0363 Da (36 ppm for a Mr 1000 peptide) (Zhang et al., 2004), which is less than the resolution of our LC/MS analysis. Consequently, we were not able to distinguish these two modifications by mass spectrometry. However, our 2-DE separation of soluble leaf proteins followed by immunoblotting with generic antibodies suggested that LysAc was much more abundant than lysine trimethylation, and with the exception of eEF-1A the proteins modified by LysAc were distinct from the proteins modified by lysine trimethylation (Supplemental Figure 3.S3). Hence, it is reasonable to conclude that the majority of the proteins we identified with a mass gain of 42 in LC/MS are sites of lysine acetylation rather than lysine trimethylation.

The identified LysAc proteins consist of a diverse group representing virtually all major plant processes (Figure 3.2), including photosynthesis, protein metabolism, cell organization and biogenesis, stress responses and secondary metabolism. Accordingly, these proteins were

localized in various cellular compartments, including the chloroplast, nucleus, plasma membrane and so on (Supplemental Figure 3.S4). Representative proteins and their Gene Ontology classifications are listed in Table 3.1. A number of lysine acetylated candidate proteins are involved in photosynthesis, including light harvesting protein LHCb1, 33 KDa subunit of photo-reaction center PSII, carboxylation enzyme Rubisco large and small subunits, and energy generator chloroplast ATP synthase (β chain). This group of proteins and their lysine acetylation are unique to plants.

The localization of lysine acetylated proteins was further characterized in immuno-localization experiments (Figure 3.3). As shown in (Figure 3.3A-D), robust anti-LysAc signals were observed in mesophyll cell chloroplasts (short arrow head) with enriched labeling on the thylakoid membranes that were visualized with FM143 membrane stain (Figure 3.3). Starch grains inside the chloroplast were not labeled, which further indicated the specificity of the labeling. The section analyzed in Figure 3.3A-D also included the epidermis and it was clear that the plasma membrane of epidermal cells also contained LysAc proteins (long arrow), suggesting that LysAc is a common modification for different cell types. We also observed anti-LysAc labeling of the nuclei, visualized with DAPI nuclear stain (Figure 3.3E-H). Highly condensed chromatin regions, or chromocenters, are visualized as the bright DAPI-positive domains, and often contain the pericentric chromosome regions. In contrast, the gene-rich portions of chromosomes are less condensed and stain more weakly with DAPI (Tessadori et al., 2007). Importantly, histones associated with chromocenters are typically methylated whereas chromatin in other regions of the nucleus tends to be associated with acetylated histones (Soppe et al., 2002; Jackson et al., 2004). Consistent with this notion, we found weak colocalization of DAPI staining with protein LysAc inside the chromocenters, suggesting that proteins in these regions may be hypo-acetylated. Finally, the specificity of the immunolabeling was demonstrated in Figure 3.3I-L, where no primary anti-LysAc antibodies were added and as a result, no signals were observed in the antibody channel, while the chlorophyll autofluorescence showed the presence of the cells. To summarize, the immunolocalization data reinforced the LC-MS identification that LysAc proteins in Arabidopsis are diverse and localized in many cellular compartments.

Differential Lysine Acetylation of Peripheral LHCb Versus Tightly PSII-bound LHCb

LHCb proteins are encoded in the nucleus, and processed into the mature form in the chloroplast. N-acetylation of LHCb has been reported (Michel et al., 1991), but ε-acetylation of these proteins is not known. In the immunoblotting results (Figure 3.1C*)*, LHCb family proteins were one of the major LysAc proteins in Arabidopsis. The mature LHCb1 polypeptide begins with Arg-36 (Michel et al., 1991), and our LC/MS analysis identified Lys-37 to be a site of acetylation in the LHCb1 Glu-C proteolytic peptide: $_{H2N}$R(ac)KTVAKPKGPSGSPWYGSD. The LC/MS spectrum also contained the N-acetylated form peptide: $_{ACETYL}$RKTVAKPKGPSGSPWYGSD, which lacked the ε-acetylation on Lys-37. This mixed identification of acetylated Lys-37 and N-acetyl-Arg-36 peptides also occurred for the phosphorylated forms of each peptide (phosphoThr-38, Supplemental Figure 3.S5). However, no peptides with double acetylation (N-Ac-R36 and acK37) or completely lacking acetylation (no N-Ac-R36 or acK37) were identified in the same digests. Thus, it is possible that the ε-acetylation of Lys-37 and N-acetylation of Arg-36 are mutually exclusive.

It is known that LHCb occurs in several complexes in the thylakoid membranes and to study the possible relation of lysine acetylation with LHCb protein association, we performed a 2-dimensional native green gel analysis of thylakoid membranes (Figure 3.4). In the first native (i.e., non-dissociating) dimension (Figure 3.4A), three chlorophyll-containing bands were found to be acetylated: Band 1, corresponding to photosystem supercomplexes; Band 2, PSII: LHCb complex; and Band 3, peripheral LHCb (14). Peripheral LHCb includes the LHCb that is loosely bound to PSII and the mobile pool of LHCb. Each of the three bands was cut out individually and the component proteins in each band were resolved by SDS-PAGE in the second dimension, which resolved two major LysAc bands at 50 kDa and 25 kDa. The highly LysAc 50 kDa protein (both in Band 1 and Band 2) was identified as RbcL by LC-MS. It is established that RbcL can interact with the thylakoid membrane (Smith et al., 1997), but the surprising observation of RbcL comigrating together with PSII and LHC in different complexes has not been reported. The 25 kDa LysAc proteins were identified as LHCb1 and LHCb2. Furthermore, it turned out that the peripheral LHCb (Band 3) had substantially higher levels of LysAc than the tightly PSII-bound LHCb (Band 2), despite the similar amount of LHCb protein (Figure 3.4B). These quantitative differences are summarized in Figure 3.4C. For both light and dark samples, the peripheral LHCb antennae (Band 3) had 2 to 3-fold higher LysAc/LHCb ratio (i.e., acetylation normalized

for protein) compared to the LHCb that was more tightly bound to PSII (Band 2). The results suggest that lysine acetylation may play a role in LHCb associations in the thylakoid membrane and thus could be of regulatory significance.

We monitored the modification of LHCb by LysAc and threonine phosphorylation during light to dark transitions (Figure 3.4D). As expected, the phosphorylation of LHCb on threonine residues decreased rapidly in the dark, while the LysAc remained constant. This result is consistent with the observation from the green gel study. Hence, unlike phosphorylation, which is a big part of LHCb regulation during state transitions (16), the LysAc of LHCb did not respond directly to short term light/dark changes.

Interestingly, LysAc was detected not only in the major antennae (LHCb1 and LHCb2), but was also in the minor antennae (LHCb3-5). We identified alternative N-terminal forms of LHCb5 starting with Leu-38, Phe-39 or Ser-40 (Figure 3.S6). However, only the peptide starting with Leu-38 contained the acetylated modification at Lys-41. Thus, the possible relation between LysAc and alternative transit peptide processing in LHCb5 emerges as an interesting topic to explore in the future. In summary, we have shown that LysAc is an important modification of LHCb proteins and may play a role in LHCb protein interactions and N-terminal processing.

Lysine Acetylation of eEF-1A Lys-306 in Relation to CaM Binding

Eukaryotic elongation factor-1A was another abundant LysAc protein identified in Arabidopsis by immunoblotting (Figure 3.1B). The five candidate sites of acetylation were located in domain I (acLys-36, acLys-79, ac Lys-187, ac Lys-227) and domain II (ac Lys-306) of the protein (Andersen et al., 2001) (Supplemental Figure 3.S8). Four of these five sites have been reported to be trimethylated in eEF-1A in maize (Lopez-Valenzuela et al., 2003). In addition, two lysine residues (Lys-44 and Lys-55) were identified as monomethylated or dimethylated in this study (Table 3.2). In order to confirm the LysAc of eEF-1A, we produced sequence- and modification- specific anibodies to recognize acetylated Lys306 (anti-eEF-1A-acK306) and acetylated Lys227 (anti-eEF-1A-acK227) and confirmed that both residues were acetylated in vivo in the shoot and root (Figure 3.5A, B). The sequence- and modification- specificity of these custom antibodies was documented with dot-blot peptide assays (Supplemental Figure 3.S7). As expected, the generic anti-LysAc antibodies could recognize the acetylated peptides corresponding to Lys-306 (eEF-1A-acK306) and Lys-227 (eEF-1A-acK227).

Carrot eEF-1A was reported to interact with calmodulin (CaM) (Durso and Cyr, 1994), but the specific sequences involved in the binding are not known. We used a predictive algorithm (Hoeflich and Ikura, 2002) for CaM-binding sequences and found the sequence from Leu-291 to Ala-314 (containing Lys-306) had the highest score for the Arabidopsis eEF-1A protein. Using synthetic peptides, we confirmed that recombinant CaM could interact with the eEF-1A Lys-306 peptide. More interestingly, the acetylated form of the Lys-306 peptide had strongly reduced binding of Ca^{2+}/CaM compared to the non-acetylated peptide (Figure 3.5C). These data suggest that lysine acetylation of eEF-1A Lys-306 may play a role in regulating the interaction of eEF-1A and Ca^{2+}/CaM.

DISCUSSIONS

Our report along with the companion manuscript (Finkemeier et al., 2011) are the first systematic studies of lysine acetylation of non-histone proteins in plants. Thus, Arabidopsis is shown to contain a lysine acetylome, as documented recently for eubacteria [*E. coli* (Zhang et al., 2009) and *Salmonella* (Wang et al., 2010)] and eukaryotes [various human cell lines: HeLa cells (Kim et al., 2006), cancer cells (Choudhary et al., 2009), and liver cells (Zhao et al., 2010)]. In our study, we identified 64 lysine modification sites on 58 proteins, which are involved in a wide variety of pathways and processes and located in various cellular compartments. One characteristic group was the photosynthesis-related proteins. From light harvesting and energy metabolism to carboxylation, proteins representative of the full photosynthetic pathway harbor LysAc modifications, as it is also reported by Finkemeier et al. (2011). Understanding the impact of the modifications on these sites holds considerable promise for a deeper understanding of the regulation of the component processes of photosynthesis.

In our LC-MS identifications, we could not distinguish lysine acetylation from trimethylation, because these two modifications only differ by 0.0363 Da. The discriminative immunion ions for LysAc or lysine trimethylation peptides reported by Zhang (Zhang et al., 2004) were not detected in most cases, perhaps due to the limited abundance of in vivo peptides. We took best advantage of ion error maps to manually verify each putative acetylation site (Carroll et al., 2008). Nonetheless, some false positives of lysine trimethyl peptides may still remain. However, our immunoblot results (Supplemental Figure 3.S3) indicated that LysAc was

a much more common modification in Arabidopsis compared to lysine trimethylation, suggesting that peptides containing a lysyl residue with a mass gain of ~42 units are most likely to be sites of acetylation. In the case of eEF-1A, the one protein that was clearly acetylated and trimethylated on lysine residues, we confirmed two in vivo acetylation sites with specific antibodies.

We studied two abundant LysAc proteins in Arabidopsis—LHCb and eEF-1A. For LHCb proteins, LHCb1 and LHCb5 were found to contain lysine modification sites close to the N-termini of the proteins (acetylated Lys-37 for LHCb1 and Lys-41 for LHCb5). These sites were isoform specific (Jansson, 1999). In the structural view of LHCb proteins, Standfuss et al. (Standfuss et al., 2005) reported that N-terminal positive residues of LHCb proteins are important in the association of LHCb trimers and cohesion of thylakoid grana. The LysAc on the LHCb N-terminal lysine residues would remove the positive charges of the lysine side chain and consequently may affect the LHCb trimer interactions and thylakoid membrane structure. In our experiments, we found the overall lysine acetylation of the peripheral LHCb was much higher than the tightly PSII-bound LHCb, although the LHCb lysine acetylation did not differ significantly between light and dark samples. This suggests that LysAc may influence the building of LHCb complexes, but may not be directly involved in shuffling LHCb complexes during state transition as is Thr38 phosphorylation (Vener et al., 2001).

In eEF-1A, we identified five potential LysAc sites and two lysine methylation sites. We showed that one of these sites, Lys-306, may be important in regulating interaction with Ca^{2+}/CaM, and thus may regulate eEF-1A function indirectly by altering protein:protein interactions. Whether calcium signaling regulates eEF-1A function in vivo is unclear at present and remains as an important topic for future studies. Acetylation of the Lys-306 site may also directly regulate eEF-1A function. In yeast EF-1α, the directed mutant E317K (equivalent to D307K in Arabidopsis eEF-1A) caused a substantial reduction in protein translation efficiency and fidelity (Sandbaken and Culbertson, 1988). As acetylation of Lys-306 would also affect charge in a similar domain of the eEF-1A protein it is reasonable to speculate that acetylation of Lys-306 might have the same effect as the E317K directed mutant of the yeast enzyme and lower protein translation fidelity. Alternatively, other functions of eEF-1A may be impacted such as actin association (Gross and Kinzy, 2005).

In addition to the characterization of LHCb and eEF-1A, we summarized other LysAc candidate sites that have potential functional implications (Supplemental Table 3.S1). One example is acetylation of Lys-252 in RbcL. In the crystal structure of the spinach Rubisco quaternary complex (L_4S_4), Lys-252 is bonded via ionic interactions with Asp-286 at the dimer interface (Knight et al., 1990). This ionic interaction is thought to be involved in the stabilization of the Rubisco hexadecameric complex (Knight et al., 1990). Acetylation of Lys-252 would neutralize the positive charge of the side chain and preclude the salt bridge with Asp-286, likely leading to less stability of the Rubisco holoenzyme. Therefore, the activity of Rubisco holoenzyme would be negatively affected (Gutteridge and Gatenby, 1995), and might explain the inhibition of Rubisco activity by acetylation that was recently observed (Finkemeier et al., 2010). Another interesting example is acetylation of Lys-178 of chloroplast ATP synthase β subunit. This residue is located in the ATP binding motif (^{172}GGAGVG<u>K</u>T^{179}) that is conserved across eukaryotic ATP synthase β subunits (Omote et al., 1992). The equivalent residue of the *E. coli* F1 ATPase β subunit (^{149}GGAGVG<u>K</u>T^{156}) when substituted with alanine or serine (to generate the K155A or K155S directed mutants, respectively) resulted in a10-fold decrease in ATP binding and 100-fold decrease in the rate of ATP catalysis (Ida et al., 1991; Omote et al., 1992). It is possible that acetylation of Lys-178 (equivalent to Lys-155 in the *E. coli* protein) would mimic the charge depletion effect of the alanine and serine substitutions, and thereby cause down regulation of ATP synthase catalytic activity.

Along with the companion paper (Finkemeier et al., 2010), our findings indicate that lysine acetylation may be an important regulatory mechanism across various pathways and processes in Arabidopsis. The findings of lysine acetylation on non-histone proteins will likely provide new insights and tools for plant biologists to engineer plants in future.

FIGURES

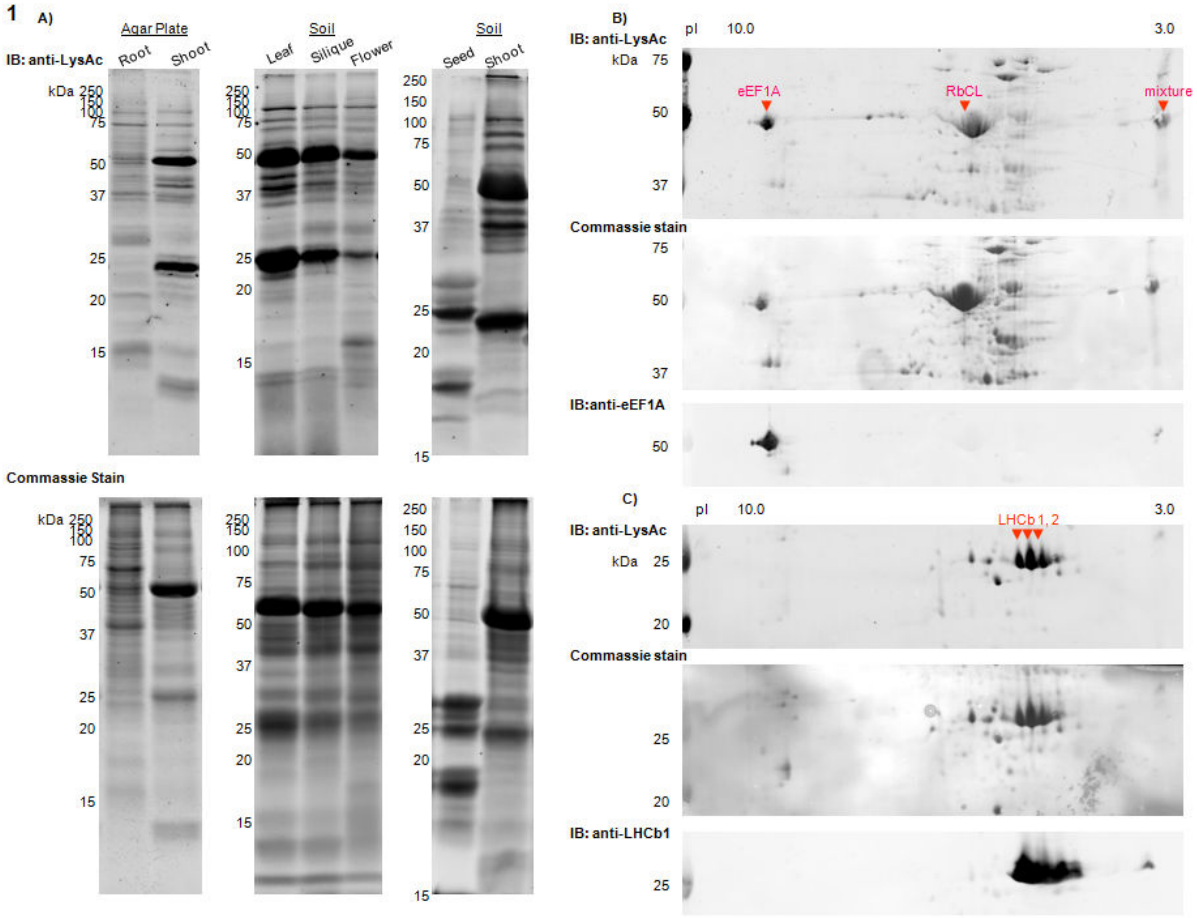


Figure 3.1 Identification of LysAc proteins by immunoblotting.

A, Representative one dimensional (1-DE) anti-LysAc immunoblots of tissues from different organs. Corresponding Coomassie stained blots are shown for comparing the level of lysine acetylation and the abundance of individual protein bands.

B, Two dimensional (2-DE) immunoblots of leaf proteins showing the 50 kDa region. eEF-1A and RbcL were two major LysAc proteins at 50 kDa.

C, 2-DE immunoblot of leaf proteins showing the 25 kDa region and identification of LHCb proteins as major LysAc proteins. The major LysAc proteins and their corresponding spots in 2-DE are indicated.

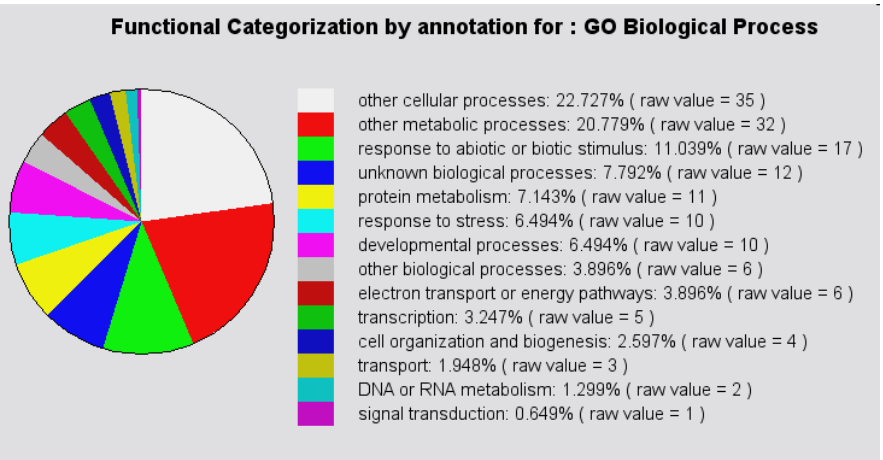


Figure 3.2 Gene ontology categorization of biological processes for identified proteins with potential LysAc sites from LC-MS analysis. The gene ontology information is based on Arabidopsis (http://www.Arabidopsis.org/tools/bulk/go/index.jsp). Categorization by cellular localization is summarized in Supplemental Fig S4.

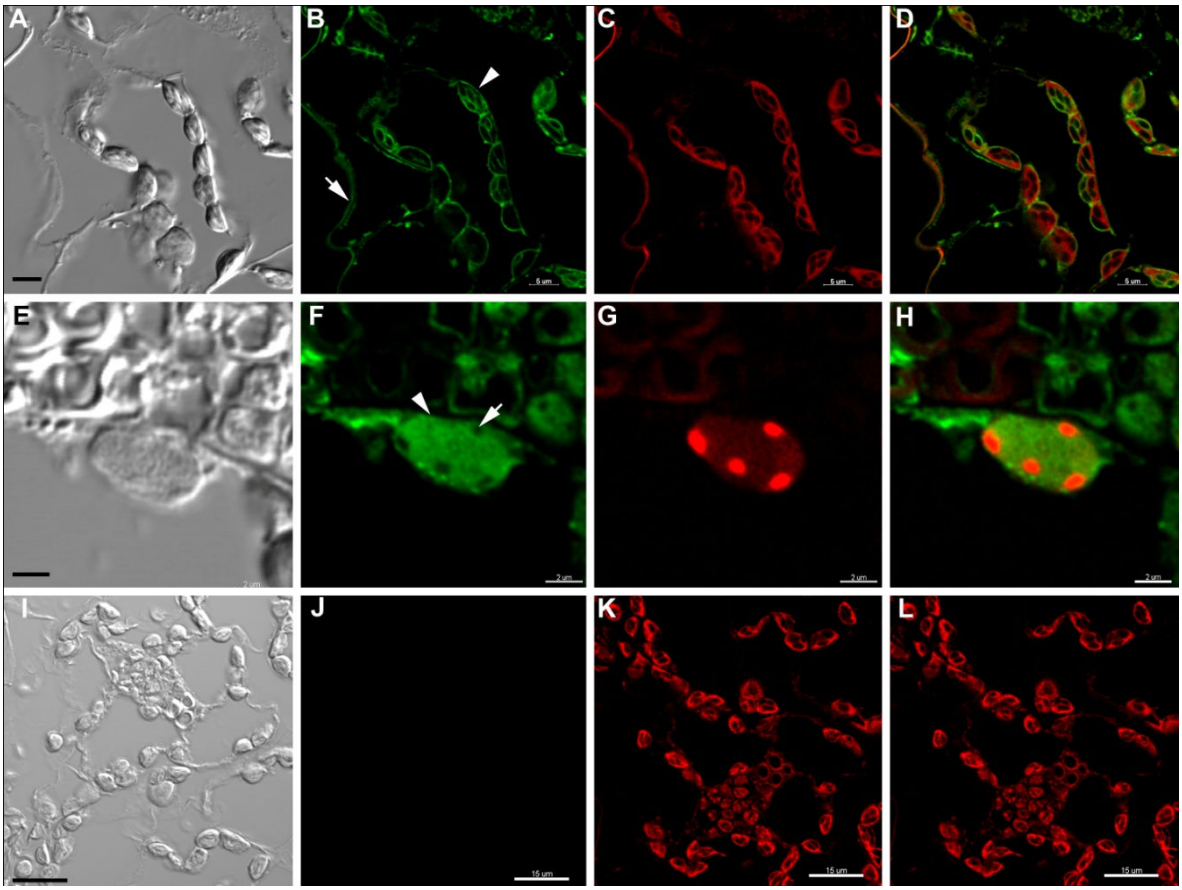


Figure 3.3 Cellular localization of LysAc proteins in Arabidopsis leaf cells by immunocytochemistry.
A-D, LysAc proteins were localized in the chloroplast membrane and plasma membrane. A, Differential interference contrast image (DIC); B, Anti-LysAc ab signals; C, FM143 membrane stain, labeling both chloroplast thylakoid membrane and plasma membrane; D, Merged image of LysAc and FM143; Scale bar 5 μm. Arrow head: chloroplast membrane (mesophyll cells). Arrow: plasma membrane (epidermal cells).
E-H, LysAc proteins were also localized in the nucleus. E, DIC; F, Anti-LysAc ab signals; G, DAPI nuclear stain; H, Merged image of LysAc and DAPI; Scale bar 2 μm. Arrow head: representative nucleus. Arrow: nucleolus inside the nucleus. The nucleolus has hypo-anti-LysAc signals compared to nuclear matrix.
I-L, Control probed only with secondary ab (without primary anti-LysAc antibodies). No false positive signals were detected. I, DIC; J, Anti-LysAc ab signals; K, Chlorophyll autofluorescence; L, Merged image of Lys Ac channel and chloroplast autofluorescence ; Scale bar 15 μm.

4

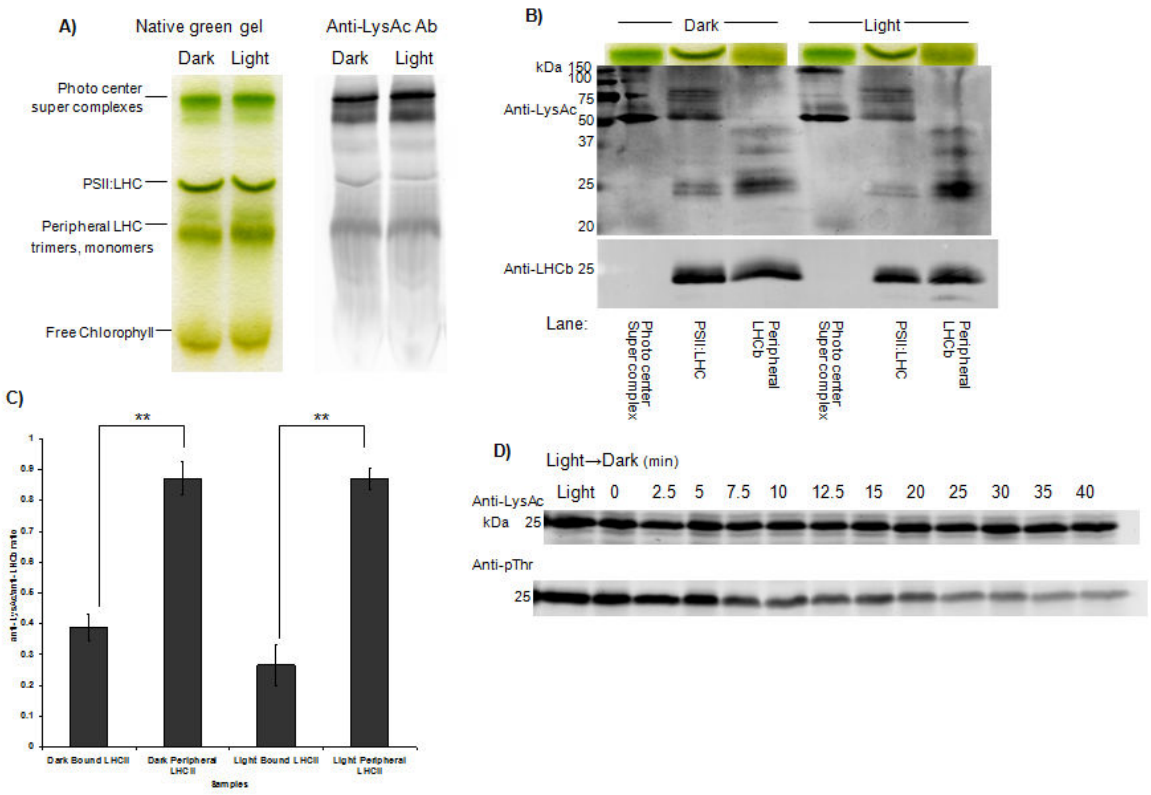


Figure 3.4 Differential lysine acetylation of peripheral LHCb versus tightly PSII-bound LHCb.
A, First dimension green native gel of solubilized thylakoid-associated proteins. Three main chlorophyll containing bands were detected by immunoblotting with anti-LysAc antibodies.B, Second dimension SDS-PAGE of the three chlorophyll-containing (and LysAc protein) bands. The peripheral pool LHCb had substantially higher LysAc levels compared to tightly PSII-bound LHCb.C, Densitometric analysis of the relative LysAc level of LHCb expressed as the ratio (anti-LysAc / anti-LHCb). ** $p < 0.0001$. Values are means of three independent experiments. Significantly higher LysAc levels for LHCb in the peripheral pool were observed in both light and dark samples.
D, Effect of a light to dark treatment on LHCb lysine acetylation and threonine phosphorylation.

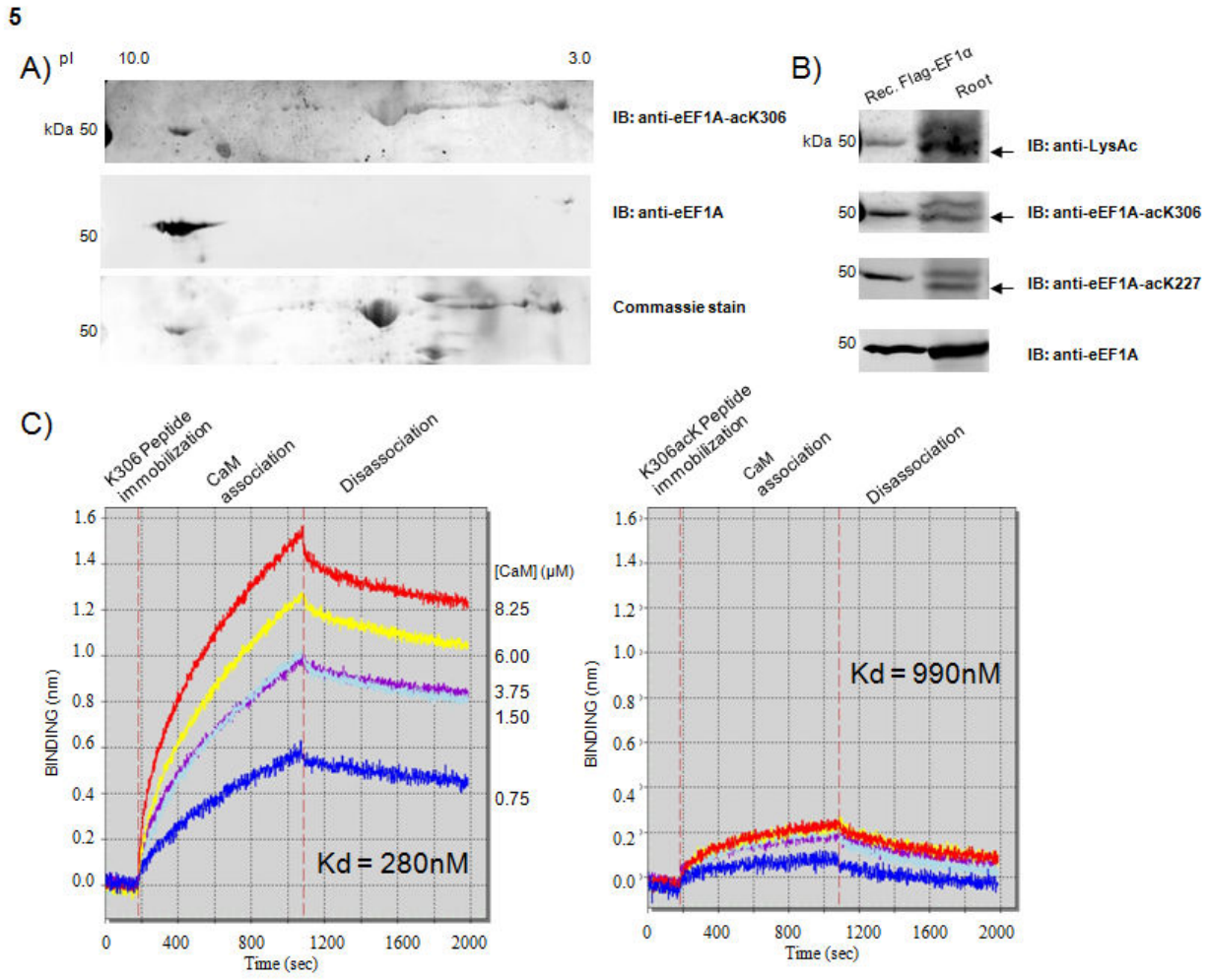


Figure 3.5 Confirmation of acetylation of eEF-1A on Lys-306 and Lys-227 and possible role in binding of Ca^{2+}/ CaM.

A, 2-DE confirmed the occurrence of LysAc K306 in shoots. The blot was sequentially probed with anti-eEF-1A-acK306 and anti-eEF-1A antibodies, before final staining with Coomassie. The modification- and site- specific antibodies also cross reacted slightly with the very abundant RbcL protein. B, 1-DE immunoblots of root samples probed with anti-LysAc, anti-eEF-1A-acK306, anti-eEF-1A-acK227, and anti-eEF-1A. The results confirm acetylation of Lys-306 and Lys-227 in the root. Note that the recombinant Flag-eEF-1A also had LysAc on both sites. C, Label-free real-time binding of Ca^{2+}/CaM to the eEF-1A-K306 synthetic peptide. Acetylation of Lys-306 (right panel) significantly decreased peptide binding to Ca^{2+}/CaM.

TABLES

Table 3.1. Summary of potential LysAc proteins and sites

Go Function	Position	Protein	AT number	Mr(expt)	Mr(calc)	Delta	Score	Peptide
Other biological processes	K252	Ribulose bisphosphate carboxylase large chain	AtCg00490, Rbcl	1949.5456	1949.9088	-0.3632	73	GHYLNATAGTCEE(ox)MI(ac)KR
Protein metabolism	K306	Eukaryotic elongation factor 1A	At5g60390, At1g07940, At1g07930, At1g07920	927.5894	927.5389	0.0505	36	NVAV(ac)KDLK
Protein metabolism	K133	ubiquitin-conjugating enzyme 29 (UBC29), E2 29	At2g16740	909.5660	909.4378	0.1283	47	(ac)KYEAMAR
Other metabolic processes	K10	Terpene synthase-like protein	At3g14490	1162.3414	1162.6597	-0.3183	22	(N-terminal-acetyl)VRD(ox)ML(ac)KSSK
Cell organization and biogenesis	K41	60S ribosomal protein L12-2	At2g37190, At3g53430, At5g60670	914.4862	914.5073	-0.0210	24	(ac)KIGEDIAK
Response to abiotic or biotic stimulus	K178	ATP synthase CF1 beta subunit	AtCg00480	2485.6756	2485.3978	0.2778	51	IGLFGGAGVG(ac)KTVLI(ox)MELINNIAK
Response to stress	K53	Disease resistance protein, phosphoinositide binding	At4g14370	820.9330	821.3701	-0.4371	41	(ac)KMDNTR
Transcription	K363	FZF; transcription factor	At2g24500	1379.6173	1379.6835	-0.0663	41	(ox)M(ac)KVMREMNKR
Developmental processes	K837	AGO1 (ARGONAUTE 1)	At1g48410	1092.5326	1092.6152	-0.0826	17	RSTGH(ac)KPLR
DNA or RNA metabolism	K764	ATP-dependent DNA helicase	At2g01440	1633.5230	1633.8821	-0.3591	22	SKCLLVGSSTNSL(ac)KR
Electron transport or energy pathways	K37	Chlorophyll a/b binding protein (LHCP AB 180)	At1g29910, At1g29920, At1g29930	2058.6688	2059.0487	-0.3799	44	R(ac)KTVAKPKGPSGSPWYGSD
Transport	K283	SEC14 cytosolic factor	At1g19650	1162.5508	1162.6234	-0.0725	19	SFLDP(ac)KTVSK

Table 3.2 Summary of Lysine modification sites in eEF-1A

Position	Modified peptides	Modification	z	m/z	d m/Z	p value	Comment
K36	LGGID(ac)KR	Acetyl_K	2	400.729	0.006	2.46E-06	
K36	LGGID(trimethyl)KR	Trimethyl_K	2	400.729	0.024	2.46E-06	
K44	FE(dimethyl)KEAAE(ox)MNKR	Dimethyl_K	3	466.206	0.028	0.00E+00	
K44	FE(methyl)KEAAEMNKR	Methyl_K	3	456.204	0.027	0.00E+00	
K55	SF(dimethyl)KYAWVLDK	Dimethyl_K	2	642.773	0.080	2.51E-10	
K79	GITIDIALW(ac)KFETTK	Acetyl_K	2	889.432	0.051	0.00E+00	
K79	GITIDIALW(trimethyl)KFETTK	Trimethyl_K	2	889.432	0.069	0.00E+00	
K187	VGYNPD(ac)KIPFVPISGFEGDNMIER	Acetyl_K	3	912.646	0.137	1.39E-33	
K187	VGYNPD(trimethyl)KIPFVPISGFEGDNMIER	Trimethyl_K	3	912.646	0.149	1.39E-33	
K227	GPTLLEALDQINEP(ac)KRPSDKPLR	Acetyl_K	3	877.021	0.127	2.18E-17	Confirmed by Ab
K227	GPTLLEALDQINEP(trimethyl)KRPSDKPLR	Trimethyl_K	3	877.021	0.139	2.18E-17	
K306	NVAV(ac)KDLK	Acetyl_K	2	465.249	-0.473	4.02E-10	Confirmed by Ab

SUPPLEMENTAL FIGURES

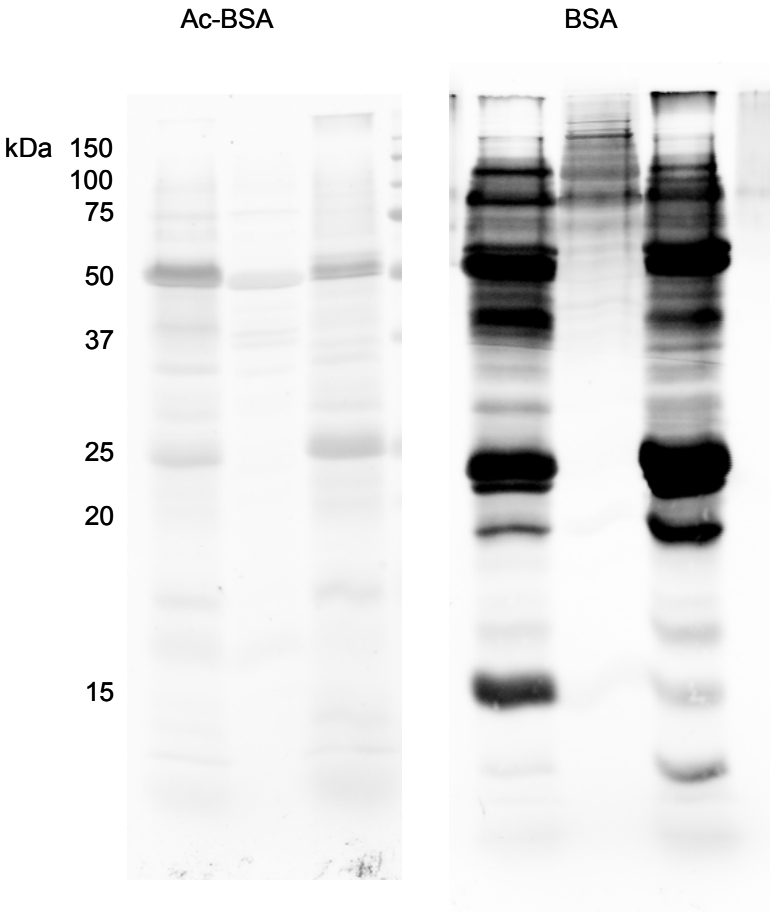


Figure 3.S1 Acetyl-BSA competition confirmed the acetylation specificity of the generic anti-LysAc antibodies.

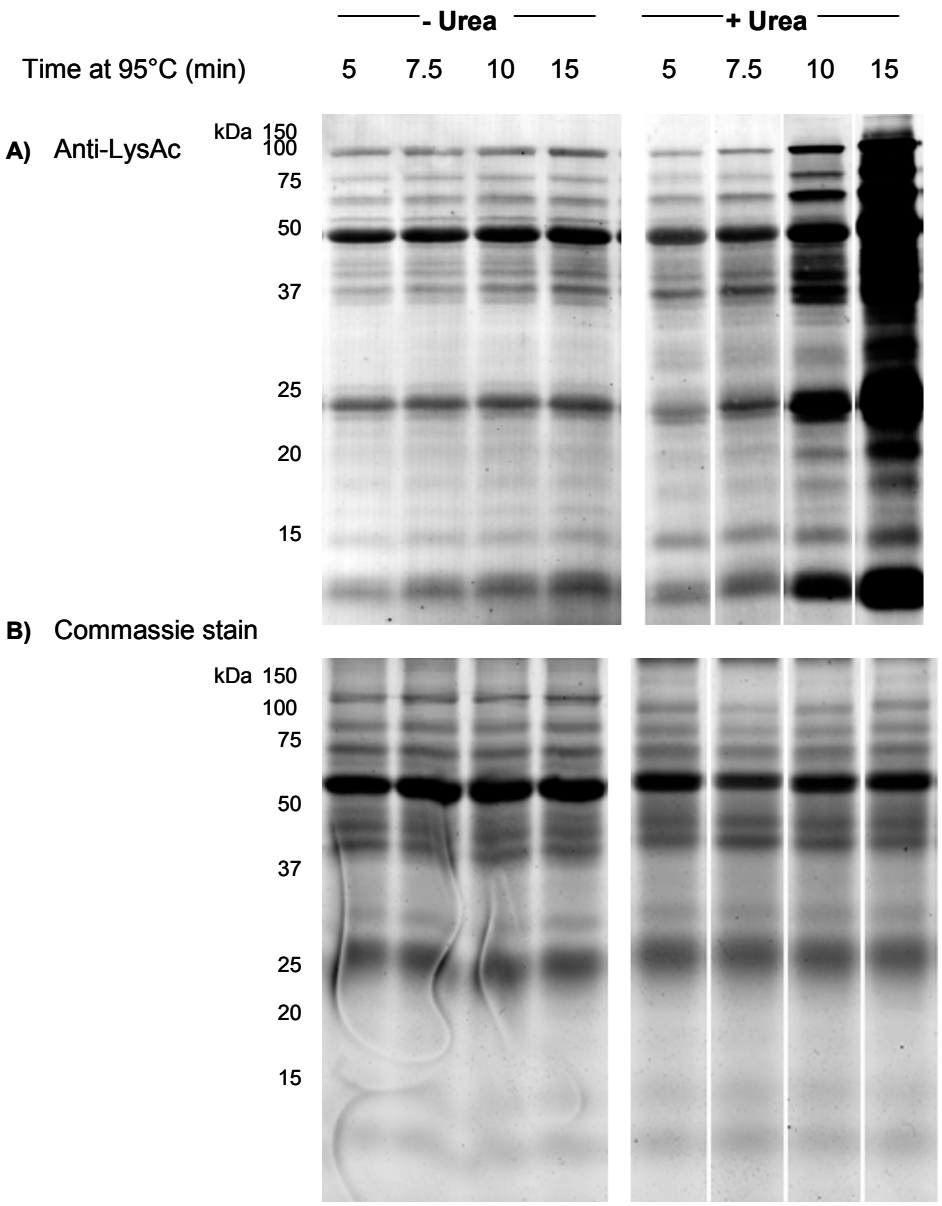


Figure 3.S2 A, Anti-LysAc antibodies cross react with carbamylated lysine residues. Extended boiling of protein extracts in SDS sample buffer (+ urea) causes chemical carbamylation of protein lysine residues. This lysine carbamylation was recognized by anti-LysAc antibodies. The artifact was dramatically minimized by removing urea from the sample buffer. B, The Coomassie stained blot showed no change in protein loading at the different time points.

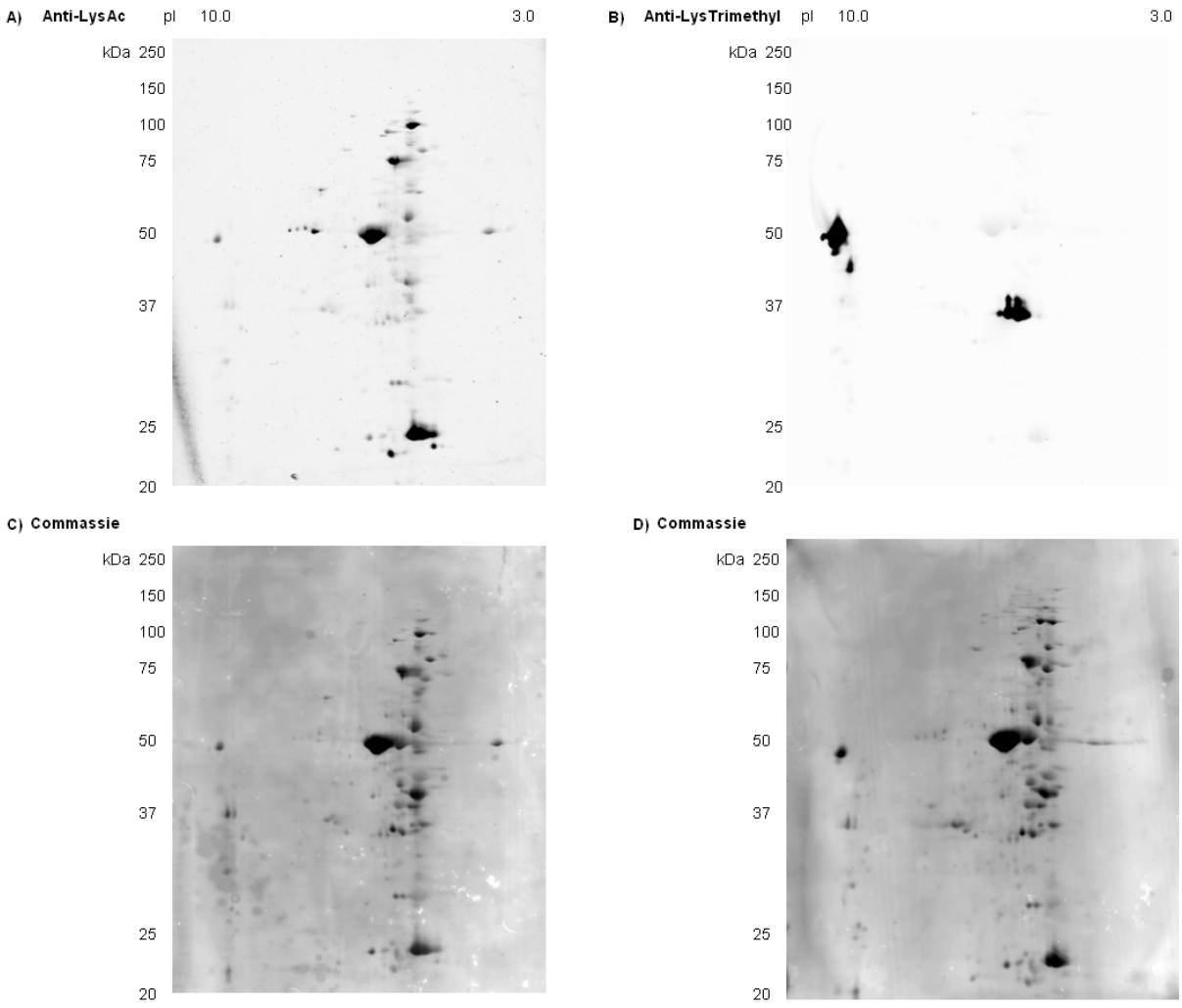


Figure 3.S3 LysAc is a more abundant protein modification compared with lysine trimethylation in Arabidopsis. Replicate 2-DE blots were probed with: A, anti-LysAc antibodies or B, anti-trimethyllysine antibodies. C- D, Corresponding Coomassie stained blots. Note that the anti-trimethyllysine antibodies only detected two clusters of proteins, one of which was eEF-1A that is also lysine acetylated.

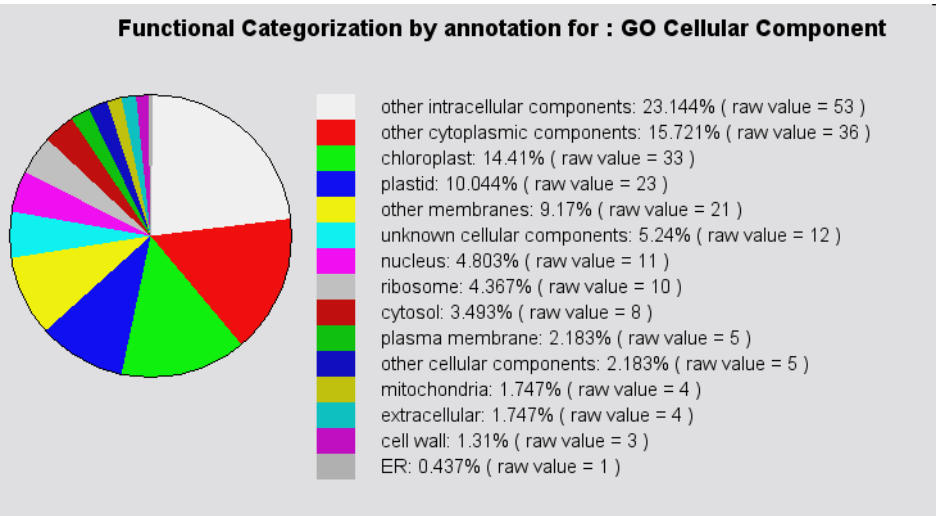


Figure 3.S4 Gene ontology categorization of cellular localization of lysine modified proteins identified by LC-MS in Arabidopsis.

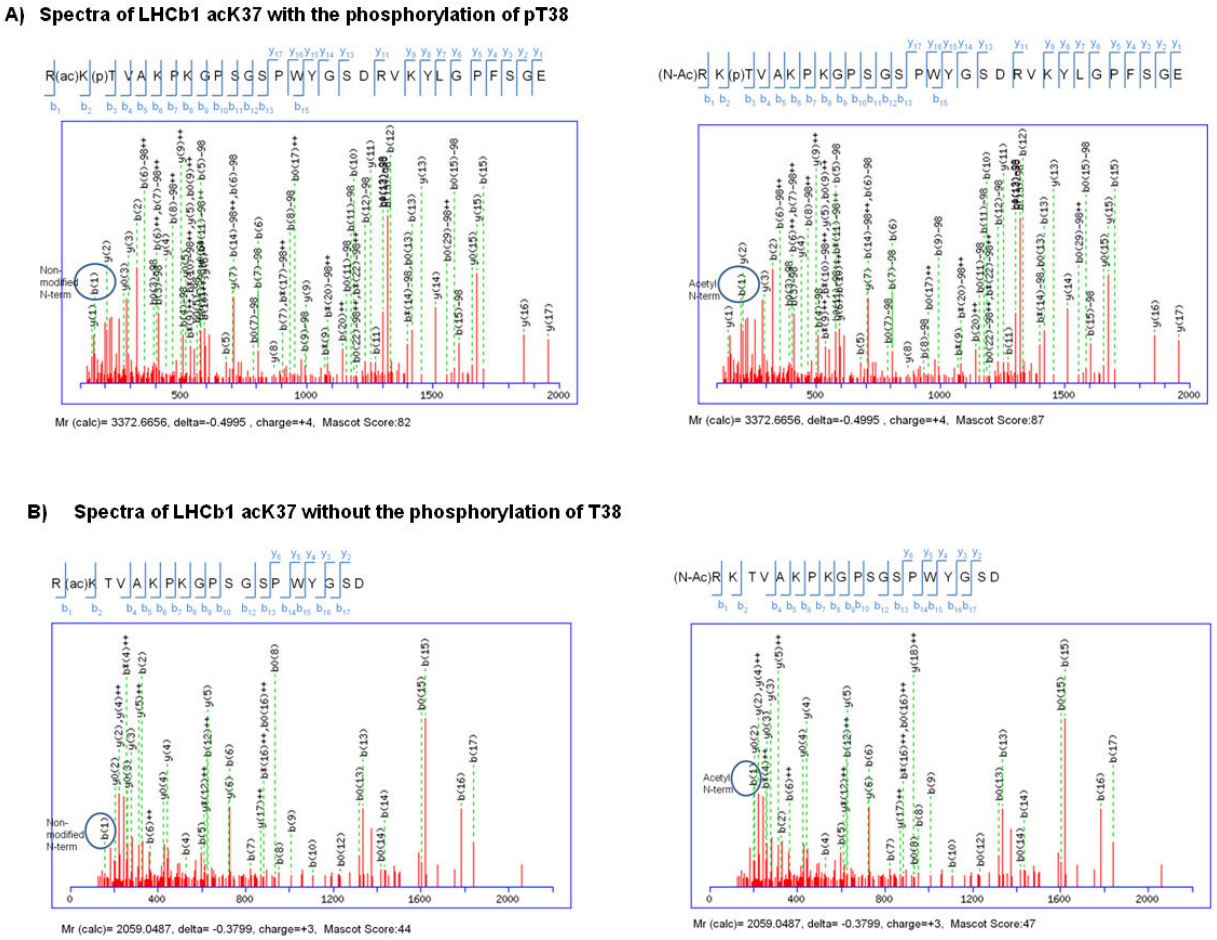


Figure 3.S5 MS/MS spectra of peptides derived from the N-terminus of LHCb1 containing acetylated Lys-37 (acK37) with (A) or without (B) phosphorylation of Thr-38. The spectra were collected from an in gel digestion of the 25 kDa band from a 1-DE gel as shown in Figure 1. Glu-C was the protease used for digestion to avoid cleavage at Lys-37. Peptides without acK37 but with N-ac-R36 were co-identified in the same peptide mixtures. However, neither double acetylation peptide (N-Ac-R36 acK37) nor null acetylation peptide (N-R36 K37) were identified in the digests.

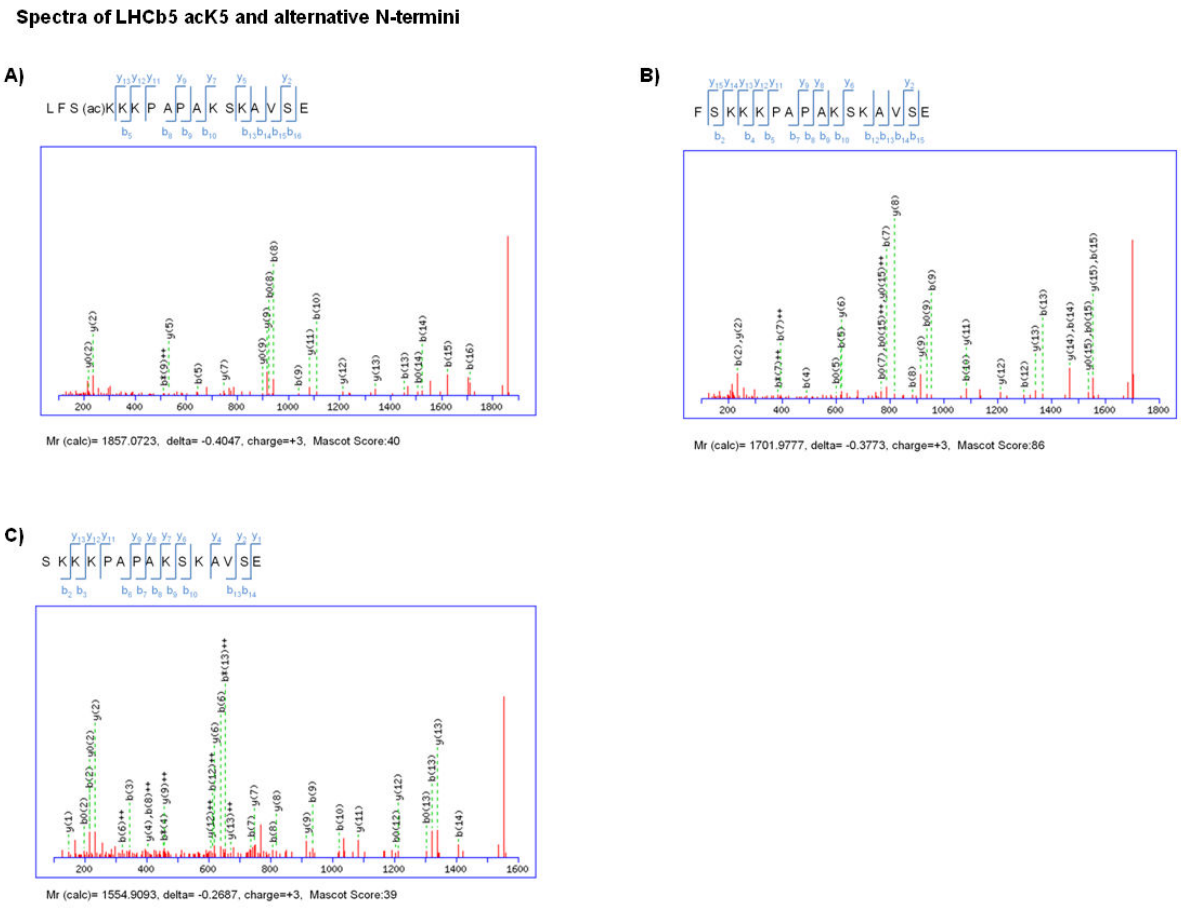


Figure 3.S6 MS/MS spectra identified acetylation of Lys-41 of LHCb5. Samples were processed as detailed in the legend of Supplemental Figure S5. Spectra shown (A-C) identified peptides with alternative N-termini of LHCb5, but only the sequence starting with Leu-38 was acetylated at Lys-41 (A).

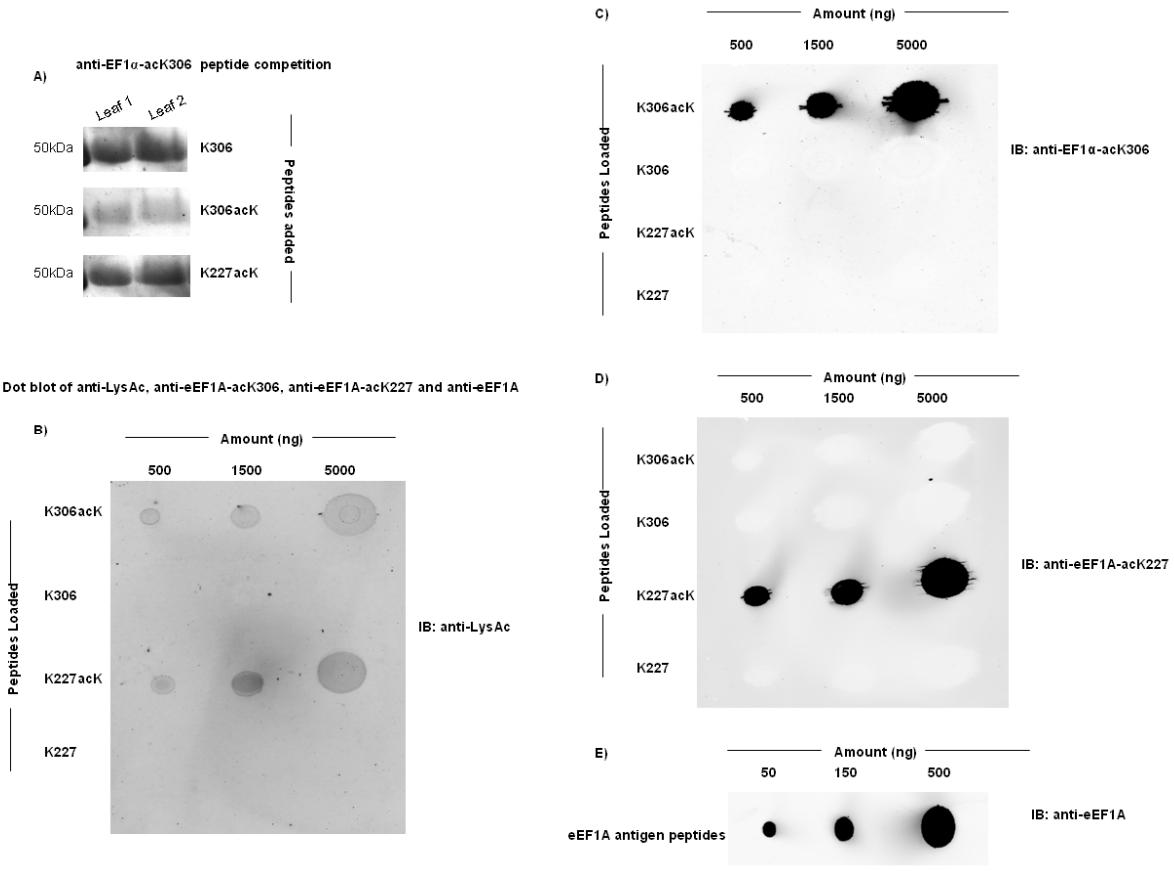


Figure 3.S7 A, Peptide competition confirmed the sequence specificity of the anti-eEF1A-acK306 antibodies. B, The generic anti-LysAc Abs cross reacted with the acetylated forms of the Lys-306 and Lys-227 peptides on dot blots. C, The anti-eEF1AacK306 and D, anti-eEF1A-acK227 antibodies only detected the acetylated form of the antigen peptides on dot blots. E, Detection of the eEF1A antigen peptide by anti-eEF-1A antibodies. In addition, immunoblot signals with all four antibodies were proportional to amount of antigen present.

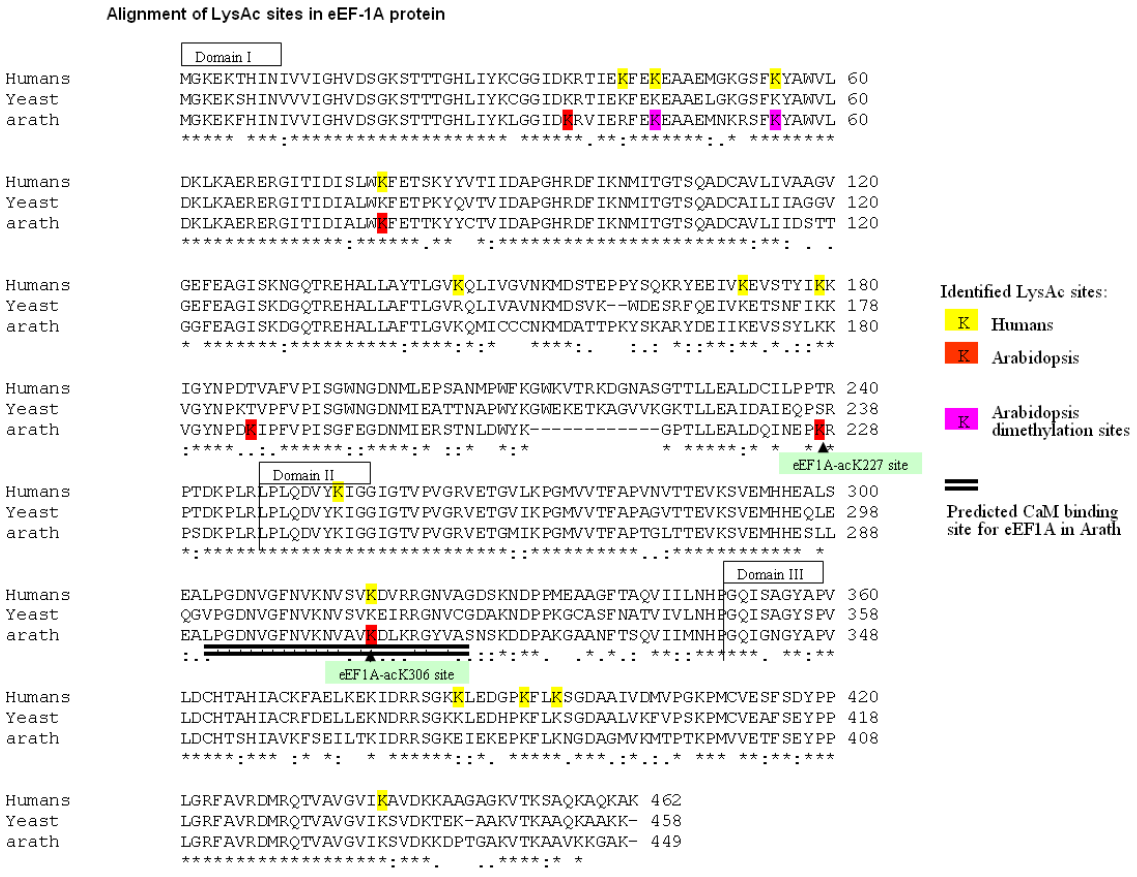


Figure 3.S8 Alignment of LysAc sites in eEF-1A protein.

SUPPLEMENTAL TABLES

Table 3.S1 Functional examples of LysAc candidate sites

Implication of the LysAc site	Position	Protein	AT number	Score	Peptide
Interfere with the inter salt bridge formation of Rubisco holoenzyme	K252	Ribulose bisphosphate carboxylase large chain	AtCg00490, Rbcl	73	GHYLNATAGTCEE(ox)MI(ac)KR
Within ATP binding domain, control ATP synthase catalytic activity	K178	ATP synthase CF1 beta subunit, chloroplastic	AtCg00480	51	IGLFGGAGVG(ac)KTVLI(ox)MELINNIAK
Inhibit translation, inhibit CaM binding	K306	Eukaryotic elongation factor 1A	At5g60390, At1g07940, At1g07930, At1g07920	36	NVAV(ac)KDLK
Play a role in LHCb trimer assoiciation	K37	Chlorophyll a/b binding protein (LHCP AB 180)	At1g29910, At1g29920, At1g29930	44	R(ac)KTVAKPKGPSGSPWYGSD
Alternative splicing	K41	Chlorophyll a-b binding protein CP26, LHCB5	At4g10340	49	LFS(ac)KKKPAPAKSKAVSE

Table 3.S2 LysAc candidate sites identified in this study

Materials	Go Function	Localization	Position	Protein	AT number	Mr(expt)	Mr(calc)	Delta	Miss Cl	Score	Peptide
Trypsin Digests											
shoot	Other biological proces	chloroplast	K252	Ribulose bisphosphate carboxyl	AtCg00490,	1949.5456	1949.9088	-0.3632	1	73	GHYLNATAGTCEE(ox)MI(ac)KR
shoot	Response to abiotic or	chloroplast, plastoglol	K178	ATP synthase CF1 beta subunit	AtCg00480	2485.6756	2485.3978	0.2778	1	51	IGLFGGAGVG(ac)KTVLI(ox)MELINN
shoot	Response to abiotic or	chloroplast, plastoglol	K178	ATP synthase CF1 beta subunit	AtCg00480	2485.6726	2485.3978	0.2748	1	46	IGLFGGAGVG(ac)KTVLI(ox)MELINN
root	Other metabolic proces	n.a.	K257	N-acetyltransferase hookless1-li	At5g67430	1140.492	1140.698	-0.206	1	29	LQV(ac)KGASRLK
shoot	Other cellular processe	chloroplast membrane	K216	33 kDa oxygen-evolving protein	At5g66570	2423.2471	2423.2737	-0.0266	1	30	VPFLFTV(ac)KQLDASGKPDSFTGK
shoot	Other cellular processe	chloroplast membrane	K216	33 kDa oxygen-evolving protein	At5g66570	2423.5612	2423.2737	0.2875	1	56	VPFLFTV(ac)KQLDASGKPDSFTGK
root	Protein metabolism, oth	ribosome, endomemb	K227	Eukaryotic elongation factor 1A	At5g60390,	2628.1221	2628.4235	-0.3014	1	91	GPTLLEALDQINEP(ac)KRPSDKPLR
root	Protein metabolism, oth	ribosome, endomemb	K79	Eukaryotic elongation factor 1A	At5g60390,	1776.8634	1776.9662	-0.1027	1	65	GITIDIALW(ac)KFETTK
root	Protein metabolism, oth	ribosome, endomemb	K79	Eukaryotic elongation factor 1A	At5g60390,	1776.8710	1776.9662	-0.0951	1	50	GITIDIALW(ac)KFETTK
shoot	Protein metabolism, oth	ribosome, endomemb	K36	Eukaryotic elongation factor 1A	At5g60390,	799.5110	799.4552	0.0559	1	23	LGGID(ac)KR
root	Protein metabolism, oth	ribosome, endomemb	K36	Eukaryotic elongation factor 1A	At5g60390,	799.4438	799.4552	-0.0113	1	26	LGGID(ac)KR
shoot	Protein metabolism, oth	ribosome, endomemb	K306	Eukaryotic elongation factor 1A	At5g60390,	927.7124	927.5389	0.1735	1	32	NVAV(ac)KDLK
shoot	Protein metabolism, oth	ribosome, endomemb	K306	Eukaryotic elongation factor 1A	At5g60390,	927.5894	927.5389	0.0505	1	36	NVAV(ac)KDLK
root	Protein metabolism, oth	ribosome, endomemb	K306	Eukaryotic elongation factor 1A	At5g60390,	927.4624	927.5389	-0.0765	1	31	NVAV(ac)KDLK
shoot	Protein metabolism, oth	ribosome, endomemb	K187	Eukaryotic elongation factor 1A	At5g60390,	2735.2684	2735.3265	-0.0581	1	57	VGYNPD(ac)KIPFVPISGFEGDNMIEI
shoot	Protein metabolism, oth	ribosome, endomemb	K187	Eukaryotic elongation factor 1A	At5g60390,	2735.3791	2735.3265	0.0526	1	55	VGYNPD(ac)KIPFVPISGFEGDNMIEI
root	Protein metabolism, oth	ribosome, endomemb	K187	Eukaryotic elongation factor 1A	At5g60390,	2735.0734	2735.3265	-0.2531	1	57	VGYNPD(ac)KIPFVPISGFEGDNMIEI
shoot	Protein metabolism, oth	ribosome, endomemb	K227	Eukaryotic elongation factor 1A	At5g60390,	2628.3433	2628.4235	-0.0802	1	75	GPTLLEALDQINEP(ac)KRPSDKPLR
shoot	Protein metabolism, oth	ribosome, endomemb	K227	Eukaryotic elongation factor 1A	At5g60390,	2628.9049	2628.4235	0.4814	1	79	GPTLLEALDQINEP(ac)KRPSDKPLR
flower	n.a.	endomembrane	K873	Putative cell expansion protein,	At5g49680,	1313.4836	1313.7779	-0.2943	2	28	IV(ac)KSSRVQISR
root	n.a.	endomembrane	K873	Putative cell expansion protein,	At5g49680,	1313.5608	1313.7779	-0.2171	2	21	IV(ac)KSSRVQISR
shoot	Developmental process	endomembrane	K141	Probable 3-ketoacyl-CoA syntha	At5g49070	883.0310	883.5239	-0.4929	2	17	KN(ac)KLSPR
root	n.a.	n.a.	K142K14	RNA recognition motif (RRM)-cc	At5g46840	799.4338	799.4552	-0.0214	2	27	(ac)KVGE(ac)KR
shoot	Response to abiotic or	chloroplast, cytosol, e	K92	Ribulose bisphosphate carboxyl	At5g38410	2365.5541	2365.1201	0.4340	1	43	(deamination)N(ac)KWIPCVEFELEH(
shoot	Response to abiotic or	chloroplast, cytosol, e	K92	Ribulose bisphosphate carboxyl	At5g38410	2365.5721	2365.1201	0.4520	1	87	(deamination)N(ac)KWIPCVEFELEH(
root	Protein metabolism, oth	n.a.	K409	DNAJ heat shock N-terminal dor	At5g37380	1059.3596	1059.5560	-0.1964	1	34	ESAD(ac)KLSLR
root	Protein metabolism, oth	n.a.	K409	DNAJ heat shock N-terminal dor	At5g37380	1059.3930	1059.5560	-0.1630	1	22	ESAD(ac)KLSLR
shoot	Other cellular processe	endomembrane	K37	Glutaredoxin-C4	At5g20500	841.4178	841.4657	-0.0479	1	27	(ac)KTISSHK
shoot	Other cellular processe	endomembrane	K37	Glutaredoxin-C4	At5g20500	841.0394	841.4657	-0.4263	1	27	(ac)KTISSHK
shoot	Other cellular processe	endomembrane	K37	Glutaredoxin-C4	At5g20500	841.0518	841.4657	-0.4139	1	29	(ac)KTISSHK
shoot	Unknown biological pro	n.a.	K180	Zinc finger (C2H2 type) family pı	At5g14140	870.5798	870.5035	0.0763	2	41	RE(ac)KLQR
root	Unknown biological pro	n.a.	K80	Calmodulin-binding protein-relat	At5g10660	1596.6354	1596.8583	-0.2229	2	32	KNNAVEENQ(ac)KLLR
shoot	Other cellular processe	n.a.	K7	SWAP (Suppressor-of-White-AF	At5g06520	1338.1996	1338.6060	-0.4064	1	25	MYTSMH(ac)KDLR
shoot	Unknown biological pro	n.a.	K294	Transducin family protein / WD-4	At4g38480,F	999.7104	999.5713	0.1392	2	33	(ac)KKDGELLR
seed	Developmental process	plasma membrane	K133	Embryo SAC development arres	At4g37890	1403.5402	1403.8071	-0.2668	2	21	LCFT(ac)KVRILNR
seed	Developmental process	plasma membrane	K134	Embryo SAC development arres	At4g37890	1403.5354	1403.8071	-0.2717	2	17	LCFT(ac)KVRILNR
seed	Developmental process	plasma membrane	K135	Embryo SAC development arres	At4g37890	1403.5388	1403.8071	-0.2682	2	16	LCFT(ac)KVRILNR
shoot	Unknown biological pro	n.a.	K519	Putative uncharacterized protein	At4g18120	1734.2986	1733.9498	0.3488	2	20	TTLMI(ac)KNIPNKYTR
shoot	Response to stress, sig	plasma membrane	K53	Disease resistance protein, phos	At4g14370	820.9330	821.3701	-0.4371	1	41	(ac)KMDNTR
root	Transcription, other me	n.a.	K217	NAC domain containing protein	At3g56530	1201.5414	1201.6918	-0.1503	1	35	AEEAENE(ac)KLK
shoot	Protein metabolism, oth	n.a.	K131	Putative uncharacterized protein	At3g49540	912.0224	912.4916	-0.4692	1	21	(ac)KAEAEPVK
shoot	n.a.	n.a.	K191	ABC transporter A family memb	At3g47770,	1199.8334	1199.6332	0.2002	0	17	MVNVS(ac)KPEVR
shoot	n.a.	n.a.	K191	ABC transporter A family memb	At3g47770,	1199.5068	1199.6332	-0.1264	1	16	MVNVS(ac)KPEVR
shoot	n.a.	n.a.	K191	ABC transporter A family memb	At3g47770,	1199.7654	1199.6332	0.1322	0	16	MVNVS(ac)KPEVR
seed	Other biological proces	endomembrane	K452	AAA-type ATPase family protein	At3g28580	1377.4162	1377.6558	-0.2395	2	17	SEKEGGETCL(ac)KR
flower	Cell organization and bi	nucleus	K27	Histone H3	At3g27360	956.3624	956.5291	-0.1666	1	55	(ac)KSAPATGGVK
seed	Unknown biological pro	n.a.	K7	Unnamed protein	At3g21320,	1107.4484	1107.5602	-0.1118	2	16	(N-terminal-acetyl) (ox)MMMKLA(ac)K
seed	Unknown biological pro	n.a.	K8	Unnamed protein	At3g21320,	1107.4484	1107.5602	-0.1118	2	15	(N-terminal-acetyl) (ox)MMMKLA(ac)K
shoot	Transcription, other me	nucleus	K66	GATA transcription factor 17, zir	At3g16870	1087.2172	1087.5920	-0.3748	2	39	(ac)KRQAALG(ox)MR
shoot	Unknown biological pro	n.a.	K462	Transposable element gene; hA	At3g14800	1808.8456	1808.8727	-0.0270	1	26	NQDNFLSSLAANM(ac)KAK
flower	Other metabolic proces	chloroplast	K10	Terpene synthase-like protein	At3g14490	1162.3414	1162.6597	-0.3183	1	22	(N-terminal-acetyl)VRD(ox)ML(ac)KS

Table 3.S2 cont-

shoot	Unknown biological pro	n.a.	K492	Pentatricopeptide (PPR) repeat-	At3g13770	898.5332	898.4872	0.0460	1	19	AVT(ac)KEPGR
seed	Protein metabolism, oth	extracellular	K136	Pectate lyase family protein	At3g09540	1325.4122	1325.8143	-0.4021	3	22	GQ(ac)KVKITGKGLR
seed	Protein metabolism, oth	extracellular	K136	Pectate lyase family protein	At3g09540	1325.4122	1325.8143	-0.4021	3	20	GQ(ac)KVKITGKGLR
shoot	Cell organization and bi	ribosome	K41	60S ribosomal protein L12-2	At2g37190,	914.4862	914.5073	-0.0210	1	24	(ac)KIGEDIAK
shoot	Cell organization and bi	ribosome	K41	60S ribosomal protein L12-1; FL	At2g37190,	957.5068	957.5131	-0.0062	1	40	(N-term carbamylation) (ac)KIGEDIAK
root	Cell organization and bi	ribosome, membrane	K4	60S ribosomal protein L12-2	At2g37190,	1794.7936	1794.9880	-0.1944	1	57	(ethyl)PP(ac)KLDPSQIVDVYVR
shoot	Developmental process	nucleus	K383	ADP-ribosylation factor GTPase	At2g35210	1007.4118	1007.4593	-0.0475	1	29	N(ox)MAEET(ac)KK
shoot	Response to stress, res	nucleus	K6K9K13I	Histone H4; DNA binding	At2g28740	1437.7700	1437.8052	-0.0351	4	80	G(ac)KGG(ac)KGLG(ac)KGGA(ac)KF
shoot	Response to stress, res	nucleus	K6K9K13I	Histone H4; DNA binding	At2g28740	1438.0842	1437.8052	0.2791	4	89	G(ac)KGG(ac)KGLG(ac)KGGA(ac)KF
shoot	Developmental process	ribosome	K90	60S ribosomal protein, L10a-2	At2g27530,	1476.5756	1476.7316	-0.1560	1	56	MGLSNMDVEAL(ac)KK
shoot	Transcription, other me	Intracellular	K363	FZF; transcription factor, encode	At2g24500	1379.6173	1379.6835	-0.0663	3	41	(ox)M(ac)KVMREMNKR
shoot	Transcription, other me	Intracellular	K363	FZF; transcription factor, encode	At2g24500	1379.9089	1379.6835	0.2253	3	36	(ox)M(ac)KVMREMNKR
shoot	Protein metabolism, oth	n.a.	K133	Ubiquitin-conjugating enzyme 2	At2g16740	909.5660	909.4378	0.1283	1	47	(ac)KYEAMAR
shoot	Protein metabolism, oth	n.a.	K133	Ubiquitin-conjugating enzyme 2	At2g16740	909.4276	909.4378	-0.0101	1	47	(ac)KYEAMAR
shoot	Protein metabolism, oth	n.a.	K133	Ubiquitin-conjugating enzyme 2	At2g16740	909.4348	909.4378	-0.0029	1	46	(ac)KYEAMAR
seed	DNA or RNA metabolism	n.a.	K764	Putative ATP-dependent DNA h	At2g01440	1633.5230	1633.8821	-0.3591	2	22	SKCLLVGSSTNSL(ac)KR
shoot	Other biological proces	extracellular	K94	GDSL esterase/lipase EXL4	At1g75910	1217.8040	1217.6404	0.1636	1	13	(ac)KLFNSPSDLR
shoot	Developmental process	nucleus, cytosol	K837	AGO1 (ARGONAUTE 1),encode	At1g48410	1092.5326	1092.6152	-0.0826	1	17	RSTGH(ac)KPLR
shoot	Unknown biological pro	n.a.	K5	Unknown protein, F2J6.14	At1g43760	643.3798	643.4017	-0.0218	1	26	LSV(ac)KR
flower	Other biological proces	n.a.	K7K10	Auxin-responsive family protein	At1g29430	914.3324	914.5623	-0.2298	2	20	(ac)KLM(ac)KLAK
root	Other biological proces	n.a.	K7K10	Auxin-responsive family protein	At1g29430	914.4764	914.5623	-0.0858	2	20	(ac)KLM(ac)KLAK
flower	Other cellular processe	mitochondria, plasma	K81	CYTC-1 (Cytochrom C-1); electr	At1g22840	1378.4898	1378.7496	-0.2598	1	61	ALYDYLLNP(ac)KK
shoot	Transport	endomembrane	K283	SEC14 cytosolic factor, putative	At1g19650	1162.5508	1162.6234	-0.0725	1	19	SFLDP(ac)KTVSK
shoot	Unknown biological pro	n.a.	K607	Aminoacyl-tRNA synthetase fam	At1g18950	943.5014	943.5385	-0.0371	3	54	A(ac)KK(ox)MPRR
shoot	Unknown biological pro	n.a.	K607	Aminoacyl-tRNA synthetase fam	At1g18950	943.4772	943.5385	-0.0613	3	42	A(ac)KK(ox)MPRR
shoot	Protein metabolism, oth	n.a.	K204	Ubiquitin-conjugating enzyme 3	At1g17280	1088.9732	1088.5098	0.4635	1	20	GDSEGGL(ac)KER
shoot	Protein metabolism, oth	n.a.	K204	Ubiquitin-conjugating enzyme 3	At1g17280	1088.9828	1088.5098	0.4731	1	17	GDSEGGL(ac)KER
shoot	Protein metabolism, oth	n.a.	K204	Ubiquitin-conjugating enzyme 3	At1g17280	1088.4758	1088.5098	-0.0339	1	24	GDSEGGL(ac)KER
root	Response to stress, res	n.a.	K92	Putative disease resistance prot	At1g10920	1006.4566	1006.6148	-0.1581	3	17	GI(ac)KKHARR
root	Unknown biological pro	n.a.	K131	Putative uncharacterized protein	At1g02380	913.4450	913.6072	-0.1622	3	23	KSL(ac)KRLK

n.a: unknown

Glu-C Digests

Materials	Go Function	Localization	Position	Protein	AT number	Mr(expt)	Mr(calc)	Delta	Miss Cl	Score	Peptide
shoot	Protein metabolism, oth	membrane, mitochon	K227	Eukaryotic elongation factor 1A	At5g60390	4208.9291	4209.2546	-0.3255	1	42	ALDQINEP(ac)KRPSDKPLRLPLQDV
shoot	Developmental process	n.a.	K180	WD40 repeat-like	At5g50230	1373.5246	1373.7224	-0.1978	1	21	EMLA(ac)KLKANGLE
shoot	Unknown biological pro	chloroplast	K3	Putative uncharacterized protein	At5g41110	1233.4934	1233.6023	-0.1089	0	19	MD(ac)KVNLSRTE
shoot	n.a.	n.a.	K25	Putative uncharacterized protein	At4g37600	1018.3906	1018.4753	-0.0847	0	19	AQ(ac)KNMLQE
shoot	Transcription, other cell	neucleus	K4	Basic helix-loop-helix (bHLH) fa	At4g16430	982.3576	982.4218	0.0642	1	21	(ox)MGQ(ac)KFWE
shoot	Electron transport or en	chloroplast	K41	Chlorophyll a-b binding protein (	At4g10340	1856.6677	1857.0723	-0.4047	0	40	LFS(ac)KKKPAPAKSKAVSE
shoot	Electron transport or en	chloroplast	K41	Chlorophyll a-b binding protein (	At4g10340	1856.7382	1857.0723	-0.3342	0	37	LFS(ac)KKKPAPAKSKAVSE
shoot	Electron transport or en	chloroplast	K41	Chlorophyll a-b binding protein (	At4g10340	1856.7816	1857.0723	-0.2907	0	49	LFS(ac)KKKPAPAKSKAVSE
shoot	Transcription, other me	nuclei	K200	Transcription factor	At3g11100	1373.5370	1373.7224	-0.1854	1	24	GK(ac)KQQIMIELE
shoot	Protein metabolism, oth	n.a.	K668	Unknown protein	At2g17110	1101.4838	1101.5562	-0.0724	0	22	M(ac)KMVLVGPGE
shoot	Transport, response to	plasma membrane	K148	PHO1-like protein	At1g68740	1517.5964	1517.7838	-0.1873	0	20	LKDAFKQ(ac)KQANGE
shoot	Transport, response to	plasma membrane	K148	PHO1-like protein	At1g68740	1517.5864	1517.7838	-0.1973	0	21	LKDAFKQ(ac)KQANGE
shoot	Unknown biological pro	n.a.	K206	Mitochondrial transcription termi	At1g62010	1304.5116	1304.7340	-0.2223	0	15	(ac)KFDASLKKVVE
shoot	n.a.	endomembrane	K453	AAA-type ATPase family protein	At1g43910	1374.4274	1374.7870	-0.3596	1	18	FLENKKLK(ac)KGE
shoot	Electron transport or en	chloroplast	K37	Chlorophyll a/b binding protein (	At1g29910,	2058.6688	2059.0487	-0.3799	0	44	R(ac)KTVAKPKGPSGSPWYGSD
shoot	Electron transport or en	chloroplast	K37	Chlorophyll a/b binding protein (	At1g29910,	3372.1661	3372.6656	-0.4995	0	82	R(ac)K(p)TVAKPKGPSGSPWYGSDF

n.a: unknown

REFERENCES

Abdiche Y., Malashock D., Pinkerton A., Pons J. (2008) Determining kinetics and affinities of protein interactions using a parallel real-time label-free biosensor, the Octet. Anal Biochem. 377: 209-217.

Allen K.D., Staehelin L.A. (1991) Resolution of 16 to 20 chlorophyII-protein complexes using a low lonic strength native green gel system. Anal Biochem. 194: 214-222.

Andersen G.R., Valente L., Pedersen L., Kinzy T.G., Nyborg J. (2001) Crystal structures of nucleotide exchange intermediates in the eEF1A-eEF1Balpha complex. Nat Struct Biol. 8: 531-534.

Carroll A.J., Heazlewood J.L., Ito J., Millar A.H. (2008) Analysis of the Arabidopsis cytosolic ribosome proteome provides detailed insights into its components and their post-translational modification. Mol Cell Proteomics 7: 347-369.

Choudhary C., Kumar C., Gnad F., Nielsen M.L., Rehman M., Walther T.C., Olsen J.V., Mann M. (2009) Lysine acetylation targets protein complexes and co-regulates major cellular functions. Science 325: 834-840.

Durso N.A., Cyr R.J. (1994) A calmodulin-sensitive interaction between microtubules and a higher plant homolog of elongation factor-1 alpha. Plant Cell 6: 893-905.

Eberharter A., Becker P.B. (2002) Histone acetylation: a switch between repressive and permissive chromatin. Second in review series on chromatin dynamics. EMBO Rep. 3: 224-229.

Finkemeier I., Laxa M., Miguet L., Howden A.J., Sweetlove L.J. (2010) Proteins of diverse function and subcellular location are lysine-acetylated in Arabidopsis. Plant Physiol. 155: 1779-1790.

Galetskiy D., Susnea I., Reiser V., Adamska I., Przybylski M. (2008) Structure and dynamics of photosystem II light-harvesting complex revealed by high-resolution FTICR mass spectrometric proteome analysis. J Am Soc Mass Spectrom. 19: 1004-1013.

Glozak M.A., Sengupta N., Zhang X., Seto E. (2005) Acetylation and deacetylation of non-histone proteins. Gene 363: 15-23.

Gross S.R., Kinzy T.G. (2005) Translation elongation factor 1A is essential for regulation of the actin cytoskeleton and cell morphology. Nat Struct Mol Biol. 12: 772-778.

Gutteridge S., Gatenby A.A. (1995) Rubisco synthesis, assembly, mechanism, and regulation. Plant Cell 7: 809-819.

Hoeflich K.P., Ikura M. (2002) Calmodulin in action: diversity in target recognition and activation mechanisms. Cell 108: 739-742.

Ida K., Noumi T., Maeda M., Fukui T., Futai M. (1991) Catalytic site of F1-ATPase of *Escherichia coli*. Lys-155 and Lys-201 of the beta subunit are located near the gamma-phosphate group of ATP in the presence of Mg2+. J Biol Chem. 266: 5424-5429.

Jackson J., Johnson L., Jasencakova Z., Zhang X., PerezBurgos L., Singh P., Cheng X., Schubert I., Jenuwein T., Jacobsen S. (2004) Dimethylation of histone H3 lysine 9 is a critical mark for DNA methylation and gene silencing in Arabidopsis thaliana. Chromosoma 112: 308-315.

Jansson S. (1999) A guide to the Lhc genes and their relatives in Arabidopsis. Trends Plant Sci. 4: 236-240.

Kim S.C., Sprung R., Chen Y., Xu Y., Ball H., Pei J., Cheng T., Kho Y., Xiao H., Xiao L., Grishin N.V., White M., Yang X.J., Zhao Y. (2006) Substrate and functional diversity of lysine acetylation revealed by a proteomics survey. Mol Cell. 23: 607-618.

Knight S., Andersson I., Branden C.I. (1990) Crystallographic analysis of ribulose 1,5-bisphosphate carboxylase from spinach at 2.4 A resolution. Subunit interactions and active site. J Mol Biol. 215: 113-160.

Lopez-Valenzuela J.A., Gibbon B.C., Hughes P.A., Dreher T.W., Larkins B.A. (2003) eEF1A isoforms change in abundance and actin-binding activity during maize endosperm development. Plant Physiol. 133: 1285-1295.

Michel H., Griffin P.R., Shabanowitz J., Hunt D.F., Bennett J. (1991) Tandem mass spectrometry identifies sites of three post-translational modifications of spinach light-harvesting chlorophyll protein II. Proteolytic cleavage, acetylation, and phosphorylation. J Biol Chem. 266: 17584-17591.

Oh M.H., Wang X., Kota U., Goshe M.B., Clouse S.D., Huber S.C. (2009) Tyrosine phosphorylation of the BRI1 receptor kinase emerges as a component of brassinosteroid signaling in Arabidopsis. Proc Natl Acad Sci U S A. 106: 658-663.

Omote H., Maeda M., Futai M. (1992) Effects of mutations of conserved Lys-155 and Thr-156 residues in the phosphate-binding glycine-rich sequence of the F1-ATPase beta subunit of *Escherichia coli*. J Biol Chem. 267: 20571-20576.

Sandbaken M.G., Culbertson M.R. (1988) Mutations in elongation factor EF-1 alpha affect the frequency of frameshifting and amino acid misincorporation in Saccharomyces cerevisiae. Genetics 120: 923-934.

Shevchenko A., Tomas H., Havlis J., Olsen J.V., Mann M. (2007) In-gel digestion for mass spectrometric characterization of proteins and proteomes. Nat. Protocols 1: 2856-2860.

Smith M.D., Ghosh S., Dumbroff E.B., Thompson J.E. (1997) Characterization of thylakoid-derived lipid-protein particles bearing the large subunit of ribulose-1,5-bisphosphate carboxylase/oxygenase. Plant Physiol. 115: 1073-1082.

Soppe W.J.J., Jasencakova Z., Houben A., Kakutani T., Meister A., Huang M.S., Jacobsen S.E., Schubert I., Fransz P.F. (2002) DNA methylation controls histone H3 lysine 9 methylation and heterochromatin assembly in Arabidopsis. EMBO J. 21: 6549-6559.

Standfuss J., Terwisscha van Scheltinga A.C., Lamborghini M., Kuhlbrandt W. (2005) Mechanisms of photoprotection and nonphotochemical quenching in pea light-harvesting complex at 2.5 A resolution. EMBO J. 24: 919-928.

Tessadori F., Chupeau M-C., Chupeau Y., Knip M., Germann S., van Driel R., Fransz P., Gaudin V. (2007) Large-scale dissociation and sequential reassembly of pericentric heterochromatin in dedifferentiated Arabidopsis cells. J Cell Sci. 120: 1200-1208.

Tian L., Chen Z.J. (2001) Blocking histone deacetylation in Arabidopsis induces pleiotropic effects on plant gene regulation and development. Proc Natl Acad Sci U S A. 98: 200-205.

Vener A.V., Harms A., Sussman M.R., Vierstra R.D. (2001) Mass spectrometric resolution of reversible protein phosphorylation in photosynthetic membranes of *Arabidopsis thaliana*. J Biol Chem. 276: 6959-6966.

Vlachonasios K.E., Thomashow M.F., Triezenberg S.J. (2003) Disruption mutations of ADA2b and GCN5 transcriptional adaptor genes dramatically affect Arabidopsis growth, development, and gene expression. Plant Cell 15: 626-638.

Wan L., Ross A.R., Yang J., Hegedus D.D., Kermode A.R. (2007) Phosphorylation of the 12 S globulin cruciferin in wild-type and abi1-1 mutant *Arabidopsis thaliana* seeds. Biochem J. 404: 247-256.

Wang Q., Zhang Y., Yang C., Xiong H., Lin Y., Yao J., Li H., Xie L., Zhao W., Yao Y., Ning Z.B., Zeng R., Xiong Y., Guan K.L., Zhao S., Zhao G.P. (2010) Acetylation of metabolic enzymes coordinates carbon source utilization and metabolic flux. Science 327: 1004-1007.

Zhang J., Sprung R., Pei J., Tan X., Kim S., Zhu H., Liu C.F., Grishin N.V., Zhao Y. (2009) Lysine acetylation is a highly abundant and evolutionarily conserved modification in *Escherichia coli.* Mol Cell Proteomics 8: 215-225.

Zhang K., Yau P.M., Chandrasekhar B., New R., Kondrat R., Imai B.S., Bradbury M.E. (2004) Differentiation between peptides containing acetylated or tri-methylated lysines by mass spectrometry: an application for determining lysine 9 acetylation and methylation of histone H3. Proteomics 4: 1-10.

Zhao S., Xu W., Jiang W., Yu W., Lin Y., Zhang T., Yao J., Zhou L., Zeng Y., Li H., Li Y., Shi J., An W., Hancock S.M., He F., Qin L., Chin J., Yang P., Chen X., Lei Q., Xiong Y., Guan K.L. (2010) Regulation of cellular metabolism by protein lysine acetylation. Science 327: 1000-1004.

CHAPTER 4: CONCLUDING REMARKS

This dissertation concerns two major PTMs in Arabidopsis – protein phosphorylation and lysine acetylation. We demonstrated that the two modifications can concur to a single protein, such as 14-3-3ω. Eight Ser/Thr residues (Thr-41, Thr-83, Thr-94, Ser-120, Thr-140, Thr-151, Ser-157, Thr-255) of 14-3-3ω were identified to be the phosphorylation sites targeted by BRI1-BAK1 complex. Lysine residue (Lys-53) of 14-3-3ω was identified as one of the acetyl-lysine sites. The acetylation mutant K53E of 14-3-3ω resulted in considerable loss of its phosphorylation by BRI1-BAK1 complex, indicating the two modifications were inter-connected. Moreover, the acetylation mutant K53E also lost its binding to BRI1 and BAK1, while the phosphorylation of 14-3-3ω appeared to enhance the binding to BRI1 and BAK1, which revealed the possible antagonistic effects of the two modifications on 14-3-3ω.

In Chapter 2, the phosphorylation of 14-3-3ω by BRI1 and BAK1 proteins was investigated in the context of BR signaling. It was shown that 14-3-3ω can be co-immunoprecipitated with BRI1-BAK1 complex in vivo. The co-immunoprecipitated 14-3-3ω was phosphorylated at Thr-94 and Thr-140 sites, and the phosphorylation was enhanced upon the activation of BRI1 and BAK1 kinases. The data suggest a new link of 14-3-3 protein phosphorylation in BR signaling. In addition, the binding of 14-3-3ω evidently enhanced the kinase activity of BRI1. Likewise, the phosphorylation of 14-3-3ω increased the co-immunoprecipitated 14-3-3ω by BRI1 from approximate 20% to 40% of the input, indicating the strong relationship of 14-3-3ω phosphorylation and its binding. Thus, we tentatively proposed a positive role of 14-3-3ω binding and phosphorylation through BRI1 proteins in BR signaling, which is a new addition to the current model of BR intracellular signaling (Figure 1.2).

The occurrence of lysine acetylome in Arabidopsis was explored in Chapter 3, and we identified 64 lysine modification peptides on 57 proteins, which potentially operate in a wide variety of pathways and processes and are located in various cellular compartments. In particular, a group of photosynthesis-related proteins was first identified to undergo lysine acetylation. The proteins that function from light harvesting, electron transport and ATP synthesis, to CO_2 fixation, carbon reduction and RuBP regeneration were all represented (Table 4.1). We further tested the role of lysine acetylation on light harvesting protein LHCb1. We found that the acetylation of LHCb1 was much higher in the LHCb1 that was loosely bound to

photoreaction center PSII as opposed to the LHCb1 that was tightly bound to PSII, which suggest the role of LysAc in modulating the interactions between LHCb1 and PSII and may directly affect the efficiency of photochemical quenching. In addition, the in silico modeling predicted the acetylation of RbCL Lys-252 and Lys-356 may interrupt the inter/intra-molecule salt bridge of the Rubisco complex and may decrease the stability and activity of the holoenzyme. This prediction was confirmed experimentally in a recent publication (Finkemeier et al., 2011). These results highlighted the functional relevance of lysine acetylation in photosynthesis. Thus, in addition to the redox control, lysine acetylation may provide another strategy to engineer plants towards higher photosynthetic efficiency.

Collectively, the dissertation indicated that protein phosphorylation and lysine acetylation are two functionally important and related modifications in Arabidopsis and hold a considerable promise in agricultural applications.

TABLES

Table 4.1 Summary of LysAc proteins related to photosynthesis identified in Chapter3

AT number	Protein annotation	Site of LysAc	Peptides	Cal Mass	Expt Mass	Score	Instrument
At1g29910, At1g29920, At1g29930	Chlorophyll a/b binding protein (LHCb1)	K37	R(ac)KTVAKPKGPSGSPWYGSD	2059.0487	2058.6688	44	Q-TOF
		K37	R(ac)K(p)TVAKPKGPSGSPWYGSDRVKYLGPFSGE	3372.6656	3372.1661	82	Q-TOF
At4g10340	Chlorophyll a-b binding protein CP26 (LHCb5)	K41	LFS(ac)KKKPAPAKSKAVSE	1857.0723	1856.7816	49	Q-TOF
At5g66570	Photosystem II reaction center subunit, 33 kDa oxygen-evolving protein	K216	VPFLFTV(ac)KQLDASGKPDSFTGK	2423.2737	2423.5612	56	Q-TOF
At1g03130	Photosystem I reaction center subunit II-2, psaD2	K187	SIG(ac)KNVSPIEVK	1312.7474	1312.7474	39	FTMS
AtCg00480	ATP synthase CF1 beta subunit, chloroplastic	K178	IGLFGGAGVG(ac)KTVLI(ox)MELINNIAK	2485.3978	2485.6756	51	Q-TOF
AtCg00490	Ribulose bisphosphate carboxylase large chain, RbcL	K356	DDYVE(ac)KDR	1081.4803	1081.4803	43	FTMS
		K252	GHYLNATAGTCEE(ox)MI(ac)KR	1949.9088	1949.5456	73	Q-TOF
At5g38410	Ribulose bisphosphate carboxylase small chain, Rbcs	K92	(deamination)N(ac)KWIPCVEFELEHGFVYR	2365.1201	2365.5721	87	Q-TOF
At1g12900, At3g26650	Glyceraldehyde-3-phosphate dehydrogenase A subunit 2 (GAPA-2)	K265	VPTPNVSVVDLVVQVS(ac)K	1822.0328	1822.0328	79	FTMS

APPENDIX: THE ORIGIN OF THE NON-RECOMBINING REGION OF SEX CHROMOSOMES IN *CARICA* AND *VASCONCELLEA*[3]

INTRODUCTION

The small family Caricaceae consists of six genera and 35 species, of which 32 are dioecious. The three non-dioecious species are from the genera *Carica* and *Vasconcellea*, including trioecious *C. papaya* and *V. cundinamarcensis* and monoecious *V. monoica*. These two closely related sister genera were once classified as two sections in the genus *Carica*. However, recent molecular and DNA marker data clearly separated these two sections, resulting in the reinstatement of these two genera (Aradhya et al., 1999; Badillo, 2000; Van Droogenbroeck et al., 2002; Kyndt et al., 2005; Ming et al., 2005). *Carica papaya* is the only species in the genus *Carica*, while *Vasconcellea* is the largest genus in the family including 21 species with monoecious (1), dioecious (19), and trioecious (1) all represented. These two genera are still considered the most closely related in the family, as intergeneric hybridization is possible with embryo rescue (Manshardt and Wenslaff, 1989). Many traits in *Vasconcellea* have the potential for papaya improvement, such as the resistance to papaya ringspot virus (PRSV) from *V. caulifora*, the pleasant fragrances of *V. stipulate*, the cold tolerance of *V. cundinamarcensis*, the ornamental qualities of pink flowered *V. parliflora*, and the monoecious habit of *V. monoica* (Manshardt and Wenslaff, 1989).

Dioecy results in outcrossing that enhances genetic diversity and is known to have a fitness advantage. Sex chromosomes have evolved multiple times independently in animals, plants, and fungi (Graves and Shetty, 2001; Fraser et al., 2004; Ming and Moore, 2007). Sex chromosomes reinforce dioecy and result from the selective pressure to link two sex determination mutations, one promoting maleness and the other suppressing femaleness (Charlesworth and Charlesworth, 1978; Charlesworth, 1991). These sex determination loci were permanently linked when suppression of recombination occurred in this region and a "proto-Y (or Z)" was formed. The absence of recombination leads to the accumulation of deleterious mutations, the degeneration of the Y (or Z) chromosome, and the formation of heteromorphic sex chromosome pairs as seen in

[3] The research of this chapter was conducted during my rotaion period in Dr. Ray Ming lab. The central content of this chapter has been published in the article Wu et al. (2010) Plant J. 63: 801-810.

ancient sex chromosome systems. A broad definition of sex chromosomes could be simply that they contain sex determination genes, even without the suppression of recombination at the sex determining region, as in strawberry (Spigler et al., 2008). A more strict definition would include suppression of recombination at the sex determining region and degeneration of its gene content, as demonstrated in ancient human sex chromosomes and nascent sex chromosomes in plants and fish (Skaletsky et al., 2003; Liu et al., 2004, Peichel et al., 2004, Yin et al., 2008).

Papaya is one of the two trioecious species in the family and sex determination is controlled by primitive sex chromosomes (Liu et al., 2004). When compared with the 166 million years old human sex chromosomes, papaya sex chromosomes are at the beginning stage of its evolution, started about 2 to 3 million years ago (Yu et al., 2008a). Dioecy appears to be ancestral in the family Caricaceae since no hermaphroditic species exist in the family. Papaya sex chromosomes are likely evolved from an ancestral sex determination system, shared at least with *Vasconcellea*, if not the entire family, because intergeneric crosses between *Carica* and *Vasconcellea* species showed no functional complementation for sex determination, indicating their sex determination genes are allelic (Magdalita et al., 1997).

Papaya has an XY system with two slightly different Y chromosomes, a male-specifice Y and a hermaphrodite Y^h (Ming et al., 2007a). At least one X chromosome is required for the survival genotypes: XX female, XY male, and XY^h hermaphrodite -- YY, Y^hY^h, and YY^h, are embryonic lethal. Moreover, the Y and Y^h chromosomes are mutually exclusive,and no papaya has been found with XYY, XYY^h, or XY^hY^h genotype. Both Y and Y^h chromosomes contain a small male specific region (MSY) about 8-9 Mb with low gene density and a high level of repetitive sequences (Yu et al., 2007, 2008a, b; Ming et al., 2008). The MSY in papaya is pericentric and likely includes the centromere (Zhang et al., 2008).

The first six papaya sex-linked genes were identified in two MSY BACs and two corresponding X BACs, including four genes on the MSY and six genes on the X (Yu et al., 2008a). These six genes were named based on their sequential location on the BACs following the example of the *Silene* sex linked genes (Filatov and Charlesworth, 2002; Nicolas et al., 2005). Four X/Y^h gene pairs were analyzed and the estimated divergence time between the X and Y^h chromosomes was 2-3 million years (Yu et al., 2008a), perhaps after the speciation event of *C. papaya* that occurred more than 3 million years ago (Aradhya et al., 1999). These results indicated that sex chromosomes could not be ancestral in the family Caricaceae. Recombination

between the X and Y chromosomes in the MSY region might have been suppressed in the past 2 to 3 million years and the X and Y sequences have diverged, sharing about 83-86% genomic sequence identity (Yu et al., 2008a, b). However, the Y and Y^h homologous BACs shared 98.8% sequence identity including the repetitive sequence, and the estimated time of divergence is about 73,000 years (Yu et al., 2008b). Considering the prevalence of dioecy in the family Caricaceae, the hermaphroditic papayas are likely evolved from the males with the Y chromosome.

Currently, it is unknown whether sex chromosomes exist in other genera of Caricaceae. The only species that is certain to have no sex chromosomes is the monoecious species *V. monoica*, because there is no sexual dimorphism among individual plants. The objective of this study was to assess the MSY homologous regions in selected *Vasconcellea* species to test whether sex chromosomes have evolved in *Vasconcellea* and if so, whether the origin of sex chromosomes was before or after the speciation events of these two genera and within *Vasconcellea*.

MATERIALS AND METHODS

Plant materials and sex allele identification

Five *Vasconcellea* species were studied concerning the homologs of papaya six sex-linked genes, including one trioecious species, *V. cundinamacensis*, three dioecious species, *V. parviflora, V. goudotiana* and *V. pulchra*, and one monoecious species, *V. monoica*. Genomic DNA was extracted using standard protocols from different sex types of the five *Vasconcellea* species, along with gynodioecious papaya variety SunUp and dioecious papaya Au9. For the allele identification in *Vasconcellea* species, the X allele sequencse were obtained from the female plant with XX genotypes; the Y allele sequences were obtained from the male plant (XY genotype) if clear sequence variations were observed after compared with the X allele of the same species. For papaya, sex specific alleles were obtained from the sex specific BAC (Yu et al., 2008a).

Degenerate primer design and degenerate PCR

The six papaya sex-linked genes in this studied were designated based onYu et al. (2008a). Autosomal *ANKYRIN* was used as the control gene. The conserved regions of each gene were selected for designing degenerate primers with the criteria of at least 20bp in length and less than 96 degeneracy. The inosines were used as neutral base match at the most divergent positions. Partial codons were included at the end of the primers for specific match.

The degenerate PCR were performed following: 1×reaction buffer, 150 μM dNTP, 1.25 μM degenerate primer or 0.5 μM specific primer,and 2 units of EconoTaq (Lucigen #30031-1, Middleton, WI, USA), 5ng genomic DNA template. The PCR program included: 94 °C 5min; 40 cycles of [94°C 30 sec, 50°C 45 sec,72°C 40 sec ~ 2min (varied by the PCR product size)]; 72 °C 10min; and 4°C for ever.

Cloning and Sequencing

The specific PCR products were purified with PCR Clean-Up Kit (Promega #A9282, Madison, WI, USA) and cloned into pGEM-T EASY vector (Promega #A1360) following the manufacturer's instructions. The ligation products were transformed into JM109 competent cells (Promega). Positive colonies were confirmed by colony PCR, with T7-pro primer (5'-GTAATACGACTCACTATAGGGC-3') and M13Rev-48 primer (5' GAACAGCTATGACCATGATTAC-3'). Plasmids of positive colonies were isolated and adjusted to concentration at 100~200 ng/μl for sequencing using both T7-pro and M13Rev-48 primers at UIUC Core Sequencing Facility (Urbana, IL, USA). Each gene fragment was sequenced at least twice to eliminate any sequence error.

Primer walking

Once the gene sequences derived from *Vasconcellea* species were available, sequence of specific primers were designed from the conserved regions of the available sequences to amplify the genes in those species that could not be amplified by degenerate primers. For the continual coverage of the target gene sequence, nested sequence-specific primers were designed to further extend the sequences.

DNA sequence divergence analysis

Pairs of sequences were sequentially aligned in the BioEdit program (Hall, 1999). The alignments were exported in .nex format file to be analyzed in the Dnasp 4.20 program (Rozas et al., 2003). Exons and introns of the X and Y gene pairs amplified from *Vasconcellea* species were designated based on the papaya gene sequence structure. The numbers of synonymous substitution per synonymous site (K_s), nonsynonymous substitution per nonsynonymous site (K_a), and synonymous and non-coding substitution per silent site (K_{sil}) were calculated according to the method of Nei and Gojobori (1986) and implemented in DnaSP 4.20 (Rozas et al., 2003).

Divergence times of X/Y pairs from each species were determined using the program BEAST v1.4 (Drummond et al, 2006; Drummond and Rambaut, 2007). We used an uncorrelated Bayesian relaxed-clock model with branch rates independently drawn from an exponential distribution with a mean substitution rate of 7.1×10^{-9} substitutions/site/year, which is the mean mutation rate in *A. thaliana* based on mutation accumulation experiments (Ossowski et al., 2010). This substation rate was used as a prior as opposed to providing calibration times for internal nodes, as fossil calibration times are not available for the divergence of *C. papaya* and *Vasconcellea* species. For each gene, the combined results of two runs with 10,000,000 steps is presented.

In a self-assemble Perl scripts, location of specific point mutations, changes of coding amino acids were documented.

Phylogenetic analysis

Multiple sequences were first aligned in ClustalW program (Larkin et al., 2007), and then, the alignments were export to MEGA (4.0) (Tamura et al., 2007) for Neighbour-joining and Maximum Parsimony analysis (both used 1000 replications for bootstrap). The alignments were also exported to MrBayes (3.1.2) (Huelsenbeck and Ronquist, 2001) for Bayesian analysis (GTR+ invgamma model, 500,000 generations). The maximum likelihood analysis was performed in PhyML 3.0 (Guindon and Gascuel, 2003) with GTR model and the best of NNIS SPRS tree topology. Homologs of *Arabidopsis thaliana* were used as outgroup in all gene tree analyses.

Gene conversion analysis

We used GENCOV (1.81 version) for gene conversion analysis. Both the global and pairwise comparison was conducted for 10,000 permutations. The fragments with higher significance than Karlin-Altschul P value were recorded (Sawyer, 1989).

RESULTS

The six X/Y gene pairs selected for this experiment are located on two pairs of papaya X/Y homologous BACs, Genes 1-3 on X/Y BACs SH53E18 and SH85B24 (GenBank Accession No. EF661026 and EF661024) and Genes 4-6 on X/Y BACs SH61H02 and SH95B12 (GenBank Accession No. EF661023 and EF661025). These two pairs of BACs are 4-5 Mb apart spanning about 60% of the 8-9 Mb papaya MSY and the gene numbers are based on their positions on the BACs (Figure A.S1). The X/Y allelic sequences of the six target genes were amplified from *Vasconcellea* species, including pairs of Genes 1 and 3 that have not been reported before. Distinct X and Y alleles of Gene 1 were obtained from three dioecious and one trioecious species, but only the X allelic form was obtained from the monoecious species *V. monoica*. For the other five gene pairs, we only obtained fragments of both sex types from one to three *Vasconcellea* species, despite our numerous attempts. The difficulty was mainly attributed to large introns and possible sequence variations. The autosomal gene *ANKYRIN* was amplified from all five *Vasconcellea* species with only one allelic form.

The X alleles of Genes 1, 2, and 3 in papaya were located on the X-specific BAC SH53E18 (Table A.S1), while the Y allele of Genes 2 was on the Y-specific BAC SH85B24 (Gene 3 was deleted from the MSY) (Yu et al., 2008a). The Y allele of Gene 1 was not identified until a MSY BAC SH69A08 was sequenced recently (GenBank Accession No. AM778093). The available sequences enabled us to locate Gene 1, which was 1.7 Mb away from BAC SH85B24. The X allele of papaya Gene 1 encoded 684 amino acids in 19 exons and the closest match to the sequence is the protein kinase-like protein from *Arabidopsis thaliana* (AT5G14720). In contrast, the Y allele encoded 678 amino acids, with a truncation of 6 amino acid residues in exon 15 (truncated sequence: LLNFTA). Since Gene 1 was predicted as a kinase-like protein, we also conducted a sequence search in the RCSB Protein data Bank (PDB). The N-terminal amino acid

sequence of Gene 1 had 43% (125/292) identity to Human STE20-like kinase 3 (MST3, STK24, PDB accession: 2j51, Pike et al., 2008), which is on the long arm of the human X chromosome (NCBI: HsX_11943).

Partial coding sequences of the six X/Y gene pairs (Genes 1- 6) and the autosomal gene *Ankyrin* were analyzed to determine the degree of synonymous (K_s) and nonsynonymous (K_a) divergence between them within species and between X alleles or Y alleles between species. The ratio of nonsynonymous to synonymous divergence (K_a/K_s) between the X and Y alleles can be assessed to infer the degree of functional constraint and the level of divergence. The total number of synonymous and nonsynonymous sites, mutations, and the degree of divergence were summarized in Table A.1 and Tables A.S2-6. All six X/Y gene pairs had K_a/K_s ratios that were less than 1, indicating functional constraint. For Gene 1 that was covered in all six species, K_a/K_s ratios ranged from 0.07 to 0.51 within species X vs. Y alleles, from 0 to 0.31 between species X vs. X alleles, and from 0.07 to 0.74 between species Y vs. Y alleles.

Besides the K_a/K_s ratios, the number of synonymous and nonsynonymous mutations is also an indication of the level of divergence. Within *Vasconcellea* species, the number of synonymous mutations between X/Y alleles ranged from 0 to 8 and nonsynonymous mutations from 1 to 7 (Table A.1). Between genera (ie. *Carica papaya* vs *Vasconcellea* species), the number of synonymous and nonsynonymous mutations increased to 13 – 30 and 6 – 24, respectively, for the X allele, and to 12 - 32 and 8 – 23 for the Y allele. Between *Vasconcellea* species, the number of synonymous and nonsynonymous mutations was 1 – 6 and 0 – 3, respectively, for the X allele, and 0 - 12 and 0 – 8 for the Y allele. Similar patterns were observed for the other 5 X/Y gene pairs (Table A.S2-S6).

For the autosomal gene *ANKYRIN*, the K_a/K_s ratios were from 0.05 to 0.13 between *Carica* and *Vasconcellea* species and from 0.32 to 0.49 among *Vasconcellea* species (Table A.2). The number of synonymous and nonsynonymous mutations was 12 and 2, respectively, for all five pair wise comparisons between *Carica* and *Vasconcellea* species, whereas the numbers ranged from 0 to 2 and 0 to 3 among *Vasconcellea* species. It should be noted that six pair wise comparisons of *ANKYRIN* showed no synonymous or nonsynonymous mutation among *Vasconcellea* species.

Divergence times of X/Y pairs from each species were determined using the uncorrelated Bayesian relaxed-clock model with branch rates independently drawn from an exponential

distribution with a mean substitution rate of 7.1×10^{-9} substitutions/site/year (Ossowski et al., 2010) as implemented in the software, BEAST 1.4 (Drummond et al, 2006; Drummond and Rambaut, 2007). For *C. papaya*, mean divergence times ranged from 0.57 to 5.4 mya for X/Y alleles (Table A.3), consistent with previous reports of the relatively recent divergence of the X and Y chromosome in this species (Yu et al., 2008a, b). The mean divergence time of the *C. papaya* male Y and hermaphroditic Y^h was consistently more recent than the X/Y divergence, ranging from 0.13 to 0.32 mya, supporting the hypothesis that hermaphrodites derived from males in the recent past. The estimated divergence times of the *Vasconcellea* species' allele pairs was on par with that found for *C. papaya* X/Y alleles. Estimated divergence times ranged from 0.89 to 4.4 mya for *V. goudotiana*, 0.80 to 3.1 mya for *V. pulchra*, 0.7 to 2.0 mya for *V. parviflora*, and 0.64 to 2.8 mya for *V. cundinamarcensis*. For all genes, the divergence times for all X/Y pairs were more recent than the mean divergence time of *Carica* from *Vasconcellea* species (6.8 to 14.6 mya), indicating independent evolution of X/Y alleles in these genera.

We tested for the existence of evolutionary strata on the *C. papaya* MSY by comparing the mean estimated divergence times of the X/Y alleles of genes 1-3 to the mean estimated divergence of genes 4-6; these groups of genes are found on separate BAC clones and are physically separated on the MSY by 4-5 Mbp. Although the mean divergence time for genes 4-6 (3.2 ± 1.1 mya) was almost twice that of genes 1-3 (1.7 ± 0.30 mya), these ages were not significantly different (t-test, $P > 0.05$). Thus, the presence of evolutionary strata is not supported based on this limited survey of MSY genes.

We analyzed the phylogenies of X/Y alleles (or triplets for papaya) among *C. papaya* and *Vasconcellea* species using Baysean method (Figure A.1). Except for Gene 4 (exon 1-2), *C. papaya* X, Y, and Y^h alleles formed a cluster that clearly separated from their *Vasconcellea* homologs in five of the six phylogenetic trees. Among *C. papaya* X, Y and Y^h alleles, the Y and Y^h alleles formed a sub-cluster before joining the X allele in Genes 4 (exon 7-18), 5, and 6.

All amplified X/Y alleles for *V. pulchra* clustered together (Genes 1, 2 and 4), as did the for *V. parviflora* (Genes 1, 3 and 4). The X/Y alleles of *V. goudotiana* was clustered in Genes 2 and 4, but not in Genes 1 and 6. Likewise, the X/Y alleles of *V. cundinamarcensis* was positioned in cluster in Gene 6, but not in Gene 1. In autosomal gene *ANKYRIN, V. monoica* was closest to *V. goudotiana*.

To verify the phylogenetic relationships, we examined single nucleotide polymorphisms (SNP) between *Carica* and *Vasconcellea*. If the sex chromosomes evolved after a speciation event, the SNP haplotype would differ between species, but not within species between the X and Y alleles. Indeed, this type of SNP haplotypes is prevalent in our data. For example, at Gene 1, exon 1, bp 45, papaya X and Y have "GAA" coding for glutamic acid, whereas all *Vasconcellea* species had "GAT" coding aspartic acid. At Gene 1, exon 1, bp 51, both papaya X and Y had "AAA" coding for lysine, but all the *Vasconcellea* species shared "AAG" also coding for lysine. Twenty polymorphic synonymous mutations and three nonsynonymous mutations were found with this pattern in the 800 bp Gene 1 exon 1-2. For the exon fragments of other genes, the SNP haplotypes of papaya are also more identical between X and Y alleles than across species. Only a few exceptions were found where only one allelic form of papaya mutated, while the other remained identical to those of *Vasconcellea* species. As shown at Gene 1, exon 1, bp 30, the papaya Y allele had a CCT synonymous mutation for proline, while the *Vasconcellea* species shared CCC codon, the same papaya X allele. Likewise, at Gene 1, exon 1, bp 105, where the papaya X allele was "TGT" (cysteine) but the Y allele coded "TGC" (cysteine), the common codon in all five *Vasconcellea* species. Nevertheless, these exceptions would not change the general conclusion that X-Y (Y^h) chromosome system in papaya evolved independently of the *Vasconcellea* genus.

SNP haplotypes from *V. pulchra* and *V. parviflora* appeared to support independent evolution of nascent sex chromosomes in each of these two species. At Gene 2, exon 6, bp 141, both X and Y alleles of *V. pulchra* shared codon "CTA" coding for leucine, whereas the other four *Vasconcellea* species shared the synonymous codon "CTC". At Gene 5, exon 11, bp 323, the X and Y alleles of *V. parviflora* shared codon "GTA" coding for proline, whereas the other four *Vasconcellea* species shared the synonymous codon "GTG".

Close examination of Gene 1 sequences showed that most variations were at the C-terminal exons. For the allele of the monoecious *V. monoica*, a deletion of two amino acid residues 'KY' occurred at bp 23-28 of exon 16. For both X and Y alleles of *V. parviflora*, an insertion of guanine at bp 12 of exon 18 resulted in a frameshift mutation for 12 amino acid residues from 'PSTPRERELMAQ' to 'RFYSWRERAHSA'. For X allele of *V. goudotiana*, a single nucleotide polymorphism (SNP) at bp 44 of exon 15 resulted in the change from TCA (Y allele sequence) to TAA (X allele sequence), a premature stop codon, whereas the Y allele coded for serine.

We examined the possibility of gene conversion of these X/Y gene pairs using the GENECONV software (Sawyer, 1989, 1999). No gene conversion was detected in Gene 3 and the autosomal gene *Ankyrin*. For the remaining five genes, only short fragments in six of the 24 pairs of sequences within species appeared to have gene conversion, including 707 bp of Gene 1 in *V. parviflora*, 111 bp sequence of Gene 2 in *V. pulchra* , 95 bp of Gene 4 in papaya, 252 bp of Gene 5 in papaya , 157 bp of of the Gene 6 in *V. cundinamarcensis*, and 371 bp of Gene 6 in *V. goudotiana* (Table A.S7). We reconstructed the phylogenetic trees after removing those sequences with gene conversion, and the resulting trees remained the same as in Figure A.1.The limited amount of gene conversion corroborated our conclusion that the divergence between MSY and its X counterpart is the consequence of recombination suppression at the sex determining region in the course of sex chromosome evolution.

A summary diagram representing the evolution of the sex chromosomes in *Vasconcellea* and *C. papaya* clade in a simplified form is shown in Figure A.2.

DISCUSSIONS

Sexual reproduction increases genetic diversity and generates novel allele combinations for natural selection to act on (Weismann, 1889; Goddard et al., 2005; Paland and Linch, 2006). The emergence of sex chromosomes requires the suppression of recombination in the genomic region harboring the sex determination genes, which leads to the degeneration of the Y (if male heterogametic) or Z (if female heterogametic) chromosome and the divergence of X/Y (or Z/W) alleles (Charlesworth and Charlesworth, 1978, Charlesworth, 1991, Ming et al., 2007b). After the primitive sex chromosomes were uncovered in papaya (Liu et al., 2004), a follow up question is whether such sex chromosomes exist in other genera of Caricaceae. We investigated selected species of *Vasconcellea*, the closest relatives of *Carica*, using six sex-linked genes cloned in papaya (Yu et al., 2008a, b). Distinctive X- and Y-specific alleles in three dioecious and one trioecious *Vasconcellea* species were identified, whereas only one allelic form was identified in the monoecious species *V. monoica*. Synonymous and nonsynonymous mutations were found between X and Y alleles and the estimated divergence times between the X and Y alleles in *Vasconcellea* species ranged from 0.64 to 4.4 mya. In contrast, only one allelic form of the

autosomal gene *Ankyrin* was found in each species, and no synonymous and nonsynonymous mutations were found in 6 of the 10 pair wise comparisons among five *Vasconcellea* species. Our results demonstrated that sex chromosomes had evolved in at least some, if not all, dioecious and trioecious *Vasconcellea* species.

The six X/Y gene pairs used in this experiment are 4-5 Mb apart, spanning more than half the 8-9 Mb papaya MSY (Yu et al., 2008a). The identification of X and Y allelic forms of six orthologous genes in *Carica* and *Vasconcellea* indicated their sex chromosomes evolved from the same ancestral autosomes. It is likely that *Carica* and *Vasconcellea*, if not the entire family, share the same ancestral sex determination genes that triggered sex chromosome evolution.

Our next question was whether sex chromosomes evolved before or after the speciation event of the two genera. If it happened before the speciation event, all alleles of the same sex type regardless of the species, should be clustered together; if it happened after the speciation event, the X and Y alleles within species would be clustered together separated from the X and Y allele cluster of other species as shown in the most recently diverged X/Y gene pairs on the sex chromosomes of selected *Silene* species (Nicolas et al., 2005). Our results showed that papaya X, Y, and Y^h alleles formed a distinct cluster from other X and Y alleles of *Vasconcellea* species (Figure A.1), showing that the sex chromosomes in *Carica* evolved after the divergence of these two genera. Furthermore, the estimated divergence time of X-Y alleles in *C. papaya* was more recent than the divergence time of these two genera (Table A.3), demonstrating X-Y alleles diverged after the papaya speciation event. Moreover, the *Carica* X and Y alleles shared SNP haplotypes that are different from those shared by *Vasconcellea* X and Y alleles in all but a few cases. The phylogenetic analysis, divergence estimation, and SNP analysis all strongly supported that the sex chromosomes in *Carica* and *Vasconcellea* have evolved independently after the speciation event that separated these two genera. This is in line with the notion that the ancestor of *C. papaya* dispersed from South America to Central America across island chains before the formation of the Isthmus of Panama 3 million years ago (Aradhya et al., 1999). The ancestor of papaya continued to evolve in isolation from its sister genus *Vasconcellea* into a distinct species before the sex chromosomes emerged.

The estimated divergence time between the X and Y alleles in *Carica* is on average higher than that within *Vasconcellea* species, although this difference is not significant (ANOVA, $P>0.05$). This is in line with the fact that *Carica* and *Vasconcellea* evolved into separate genera

before the speciation events within *Vasconcellea*. The number of synonymous and nonsynonymous mutations between X and Y alleles in papaya is consistently higher than those in *Vasconcellea* species. Furthermore, the Y allele of Gene 3 appeared to be degenerated in *Carica*, but still exists in *Vasconcellea*. These data support that the *Vasconcellea* sex chromosomes in some species may have evolved more recently than in *C. papaya*; in particular the chromosomes of *V. pulchra*, *V. parviflora*, and *V. cundinamarcensis*, with average mean divergence times between 1.2 and 2.3 mya., as opposed to the average mean divergence of 2.7mya in *C. papaya* (Table A.3).

We addressed the alternative hypothesis that gene conversion has homogenized X/Y allele sequences and is the cause of the low divergence of X/Y alleles in *C. papaya* and *Vasconcellea* species. While we did find evidence for tracts of conversion in some X/Y allele pairs, our analysis does not support this alternative hypothesis. First, the detected conversion events were inconsistently distributed among species' X/Y allele pairs for any gene analyzed. For example, in Gene 1, conversion was detected among the X/Y alleles of *V. paviflora*, but not in *C. papaya* or other *Vasconcellea* species. Similarly, in other genes, we found evidence for conversion in one or two species, but not in all species analyzed. Second, the detected gene conversion events were limited to tracts of a hundred to a few hundred bps and none spanned the entire length of the gene. Importantly, we obtained the same evolutionary relationships of X/Y alleles when we removed the conversion tracts from our alignments. Thus, while we do find evidence of limited gene conversion among some species' X/Y alleles, we suggest that the conversion was not sufficient to cause the evolutionary patterns that we see among X/Y alleles. Instead, we suggest that these patterns are caused by independent origins of suppressed recombination in the genetic regions containing these genes in the separate species.

Papaya is the only species in *Carica*, but there are 21 species in *Vasconcellea*, including monoecious, dioecious, and trioecious species (Ming et al., 2005). The fact that a monoecious species exists in this genus hints that sex chromosomes are not ancestral for the entire genus, although reverse evolution could account for the monoecious species. Our data support that sex chromosomes have evolved independently at the species level in *V. parviflora* and *V. pulchra,* and likely in *V. goudotiana* and *V. cundinamarcensis* as well, because distinctive clusters of X/Y alleles formed in all genes analyzed in *V. parviflora* and *V. pulchra* and some genes in *V. goudotiana* and *V. cundinamarcensis*.

Is it possible that these six genes are located in a recently evolved evolutionary stratum while the sex chromosomes are ancient? Genes 1-3 and Genes 4-6 are 4-5 Mb apart across more than half the MSY, but the mean estimated divergence times of X/Y alleles in *C. papaya* are not significantly different. We cannot test for strata in *Vasconcellea sp.*, however, in the absence of data detailing the physical and/or genetic position of these loci in these species. We hypothesize that the MSY region in *Carica* and *Vasconcellea* likely expanded from the initial recombination suppression in a region containing a shared pair of sex determination genes, but it appears to have happened too recently to allow the formation of detectable evolutionary strata.

Although sex chromosomes in these two genera evolved recently, degeneration of the Y chromosome is already in progress. Besides the Y allele of Gene 3 deleted in papaya, the Y allele of Gene 1 in *V. goudotiana* might be a pseudogene due to a point mutation resulting in a premature stop codon.

FIGURES

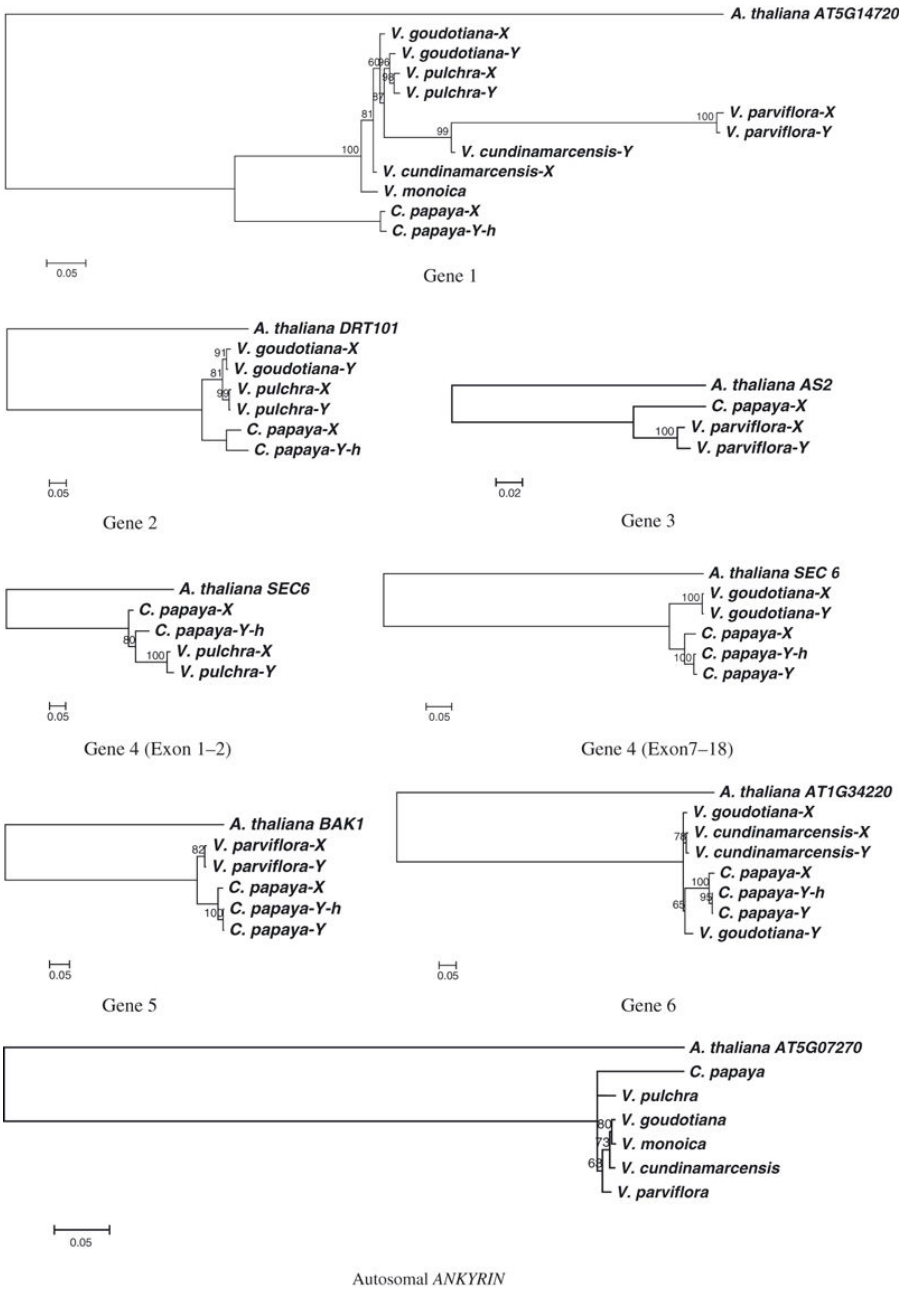


Figure A.1 Bayesian phylogenetic trees of papaya sex-linked Genes1 to 6 and autosomal gene *ANKYRIN*. All trees were generated from genomic sequence alignments (using all sites except gaps) with MrBayes (3.1.2) method (Huelsenbeck and Ronquist, 2001). Other methods (maximum likelihood, maximum parsimony and neighbor-joining) yielded similar results. Branch lengths were shown in proportion to total sequence divergence. Numbers at nodes are bootstrapping values exceeding 50% (based on 1000 replicates). Corresponding homologs of *A. thaliana* were used as an outgroup. The X and Y represented X- and Y-specific allele, respectively. For papaya, the Y represents male Y allele and Y-h hermaphrodite Y^h allele.

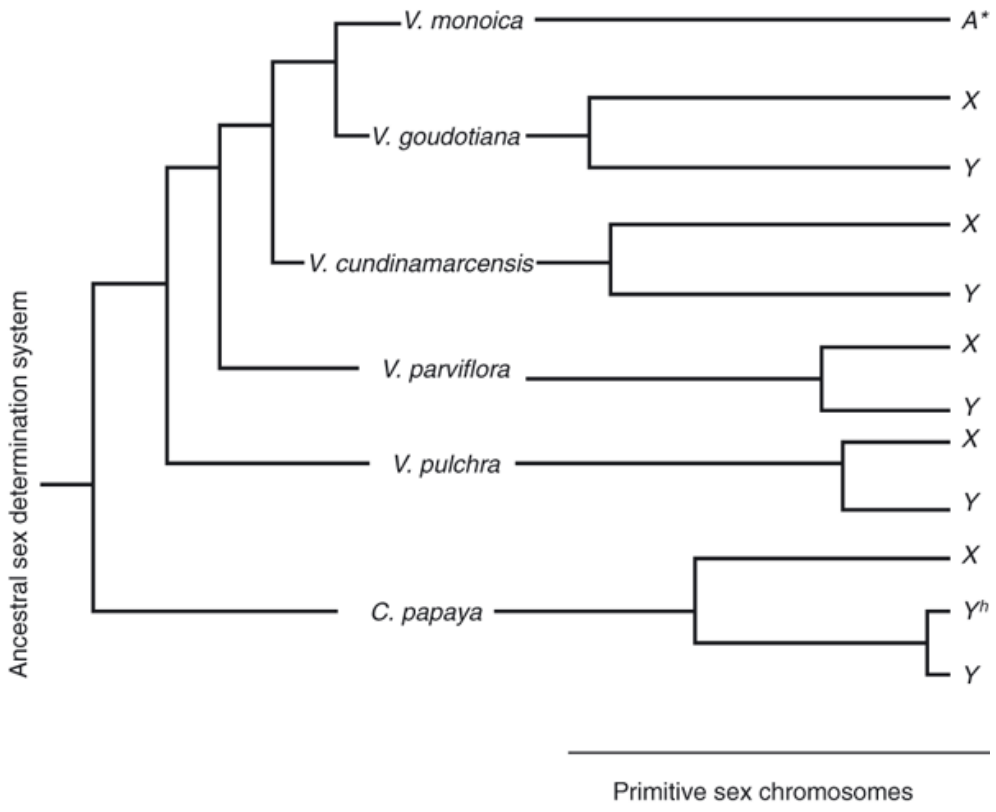


Figure A.2 Composite summary diagram based on Figure A.1 showing the evolution of the sex chromosomes in *Vasconcellea* and *Carica* clade in a simplified form. A* - autosomal allele.

TABLES

Table A.1 Estimates of synonymous and nonsynonymous nucleotide divergence within and between species of Gene 1.

Species	Total sites	Total coding sites	Syn. sites	Non-syn. sites	Syn. Mut.	Non-syn. Mut.	Ks	Ka	Ka/Ks
Within species X vs Y alleles									
C. papaya (Cp)	10732	2034	457.3	1576.8	4	7	0.009	0.004	0.51
V. cundinamarcensis (Vc)	766	255	59.8	195.2	0	2	0.000	0.010	--
V. goudotiana (Vg)	2076	768	179.9	588.1	8	2	0.046	0.003	0.07
V. parviflora (Vpa)	1680	510	123.8	386.2	3	3	0.025	0.008	0.32
V.pulchra (Vpu)	782	273	64.4	208.6	2	1	0.032	0.005	0.15
Between species X allele									
Cp vs Vc	885	375	91.3	283.8	16	6	0.200	0.021	0.11
Cp vs Vg	2951	990	233.2	756.8	30	24	0.141	0.031	0.22
*Cp vs Vm**	2104	795	185.1	609.9	26	10	0.156	0.017	0.11
Cp vs Vpa	1739	576	140.3	435.8	16	19	0.124	0.045	0.36
Cp vs Vpu	826	321	75.1	245.9	13	6	0.197	0.025	0.13
Vc vs Vg	886	375	92.2	282.8	1	0	0.011	0.000	0.00
Vc vs Vm	888	375	92.3	282.7	2	1	0.022	0.004	0.16
Vc vs Vpa	887	372	91.5	280.5	4	0	0.045	0.000	0.00
Vc vs Vpu	826	321	75.9	245.1	5	1	0.069	0.004	0.06
Vg vs Vm	2116	783	184.8	598.2	3	3	0.016	0.005	0.31
Vg vs Vpa	910	396	98.2	297.8	3	0	0.031	0.000	0.00
Vg vs Vpu	825	321	75.9	245.1	5	1	0.069	0.004	0.06
Vm vs Vpa	1761	519	125.9	393.1	5	3	0.041	0.008	0.19
Vm vs Vpu	827	321	76.1	244.9	6	2	0.083	0.008	0.10
Vpa vs Vpu	828	321	75.9	245.1	4	1	0.055	0.004	0.07
Between species Y allele									
Cp vs Vc	762	255	58.7	196.3	12	8	0.239	0.042	0.18
Cp vs Vg	3046	999	233.8	765.2	32	23	0.151	0.033	0.22
Cp vs Vm	2067	768	178.1	589.9	28	10	0.176	0.017	0.10
Cp vs Vpa	1610	456	107.2	348.8	15	15	0.155	0.044	0.29
Cp vs Vpu	779	279	63.8	215.2	12	6	0.216	0.028	0.13
Vc vs Vg	790	255	59.8	195.3	5	3	0.089	0.016	0.17
Vc vs Vm	767	252	59.7	192.3	0	3	0.000	0.016	--
Vc vs Vpa	768	252	59.5	192.5	4	2	0.070	0.010	0.15
Vc vs Vpu	760	252	59.8	192.2	3	2	0.052	0.010	0.20
Vg vs Vm	3027	999	238.5	760.5	12	8	0.052	0.011	0.20
Vg vs Vpa	1138	438	105.4	332.6	8	4	0.080	0.012	0.15
Vg vs Vpu	782	294	69.3	224.8	4	1	0.060	0.004	0.07
Vm vs Vpa	1739	510	123.3	386.8	8	7	0.068	0.018	0.27
Vm vs Vpu	781	273	64.5	208.5	4	1	0.065	0.005	0.07
Vpa vs Vpu	782	273	64.3	208.7	3	0	0.048	0.036	0.74

**Vm: V. monoica*

Table A.2 Estimates of synonymous and nonsynonymous nucleotide divergence within and between species of autosomal *ANKYRIN* Gene

Species	Total sites	Total coding sites	Syn. sites	Non-syn. sites	Syn. Mut.	Non-syn. Mut.	Ks	Ka	Ka/Ks
Between species									
Cp vs Vc	1477	453	111.2	341.8	12	2	0.117	0.006	0.05
Cp vs Vg	1583	456	111.8	344.2	12	2	0.116	0.006	0.05
*Cp vs Vm**	1582	456	111.8	344.2	12	2	0.116	0.006	0.05
Cp vs Vpa	1579	456	111.8	344.2	12	2	0.116	0.006	0.05
Cp vs Vpu	1581	456	112.0	344.0	12	5	0.116	0.015	0.13
Vc vs Vg	1549	453	111.3	341.7	0	0	0.000	0.000	/
Vc vs Vm	1550	453	111.3	341.7	0	0	0.000	0.000	/
Vc vs Vpa	1547	453	111.3	341.7	0	0	0.000	0.000	/
Vc vs Vpu	1545	453	111.5	341.5	2	3	0.018	0.009	0.49
Vg vs Vm	1660	456	112.0	344.0	0	0	0.000	0.000	/
Vg vs Vpa	1653	456	112.0	344.0	0	0	0.000	0.000	/
Vg vs Vpu	1650	456	112.2	343.8	2	3	0.018	0.009	0.49
Vm vs Vpa	1653	456	112.0	344.0	0	0	0.000	0.000	/
Vm vs Vpu	1650	456	112.2	343.8	2	2	0.018	0.006	0.32
Vpa vs Vpu	1648	456	112.2	343.8	2	3	0.018	0.009	0.49

C. papaya = (Cp)
V.cundinamarcensis = (Vc)
V. goudotiana = (Vg)
V. parviflora = (Vpa)
V.pulchra = (Vpu)

Table A.3 Estimated divergence times (MYA) for X/Y alleles in *C. papaya* and *Vasconcellea* species.

Comparison[a]	Gene ID						
	1	2	3	4 (region 1)	4 (region 2)	5	6
C. papaya	1.4[b] (0.23, 3.4)[c]	2.0 (0.36, 4.5)	-	5.4 (1.2, 12.6)	4.5 (1.0, 10.4)	2.5 (0.52, 6.1)	0.57 (0.03, 1.5)
C. papaya (Y/Y^h)[d]	n.d.	0.19 (0, 0.64)	-	-	-	0.13 (0, 0.47)	0.32 (0, 1.0)
V. goudotiana	4.4 (1.4, 9.6)	0.89 (0.09, 2.1)	-	-	0.74 (0.04, 2.2)	-	3.2 (0.79, 7.2)
V. pulchra	0.80 (0.15, 1.8)	0.44 (0.005, 1.3)	-	3.1 (0.56, 8.0)	-	-	-
V. parviflora	1.0 (0.21, 2.3)	-	2.0 (0.21, 5.4)	-	-	0.70 (0.06, 1.8)	-
V. cundinamarcensis	2.8 (0.66, 5.8)	-	-	-	-	-	0.64 (0.09, 1.5)
C. papaya/Vasoncellea sp.[e]	13.9 (4.4, 28.7)	13.2 (4.7, 26.4)	10.5 (3.0, 22.3)	14.7 (4.4, 31.6)	13.2 (4.3, 27.4)	7.2 (2.3, 14.5)	6.8 (2.4, 14.1)

[a]Comparisons between X and Y alleles unless otherwise noted; [b]mean estimated divergence time in millions of years; [c]lower and upper bounds of the 95% highest posterior density interval; [d]divergence time estimates for the male Y and hermaphroditic Y^h; [e]estimated mean divergence time of *C. papaya* and *Vasconcellea* species

SUPPLEMENTAL FIGURES

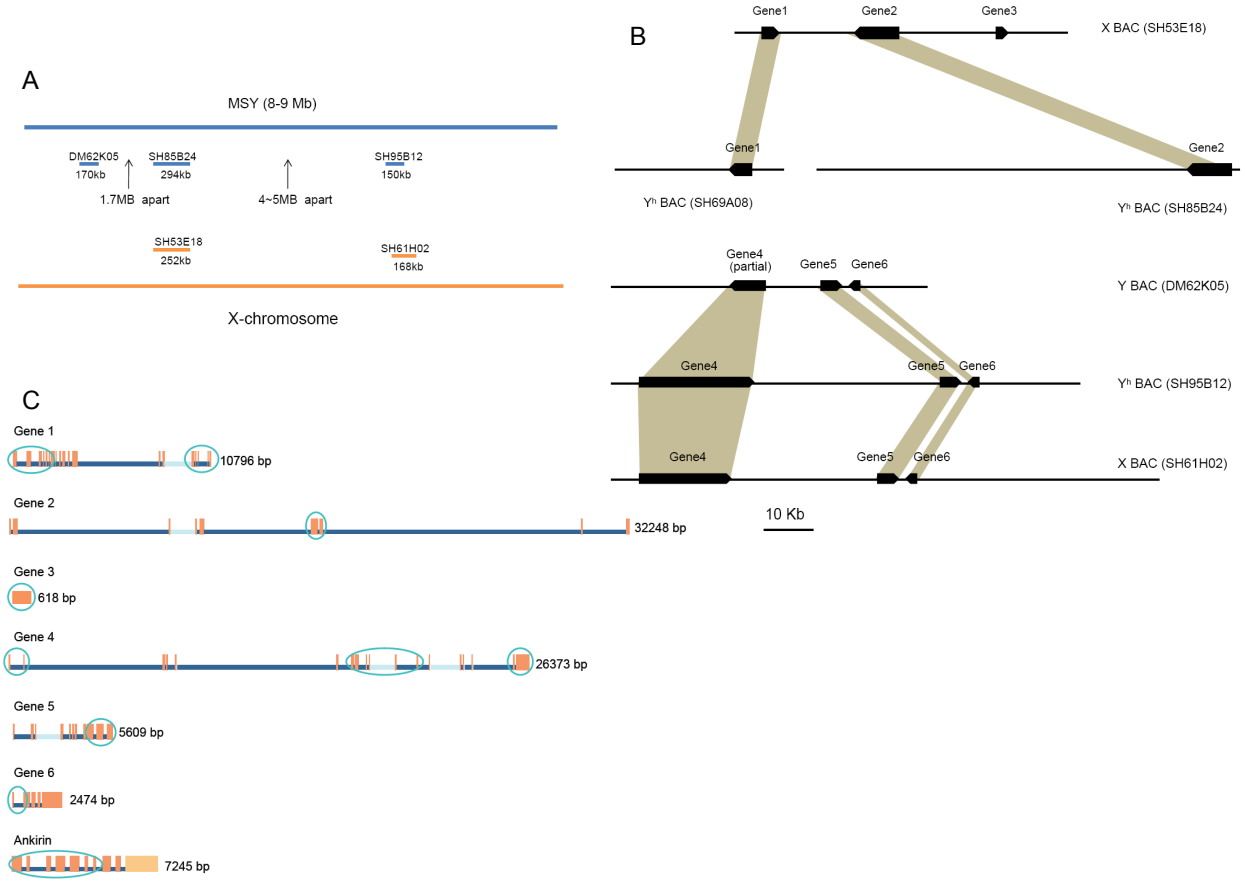


Figure A.S1 Positions of five sex-linked BACs and the structure of six sex-linked genes. **A.** The position of BACs in the MSY region of papaya. **B.** The position and orientation of Genes 1-6. The line represented the BAC and the box with arrow represented the gene and its orientation. The shaded areas connected corresponding genes. Gene3 had not been found in Y nor Y^h chromosome. Only C-terminal of Gene4 was found in the Y BAC (DM62K05). **C.** The structure of Genes 1-6. The length of the gene was shown in proportion. The orange bar represented exons and the blue line the introns. The amplified genomic sequences were indicated as blue circle.

SUPPLEMENTAL TABLES

Table A.S1 The location of the six sex-linked genes in papaya and their homologs in *A. thaliana*

Gene Number	Location on X-BAC ID	Location on Y-h BAC ID	Location on Y-BAC ID	*Arabidopsis thaliana* homologs	Gene Bank ID	Amino Acid Identity
Gene 1	19577-30372(53E18)	N/A	125814-136564(69A08)	Protein kinase family protein	AT5G14720	483/680(71%)
Gene 2	119229-86982C(53E18)	257412-285131(85B24)	N/A	DRT101 (DNA-Damage-Repair/Toleration 101)	AT5G18070	376/559(67%)
Gene 3	201739-202356(53E18)	N/A	N/A	AS2 (Asymmetric Leaves 2);	AT1G65620	154/216(71%)
Gene 4	6956-33328(61H02)	8030-43059(95B12)	Partial 41375-42176(62K05)	exocyst complex SEC6	AT1G71820	497/540(92%)
Gene 5	79843-77379C(61H02)	89773-95349(95B12)	13589-19165(62K05)	Somatic Embryogenesis Receptor-like Kinase 1 (SERK1)	AT1G34210	507/551(92%)
Gene 6	79843-77370C(61H02)	97133-99604(95B12)	20962-23435(62K05)	Hypothetical protein	AT1G34220	292/560(52%)
Autosome Gene	30188-37432(Contig 17758)			*ANKYRIN* repeat family protein	AT5G07270	135/160(84%)

Sequences of BAC 53E18, 61H02, 85B24, 95B12 and 62K05 are available in Genebank databse (Yu et al. (b) 2007 and Yu et al. 2008). BAC69A08 is the new published sequence.

Table A.S2 Estimates of synonymous and non-synonymous nucleotide divergence within and between species of Gene 2

Species	Total sites	Total coding sites	Syn. sites	Non-syn. sites	Syn. Mut.	Non-syn. Mut.	Ks	Ka	Ka/Ks
Within species X vs Y alleles									
C. papaya (Cp)	462	375	91.67	283.33	4	3	0.041	0.011	0.26
V. goudotiana (Vg)	457	375	90.58	284.42	2	0	0.024	0.000	0.00
V.pulchra (Vpu)	457	375	91.5	283.5	1	0	0.006	0.000	0.00
Between species X allele									
Cp vs Vg	462	378	91.17	286.83	17	10	0.208	0.036	0.17
Cp vs Vpu	462	378	91.67	286.33	17	10	0.199	0.036	0.18
Vg vs Vpu	457	375	91	284	8	2	0.074	0.007	0.10
Between species Y allele									
Cp vs Vg	465	375	90.92	284.08	14	12	0.169	0.044	0.26
Cp vs Vpu	465	375	91.33	283.67	15	12	0.184	0.044	0.24
Vg vs Vpu	457	375	91.08	283.92	7	2	0.055	0.007	0.13

Table A.S3 Estimates of synonymous and non-synonymous nucleotide divergence within and between species of Gene 3

Species	Total sites	Total coding sites	Syn. sites	Non-syn. sites	Syn. Mut.	Non-syn. Mut.	Ks	Ka	Ka/Ks
Within species X vs Y alleles									
V. parviflora (Vpa)	587	585	136.67	448.33	6	1	0.045	0.002	0.05
Between species X allele									
Cp vs Vpa	630	575	132.75	437.25	42	5	0.411	0.012	0.03
Between species Y allele									
Cp vs Vpa*									

The sequence of the Gene 3 Y allele of *Cp** is not available.

Table A.S4 Estimates of synonymous and non-synonymous nucleotide divergence within and between species of Gene 4

Species	Total sites	Total coding sites	Syn. sites	Non-syn. sites	Syn. Mut.	Non-syn. Mut.	Ks	Ka	Ka/Ks
Exon 1-2									
Within species X vs Y alleles									
C. papaya (Cp)	785	102	20.25	81.75	1	1	0.073	0.012	0.17
V.pulchra (Vpu)	822	102	22.83	79.17	0	1	0.024	0.013	0.54
Between species X allele									
Cp vs Vpu	834	102	20	82	1	3	0.114	0.038	0.33
Between species Y allele									
Cp vs Vpu	826	102	20.42	81.58	0	3	0.148	0.038	0.25
Exon 7-18									
Within species X vs Y alleles									
C. papaya (Cp)	2172	492	110.75	381.25	8	1	0.048	0.008	0.17
V. goudotiana (Vg)	2131	495	111	384	0	1	0.003	0.003	0.76
Between species X allele									
Cp vs Vg	2209	489	110.17	378.83	8	5	0.124	0.013	0.11
Between species Y allele									
Cp vs Vg	2170	498	111.75	386.83	9	2	0.132	0.010	0.08

Table A.S5 Estimates of synonymous and non-synonymous nucleotide divergence within and between species of Gene 5

Species	Total sites	Total coding sites	Syn. sites	Non-syn. sites	Syn. Mut.	Non-syn. Mut.	Ks	Ka	Ka/Ks
Within species X vs Y alleles									
C. papaya (Cp) X-Y	5572	1851	444.75	1406.25	22	3	0.031	0.002	0.07
C. papaya (Cp) X-Y-h	5572	1866	445.58	1420.42	24	3	0.031	0.002	0.07
V. parviflora (Vpa)	1146	765	180.83	584.17	2	5	0.006	0.003	0.62
Between species X allele									
Cp vs Vpa	1156	780	183.58	596.42	28	3	0.152	0.005	0.03
Between species Y allele									
Cp-Y vs Vpa	1142	768	181	587	30	8	0.142	0.009	0.06
Cp-Y-h vs Vpa	1156	768	180.5	587.5	30	8	0.142	0.009	0.06

Table A.S6 Estimates of synonymous and non-synonymous nucleotide divergence within and between species of Gene 6

Species	Total sites	Total coding sites	Syn. sites	Non-syn. sites	Syn. Mut.	Non-syn. Mut.	Ks	Ka	Ka/Ks
Within species X vs Y alleles									
C. papaya (Cp) X-Y	2474	1599	366.42	1232.58	14.5	31.5	0.041	0.026	0.64
C. papaya (Cp) X-Y-h	2474	1599	366.25	1232.75	14.5	32.5	0.041	0.027	0.66
V.cundinamarcensis (Vc)	648	153	33.17	119.83	1	2	0.031	0.017	0.55
V. goudotiana (Vg)	598	156	34.17	121.83	1	0	0.030	0.000	/
Between species X allele									
Cp vs Vc	654	156	34.33	121.67	5	2	0.096	0.017	0.17
Cp vs Vg	658	156	34.33	121.67	7	2	0.096	0.017	0.17
Vc vs Vg	652	150	32.83	117.17	2	0	0.025	0.000	0.00
Between species Y allele									
Cp-Y vs Vc	594	156	34.33	121.67	6	2	0.199	0.017	0.08
Cp-Y vs Vg	643	153	33.33	119.67	6	5	0.206	0.034	0.17
Vc vs Vg	596	153	33.17	119.83	2	3	0.063	0.017	0.27

Table A.S7 Fragments with possible gene conversion detected by GENECONV

Gene	Seq #	Sim Names	P value	KA Pvalue	Aligned Begin	Offsets End	Num Len	Num Poly	Tot Dif	MisM Difs	MisM Pen.	Align len	% conv
1	PI	*V. pariflora* X/Y	0.012	0.205	147	853	707	369	0	3	None	2000	35%
2	PI	*V. pulchra* X/Y	0.029	0.311	16330	16441	111	196	0	1	None	467	24%
4	PI	*C. papaya*-X/Y^{h}	0.018	0.029	242	336	95	59	0	56	None	895	11%
	GI	*C. papaya*-X/Y^{h}	0.041	0.324	5434	5685	252	104	0	26	None	5668	4%
5	GI	*C. papaya*-X/Y	0.041	0.324	5434	5685	252	104	0	26	None	5668	4%
	PI	*C. papaya*-X/Y^{h}	0.007	0.022	5434	5685	252	104	0	26	None	5668	4%
	PI	*C. papaya*-X/Y	0.007	0.022	5434	5685	252	104	0	26	None	5668	4%
6	PI	*V. goudotiana*-X/Y	0.019	0.050	635	792	157	88	0	23	None	719	22%
	PI	*V. cundinamarcensis*-X/Y	0.028	0.130	300	670	371	190	0	7	None	719	52%

GI is Inner fragments with significant global BLAST-like scores
PI is Inner fragments with significant pairwise KA P values.
KA Pvalues are NOT corrected for multiple pairwise comparisons.
Num Len is the length of DNA sequence for the gene conversion
Num Poly is the number of polymorphic sites in the fragment.
Tot Dif is the total number of mismatches between two sequences.
MisM Difs is the number of mismatches within the fragment.
MisM Pen is the penalty per mismatch for these two sequences.
Align len is the total length of DNA sequence in the alignment.
%conv is the ratio of (num Length)/(Alignment Length).

REFERENCES

Aradhya M.K., Manshardt R.M., Zee F., Morden C.W. (1999) A phylogenetic analysis of the genus Carica L. (Caricaceae) based on restriction fragment length variation in a cpDNA intergenic spacer region. Genet. Resour. Crop Evol. 46: 579-586.

Badillo V.M. (2000) Carica L. vs. Vasconcella St. Hil (Caricaceae): con la rehabilitacion de este ultimo. Ernstia. 10: 74-79.

Charlesworth B. (1991) The evolution of sex chromosomes. Science 251: 1030-1033.

Charlesworth B. and Charlesworth D. (1978) A model for the evolution of dioecy and gynodioecy. Am Nat. 112: 975-997.

Drummond A.J., Ho S.Y.W., Phillips M.J., Rambaut A. (2006) Relaxed phyogenetics and dating with confidence. PLoS Biol. 4: 699-710.

Drummond A.J. and Rambaut A. (2007) BEAST: Bayesian evolutionary analysis by sampling trees. BMC Evol. Biol. 7: 214.

Filatov D.A. and Charlesworth D. (2002) Substitution rates in the X- and Y- linked genes of the plants, Silene latifolia and S. dioica. Mol. Biol. Evol. 19: 888-907.

Fraser J.A., Diezmann S., Subaran R.L., Allen A., Lengeler K.B., Dietrich F.S., and Heitman J. (2004) Convergent evolution of chromosomal sex-determining regions in the animal and fungal kingdoms. PLoS Biol 2: e384.

Goddard M.R., Godfray H.C. and Burt A. (2005) Sex increases the efficacy of natural selection in experimental yeast populations. Nature 434: 636-640.

Graves J.A.M. and Shetty S. (2001) Sex from W to Z: evolution of vertebrate sex chromosomes and sex determining genes. Journal of Experimental Zoology 290: 449-462.

Guindon S. and Gascuel O. (2003) A simple, fast, and accurate algorithm to estimate large phylogenies by maximum likelihood. Systematic Biology 52: 696-704.

Hall, T. (1999) BioEdit: a user-friendly biological sequence alignment editor and analysis program for Windows 95/98/NT. Nucleic Acids Symp. Ser. 41: 95-98.

Huelsenbeck J.P. and Ronquist F. (2001) MrBayes: Bayesian inferences of phylogeny. Bioinformatics 17: 754-755.

Koch M.A., Haubold B. and Mitchell-Olds T. (2000) Comparative Evolutionary Analysis of Chalcone Synthase and Alcohol Dehydrogenase Loci in Arabidopsis, Arabis, and Related Genera (Brassicaceae). Mol. Biol. Evol. 17: 1483-1498.

Kyndt T., Romeijn-Peeters E., Van Droogenbroeck B., Romero-Motochi J.P., Gheysen G. and Goetghebeur P. (2005) Species relationships in the genus Vasconcellea (Caricaceae) based on molecular and morphological evidence. American Journal of Batony 92: 1033-1044.

Kyndt T., Van Droogenbroeck B., Haegeman A., Roldán-Ruiz I. and Gheysen G. (2006) Cross-species microsatellite amplification in Vasconcellea and related genera and their use in germplasm classification. Genome 49: 786-798.

Larkin M.A., Blackshields G., Brown N.P., et al. (13 co-authors). (2007). ClustalW and ClustalX version 2. Bioinformatics 23: 2947-2948.

Li, W.H. (1997) Molecular Evolution. Sunderland, MA, USA: Sinauer Associates.

Liu Z., Moore P.H., Ma H., Ackerman C.M., Ragiba M., Yu Q., Pearl H.M., Kim M.S., Charlton J.W., Stiles J.I., Zee F.T., Paterson A.H. and Ming R. (2004) A primitive Y chromosome in papaya marks incipient sex chromosome evolution. Nature 427: 348-352.

Magdalita P. M., Drew R. A., Adkins S. W. and Godwin I. D. (1997) Morphological, molecular and cytological analyses of Carica papaya×C. cauliflora interspecific hybrids. Theor. Appl. Genet. 95: 224-229.

Manshardt R.M. and Wnslaff T.F. (1989) Interspecific hybridization of papaya with other carica species. J. Amer. Soc. Gort. Sci. 114: 689-694.

Ming R., Van Droogenbroeck B., Moore P.H., Zee F.T., Kyndt T., Scheldeman X., Sekioka T. and Gheysen G. (2005) Molecular diversity of Carica papaya and related species. In: Sharma A.K, Sharma A., editors. Plant Genome: Biodiversity and Evolution. Enfield, New Hampshire, USA: Science Publishers, pp. 230-254.

Ming R., Yu Q. and Moore P.H. (2007a). Sex determination in papaya. Seminars in Cell and Developmental Biology 18: 401-408.

Ming R., Wang J.P., Moore P.H. and Paterson A.H. (2007b) Sex Chromosomes in Flowering Plants. American Journal of Botany 94: 141-150.

Ming R., Hou S., FengY. et al. (85 co-authors). 2008. The draft genome of the transgenic tropical fruit tree papaya (Carica papaya Linnaeus). Nature 452: 991-996.

Nei M. and Gojobori T. (1986). Simple methods for estimating the numbers of synonymous and non-synonymous nucleotide substitutions. Mol. Biol. Evol. 3: 418-426.

Nicolas M., Marais G., Hykelova V., Janousek B., Laporte V., Vyskot B., Mouchiroud D., Negrutiu I., Charlesworth D. and Monéger F. (2005) A gradual process of recombination restriction in the evolutionary history of the sex chromosomes in dioecious plants. Plos Biology, 3: e4.

Ossowski S., Schneeberger K., Lucas-Lledó J.I., Warthmann N., Clark R.M., Shaw R.G., Weigel D., and Lynch M. (2010). The rate and molecular spectrum of spontaneous mutations in Arabidopsis thaliana. Science 327: 92-94.

Paland S. and Lynch M. (2006) Transitions to asexuality result in excess amino acid substitutions. Science 311: 990-992.

Peichel C.L., Ross J.A., Matson C.K., Dickson M., Grimwood J., Schmutz J., Myers R.M., Mori S., Schluter D., Kingsley D.M.(2004) The master sex-determination locus in threespine sticklebacks is on a nascent Y chromosome. Curr Biol. 14:1416-1424.

Pike A.C.W., Rellos P., Niesen F.H., Turnbull A., Oliver A.W., Parker S.A., Turk B.E., Pearl L.H., Knapp S. (2008) Activation segment dimerization: A mechanism for kinase autophosphorylation of non-consensus sites. EMBO J. 27: 704-714.

Rozas J., Sánchez-DelBarrio J.C., Messeguer X., Rozas R. (2003) DnaSP, DNA polymorphism analyses by the coalescent and other methods. Bioinformatics 19: 2496-2497.

Sawyer S. A. (1989) Statistical tests for detecting gene conversion. Mol. Biol. Evol. 6: 526-538.

Sawyer S. A. (1999) GENECONV: A computer package for the statistical detection of gene conversion. Distributed by the author, Department of Mathematics, Washington University in St. Louis, available at http://www.math.wustl.edu/~sawyer.

Skaletsky H., Kuroda-Kawaguchi T., Minx P.J., Cordum H.S., Hillier L., et al. (2003) The male-specific region of the human Y chromosome is a mosaic of discrete sequence classes. Nature 423: 825-837.

Spigler R.B., Lewers K.S., Main D.S., Ashman T.L. (2008) Genetic mapping of sex determination in a wild strawberry, Fragaria virginiana, reveals earliest form of sex chromosome. Heredity 101: 507-517.

Tamura K., Dudley J., Nei M., Kumar S. (2007) MEGA4: Molecular Evolutionary Genetics Analysis (MEGA) Software Version 4.0. Mol. Biol. Evol. 24: 1596–1599.

Van Droogenbroeck B., Breyne P., Goetghebeur P., Romeijin-Peeters E., Kyndt T., Gheysen, G. (2002) AFLP analysis of tenetic relationship among papaya and its wild relative (Caricaeae) from Ecuador. Theor Appl Genet. 105: 289-297.

Weismann A. (1889) The significance of sexual reproduction in the theory of natural selection. In E.B. Poulton, S. Schönland, and A.E. Shipley [eds.], Essays upon heredity and kindred biological problems, 261-305. Clarendon, Oxford, UK.

Yin T., DiFazio S.P., Gunter L.E., Zhang X., Sewell M.M., Woolbright S.A., Allan G.J., Kelleher C.T., Douglas C.J., Wang M., Tuskan G.A. (2008) Genome structure and emerging evidence of an incipient sex chromosome in Populus. Genome Res. 18: 422–430.

Yu Q., Hou S., Hobza R., et al. (16 co-authors). (2007) Chromosomal location and gene paucity of the male specific region on papaya Y chromosome. Mol Genet Genomics 278: 177-185.

Yu Q., Hou S., Feltus F.A., et al. (16 co-authors). (2008a) Low X/Y divergence in four pairs of papaya sex-lined genes. Plant J. 53:124-32.

Yu Q., Navajas-Perez R., Tong E., Robertson J., Moore P.H., Paterson A.H., Ming R. (2008b) Recent origin of dioecious and gynodioecious Y chromosomes in papaya. Tropical Plant Biol. 1: 49–57.

Zhang W., Wang X., Yu Q., Ming R., Jiang, J. (2008) DNA methylation and heterochromatinization in the male-specific region of the primitive Y chromosome of papaya. Genome Research 18: 1938-1943.

CURRICULUM VITAE

Xia Wu

xiawu2@illinois.edu
217-417-9008

Education

Ph.D.	2006-2011(expected)	University of Illinois
B.S.	2002-2006	South China Agricultural University

Qualifications

- Protein purification, protein-protein interaction study and functional characterization
- Mass Spectrometry, peptide affinity enrichment and proteomics analysis
- Plant physiology and phenotypic characterization
- Molecular genetics and genome biology

Professional Experiences

- Research Assistant, Global Change and Photosynthesis Research Unit, USDA (2006-present)
  - Characterize post-translational modifications of 14-3-3 proteins
  - Identify novel binding partners for 14-3-3 proteins
  - Analyze lysine acetylome and its functional significance
- Teaching Assistant, MCB 151 Molecular and Cellular Biology Lab, UI (2010)
  - Teach 15 students for 2 sessions
- Certificate in Business Administration, UI (2009)
- Counseling Center Advisory Committee, UI (2008-2009)
- Internship, Institute of Animal Sci., Guangdong Academy of Agri. Sci. (2006)
  - Study swine physiology in response to isoflavone
  - Manage swine cell lines
- Undergraduate thesis, South China Agri. Univ. (2004-2006)
  - Genetic variations of *Momordica charantia* seeds in the farm markets evaluated by RAPD markers
- Lecturer, Baiwan Middle School (2004)
  - Teach 120 students in the class of Introductory Plant Biology

Honors and Awards

- International Plant Molecular Biology Congress Travel Award (2009)
- Conference chair's fund, Gordon Research Conference (2008)
- Conference travel award for graduate students, UI (2007,2008)
- Honored graduation, SCAU (2006)
- Research funds for undergraduates, SCAU (2005)

Publications

- Wu X, Oh M-H, Yau PM, Clouse SD, Huber SC. (2011) Phosphorylation of 14-3-3ω by the receptor kinases BRI1 and BAK1 that function in brassinosteroid signaling. In prepration.
- Oh M-H, Wu X, Clouse SD, Huber SC. (2011) Functional importance of BAK1 tyrosine

phosphorylation in vivo. Plant Signal Behav. 6(3). [Epub ahead of print].

- Wu X, Oh M-H, Schwarz E, Larue CT, Sivaguru M, Imai BS, Yau PM, Ort DR, Huber SC. (2011) Lysine acetylation is a widespread protein modification for diverse proteins in Arabidopsis. Plant Physiol. Feb 10. [Epub ahead of print]
- Oh M-H, Wang X, Wu X, Zhao Y, Clouse SD, Huber SC. (2010) Phosphorylation of Tyr-610 in the receptor kinase BAK1 plays a role in brassinosteroid signaling and affects basal defense gene expression. Proc. Natl. Acad. Sci. USA, 107: 17827-17832.
- Wu X, Wang J, Na JK, Yu Q, Moore RC, Zee F, Huber SC, Ming R. (2010) The origin of the non-recombining region of sex chromosomes in *Carica* and *Vasconcellea*. Plant J. 63: 801-810.
- Oh M-H, Huber JL, Shen W, Athwal GS, Wu X, and Huber SC. (2009) Overexpression of a directed mutant of 14-3-3ω in Arabidopsis leaves affects phosphorylation and protein content of nitrate reductase. Botany 87: 691–701.

Posters and Presentations

- Wu X, Oh M-H, Schwarz EM et al. Lysine acetylation – a new component in photosynthesis. 2010 Fall Welcome & Graduate Research Symposium, University of Illinois, Urbana, IL. October 8, 2010.
- Wu X, Oh M-H, Huber SC. Phosphorylation of 14-3-3 proteins by the Brassinosteroid Receptor Kinases, BRI1 and BAK1. 9th International Plant Molecular Biology Congress, St. Louis, MO. October 25-30, 2009.
- Wu X, Wang J, Na J-K et al. Speciation and the origin of sex chromosomes in *Carica* and *Vasconcellea*. American Society of Plant Biologists annual meeing, Mérida, Mexico. June 26-July 1, 2008
- Wu X, Oh M-H, McGrath JM et al. Overexpression of 14-3-3ω delays flowering in arabidopsis. GRC Gordon Research Conferences: Biology of 14-3-3 Proteins, Ventura, CA. February 24-29, 2008.

Membership in Scientific Communities

American Association for the Advancement of Science
American Society of Plant Biologists
American Society for Biochemistry and Molecular Biology
American Society of Mass Spectrometry